AN ABSTRACT OF THE THESIS OF

Said S. Al-ismaily for the degree of Master of Science in Soil Science presented on May 12, 1997. Title: Genesis of Silica-Enriched Agricultural Pans in Soils Managed Under Wheat-Fallow Cropping Systems.

Redacted for Privacy

Abstract approved: _____

John Baham

Agricultural practices, including nitrogen application and surface tillage for moisture conservation, have been used intensively to increase yields of wheat (*Triticum aestivum* L.) in the wheat-fallow cropping system practiced in eastern Oregon. Many agricultural soils in this region are prone to the formation of weakly-cemented Si-enriched pans. The pans alter the chemical, mineralogical, and most notably the physical properties leading to a decrease in hydraulic conductivity. This change in internal drainage can result in episodes of erosion during periods of intense rainfall.

The physical, chemical, mineralogical, and micromorphological characteristics of a Walla Walla soil, managed under different rates of N application, and surface tillage were examined to better understand the influence of the wheat-fallow cropping system on the genesis of Si-enriched pans. The management treatments included tillage during the summer fallow cycle to control weeds and affect moisture conservation at four rates of N application: (i) no N, (ii) 45 kg N ha^{-1}, (iii) 90 kg N ha^{-1} , and (iv) straw plus 22 Mg ha^{-1} strawy manure (110 kg N ha^{-1}).

Bulk density and penetrometer readings suggest the strength of the pans can not be explained by soil compaction alone. A significant lowering of the surface soil pH and increase in exchangeable acidity have taken place in the N-45 and N-90 plots. Soil pH

and exchangeable acidity were higher and lower in the strawy manure, respectively, as the result of the return of "basic" cations (alkalinity) to the soil. Exchangeable acidity values were consistent with the estimated potential acidity generated by cation uptake/harvest and nitrification. High concentrations of water soluble (Si_w) with well defined maxima for the N-45 and N-90, and strawy manure treatments occurred at or just below the horizon with the maximum strength and bulk density. This suggests a mineral source of Si_w is acting as a cementing agent. Treatments N-45 and N-90 also have less Si_w in the Ap suggesting a removal of Si_w as a result of acidity induced agriculturally weathering.

Soil samples from the pans have a compacted dense fabric of silty material with fine pores which appear to be filled with amorphous Si oxides as examined by SEM and soil optical techniques. The fabric appears to be less dense and without the appearance of a cementing agent for samples collected just above and below the pan region. Chemical extraction with KOH and direct microscopic examination shows the Ap horizon contains abundance sources of amorphous Si as volcanic glass, pumice, and opal phytoliths.

Although acidification and weathering of Si-rich materials undoubtedly plays a role in Si-pan genesis, the dominant formation process involves the upward movement of Si-rich soil solution and the evaporation of water at the boundary between the Ap horizon and untilled subsoil. This contrast is produced as a result of repeated tillage during the summer cycle. Our observations on the genesis of Si-enriched pans suggests their management will continue to be a concern in soils high in amorphous Si as long as moisture conservation tillage is employed as part of the agricultural management system.

Genesis of Silica-Enriched Agricultural Pans in Soils Managed Under Wheat-Fallow Cropping Systems

by

Said S. Al-ismaily

A THESIS

submitted to

Oregon State University

in partial fulfillment of
the requirements for the
degree of

Master of Science

Completed May 12, 1997
Commencement June, 1998

Master of Science thesis of Said S. Al-ismaily presented on May 12, 1997

APPROVED:

Redacted for Privacy

Major Professor, representing Soil Science

Redacted for Privacy

Chair of Department of Crop and Soil Science

Redacted for Privacy

Dean of Graduate School

I understand that my thesis will become part of the permanent collection of Oregon State University libraries. My signature below authorizes release of my thesis to any reader upon request.

Redacted for Privacy

Said S. Al-ismaily, Author

ACKNOWLEDGMENT

I would like to thank my major advisor Dr. John Baham for his moral support, guides, encouragement, time and, patient from the beginning of my program to the end. I really had good memories with him. Dr. Reed Glasmann deserve special thanks for his knowledge feedback and support for completion of my studies. Dr. Herb Huddleston has been a great help for his appreciable comments while reviewing my thesis manuscript. I appreciate Dr. Tom Cook for serving as my graduate school representative. Appreciation also goes to the crew at the Columbia Basin Agricultural Research Center specifically Clyde Douglas, Don Wysocki, Paul Rasmussen, Btty Klepper, and Roger Goller for their technical and knowledgeable support on my research.

Thanks to Al Soeldner for his teachings and help while using the SEM instrument. Thanks also goes to Dr. Larry Boersma and Dr. Benno Warkentin for their friendship and to Pam Wegner for being there answering my questions while typing my thesis. Thanks to my fellow graduate students in the soil department for their friendship.

Warm thanks to Mrs. Ruth Chadwick and Don Lyall for their kindness and help during my staying here in Oregon.

I also appreciate the support that I had from Sultan Qaboos University (SQU) and my fellows in the College of Agriculture.

Finally, I would like to express my unlimited respect with heart full of love and joy to my father, mother, and wife for their day and night prayers, love, kindness and endeavors. May Allah always bless them. Extended love and regards also pointed to my brothers, sisters, uncles, and aunts for their endless love and encouragement.

TABLE OF CONTENTS

TABLE OF CONTENTS (Continued)

Page

LIST OF FIGURES

LIST OF FIGURES (Continued)

Figure Page

LIST OF FIGURES (Continued)

Figure | Page

LIST OF TABLES

LIST OF FIGURES IN APPENDICES

Dedicated to my father Salim Mohammed Al-ismaily

Genesis of Silica-Enriched Agricultural Pans in Soils Managed Under Wheat-Fallow Cropping Systems

INTRODUCTION

Weakly Si-cemented plow pans have been observed in Colombia Plateau Basin and Palouse region agricultural soils (Allmaras et al., 1982; Brown and Mahler, 1987). Soil pans affect infiltration rate, drainage of excess water, distribution of water, soil strength, and cementation (Allmaras et al., 1982). During periods of intensive precipitation the pans may limit the infiltration of water leading to episodes of surface erosion. Pathogen activity may be enhanced under the drier environment that occurs below the pan (Allmaras et al., 1982).

The strength or hardness of Si-enriched pan appears to be ephemeral in nature. They are hard in the dry season, but considerably weaker after the soil has been moistened by winter rainfall (Wilson et al., 1996). This temporal behavior points to the role of amorphous $SiO_{2(s,am)}$ as a cementing agent (Chartres et al., 1990). The mechanism by which Si pans form, however, is not well understood. Surface acidification of the plow zone could lead to increased mineral weathering with the release of soluble Si (Brown and Mahler, 1987; Douglas et al., 1984).

Ammonia/ammonium fertilizers have been used as the dominant N source in summer fallow wheat rotation cropping systems practiced in the Columbia Plateau Basin over the last 64 years. As a result of nitrification, the soil pH has been markedly lowed to a depth of 20 cm (Allmaras et al., 1982). Accelerated weathering of silicate minerals that accompanies agricultural acidification may play a role in the

genesis of the Si-enriched pans (Brown and Mahler, 1987). A fundamental understanding of how agricultural practices influence the genesis and behavior of Si-pans serve us in dealing with their potential adverse effects on agricultural production.

The primary objective of this research was to investigate the relationship of agricultural management practices to the genesis of Si-enriched pans. We hypothesize that soil acidification accelerates the weathering and release of Si. Silica is subsequently re-precipitated in the form of amorphous cement at the lower boundary of the Ap zone as a result of evaporation during the summer-fallow season. The following specific objectives were designed to test our hypothesis:

(i) Evaluate the influence of N fertilizer rate addition on the total exchangeable acidity and pH of the soil profile;

(ii) Analyze the relationship between soil acidification and soluble Si distribution in the soil profile;

(iii) Identify the major mineral sources of soluble Si; and,

(v) Explore the formation of Si cements and relate to management practices and examine the cements impact on soil fabric using SEM and optical microscopy techniques.

LITERATURE REVIEW

Overview

Physical characteristics of soils may be markedly altered by the presence of Si-enriched pans. These include bulk density and soil strength. As a result, high density layers or horizons are formed which may affect root penetration and water infiltration. The presence of these pans may contribute to the potential for soil erosion during periods of intense rainfall. This is especially a problem if the profile was already saturated with water. Basic to the understanding of the genesis of the Si-pans are micro- and macro environmental properties which affect Si behavior. The following review will discuss some of these properties and their interaction with Si.

Agricultural Acidification

Acidification of dryland and irrigated soils as a result of agricultural practices has been recently reported by many authors. Jackson and Reisenauer (1984) found that the pH of the plow layer of the many soils has dropped dramatically from their original near-neutral values. Similar decreases in surface soil pH values have been reported for the soils of the Columbia Plateau and Palouse regions (Brown and Mahler,1988; Allmaras et al., 1982; Pikul et al., 1986). This decrease in soil pH has taken place since 1960 (Jackson and Reisenauer, 1984). The decline in soil pH values is attributed to nitrification and the removal of "basic" cations through crop harvesting (Jackson and Reisenauer, 1984). Nitrification and the removal of "basic" cations in crop harvest are

the major sources of agricultural acidification (Stumm, 1992; Bouman et al., 1995; Breemen et al., 1983).

Fertilization with anhydrous NH_3 produces acidity by biologically mediated nitrification through the following equation (Adams, 1984).

$$NH_3 + 2O_2 \rightarrow NO_3^- + H^+ + H_2O. \qquad \text{Eq. [1]}$$

According to the stoichiometry in Eq. [1], each mole of anhydrous NH_3-N oxidized to NO_3^- produces one mole of H^+. The acidification produced by nitrification can be neutralized when plants take up NO_3^-, releasing an equivalent amount of OH^- into the rhizosphere (Bouman et al., 1995). Total neutralization of the acidity produced by nitrification would require that all NO_3^- produced via nitrification be consumed by plants and assimilated as organic N (Bolan et al., 1991).

The neutralization of H^+ as a result of plant uptake of NO_3^- becomes uncoupled when NO_3^- is leached from the root zone. A permanent acidification of the soil is produced if NO_3^- is leached beyond the rooting zone (Bouman et al., 1995; Breemen et al., 1983). Crop harvesting accelerates acidification by the removal of "basic" cations (Ca^{2+}, Mg^{2+}, K^+, and Na^+) relative to anions (Cl^-, $SO_4^=$, $H_2PO_4^-$, and NO_3^-) (Pierre and Banwart, 1973). Thus, usage of N fertilizers can also increase the export of "basic" cations by increasing crop yield (Bolan et al., 1991).

Weathering rates and clay mineral genesis in freely drained agricultural soils are partially determined, with respect to climate and parent material, by the supply of acidity through plant harvest and nitrification. The annual supply of H^+ influences the rate of Si weathering. However, the relationship between the H^+ supply rate and Si behavior is still poorly understood from a field perspective.

Silica Solubility in Soil

Silica ($SiO_{2(s,am)}$) has been identified as a cementing agent in hard-setting soils (Chartres et al., 1990). Several investigations showed that amorphous Si can form bridges between soil particles at points of grain contact (Chadwick, 1989; Chartres et al., 1990). For this reason Si solubility relationships should be thoroughly investigated.

Soluble silica in solution is present almost entirely as silicic acid, $H_4SiO_4^{\circ}{}_{(aq)}$, (Alexander et al., 1954; Krauskopf, 1956; Jones and Handreck, 1967; McKeague and Cline, 1963a; Beckwith and Reeve, 1964). Silicic acid forms as a weathering product of mineral solids. It then can precipitate as either amorphous Si or polymorphic crystalline forms (Eq. [2], Faure, 1991).

$$SiO_2 \text{ (quartz)} + 2H_2O \rightleftharpoons H_4SiO_4^{\circ}{}_{(aq)} \qquad \text{Eq. [2]}$$

$$K = 10^{-2.74}.$$

Uncharged $H_4SiO_4^{\circ}{}_{(aq)}$ is the dominant species of Si below pH 8 (Elgawary and Lindsay, 1972). At pH values above 8 several other ionic species become significant (Faure, 1991). The degree of dissociation of silicic acid at pH 7 was calculated by Faure (1991) based on the following equation [3].

$$H_4SiO_4^{\circ} \rightleftharpoons H_3SiO_4^{-} + H^{+} \qquad \text{Eq. [3]}$$

$$K = 10^{-9.71}.$$

Based on equations [2] and [3], he estimated the activity of $H_3SiO_4^{-}$ at pH 7 by the following equations.

$$(H^{+})\,(H_3SiO_4^{-}) / (H_4SiO_4) = 10^{-9.7} \qquad \text{Eq. [4]}$$

$$(H_3SiO_4^{-}) = [10^{-9.7} \times 10^{-2.74}] / 10^{-7.0}$$

$$= 10^{-5.45} \text{ mol } L^{-1}.$$

Using Eq. [2] and the activity value of Eq. [4], he calculated the dissolution percentage (D) of $H_3SiO_4^-$ as shown in Eq. [5].

$$D = [10^{-5.45} / 10^{-2.74}] \times 100 \qquad \text{Eq. [5]}$$

$$= 0.19\ \%.$$

Therefore $H_3SiO_4^-$ represents only 0.19 % to the total solubility of the pure SiO_2 at pH 7.

Although most authors now agree that monosilicic acid is the main form of soluble Si in the soil solution, the correlation between soil pH and Si solubility in soils of mixed mineralogy is still questionable. McKeague and Cline (1963b) and Beckwith and Reeve (1964) concluded that pH plays a major role in controlling the solubility of Si in soils. They attributed the pH effect to its influence on Si sorption and release by soil particles. McKeague and Cline (1963b) found lower concentrations of dissolved Si in soil solution with higher pH values, and increased Si adsorption as pH increased in the range of 4.8 to 9.7. In another study, Jones and Handreck (1965) studied adsorption and release of monosilicic acid from soils maintained at field capacity. After treating these soils with various amounts of acidifying agents, they reported that silica concentrations in soil solution decreased from 33 to 11 mg L^{-1} Si as pH increased from 5.4 to 7.2. Raupach and Piper (1959) found that Si concentration in saturated extracts of Australian soils decreased with increasing soil pH in the range of 4 to 9. Beckwith and Reeve (1963) extended the study of the relationship between Si solubility and soil pH by using soils with different minerals. They concluded that Si sorption varies with different soil minerals. Amorphous silicate minerals were found to release a significant amount of $H_4SiO_{4(aq)}$ into soil solution under acidic conditions (Beckwith and Reeve, 1963). This attributed to the weak packing density of the Si tetrahedra on these minerals (Drees et al.,

1989). Dahlgren et al. (1993) claimed that the substitution of "basic" cations by aqueous H^+ under acidic conditions is responsible for the release of Si from amorphous silicate minerals.

Kaolinite and montmorillonite appear to have low dissolution rates under low or near neutral soil pH conditions (Beckwith and Reeve, 1964). Feldspars are postulated to weather to sesquioxides in local alkaline regimes wherein the Si may be dissolved in alkaline soil solution (Jackson and Sherman, 1953). The solubility of pure quartz is essentially constant between the pH limits of 2 and 8.5, but increases rapidly above pH 9 (Drees et al., 1989). Faure (1991) and Drees et al. (1989) reasoned the rapid increase in solubility above pH 9 was due to ionization of $H_4SiO_4^\circ$ and the release of $H_3SiO_4^-$ species into soil solution. Brown's and Mahler's (1987) laboratory investigations indicated that low pH conditions can result in increased levels of Si in the Palouse silt loam soils. Apparently the Si mentioned by the latter authors comes from sources other than quartz. Douglas (1984) reported that silicic acid concentrations and transfers are sensitive to short and long term soil pH changes in the Walla Walla silt loam. He concluded that concentrations of silicic acid in soil solution decreased as pH increased.

Volcanic ash soils have been reported to weather rapidly under conditions of high acidity. White and Claassen (1980) found high concentrations of $H_4SiO_{4(aq)}$ from rhyolitic glass under low pH values of 1.0 to 6.2. Dahlgren et al. (1993) stated that volcanic glass is very susceptible to weathering and release of Si under acidic soil conditions.

The foregoing discussion has demonstrated that Si solubility is a function of soil pH. In addition, the mineral source of soluble Si is important. Amorphous forms of Si (volcanic glass) are more readily soluble than crystalline sources (quartz, feldspar, and/or clays).

Volcanic Materials

Volcanic materials, including glass shards and pumice, are generally defined as metastable supercooled materials which form as a result of low nucleation and crystallization rates during rapid magma cooling (White and Claassen, 1980). Glass shards isolated from volcanic ash and tuff occur in crescentic and cuspate forms (Tomkeieff, 1983). Pumice, on the other hand, occurs as glassy lava or pyroclastic ejecta which have been highly vesiculated by expanding gases. Pumice is usually of acid or intermediate composition (Tomkeieff, 1983).

Volcanism has a dramatic influence on soil parent material in the Pacific northwest region (Dingus, 1973). Many Oregon soils either have been formed directly from volcanic materials or have had significant quantities of tephra added to them (Dingus, 1973). Volcanic ash deposited from the Mt. Mazama (present site of Crater Lake) eruption is considered to be the largest surficial ash deposit on many of the soils east of the Cascade range (Dudas, 1973). The ash from this eruption is a significant component of soils of the Columbia plateau region. The genesis of Si-enriched pans has been linked to the presence of volcanic glass. Wilson et al. (1996) reported that volcanic glass is a source of the soluble Si that is regarded as a possible cementing agent in the Olympic peninsula region soils of western Washington. Chadwick et al. (1989)

demonstrated that volcanic glass is a major source of Si cementation of the Holocene soils of Nevada.

Dissolution of primary silicates and translocation of soluble Si in solution take place rapidly and extensively during the weathering of volcanic ash soils (Wada, 1974). Volcanic glass is one of the most soluble forms of Si in soils (Tan, 1993; Drees et al., 1989). This is attributed to the low packing density of the Si tetrahedra and short-range crystal order of these materials (Drees et al., 1989).

The primary reaction in the dissolution of volcanic glass soils involves the consumption of H^+. Therefore, the weathering rates are dependent on the concentration of H^+ ions that reach the surface of volcanic grains (Dahlgren et al., 1993). White (1983) designed an experiment to investigate the effects of acidity on glass weathering. He concluded that higher $H_4SiO_4^\circ{}_{(aq)}$ concentrations are released into aqueous solution with increased H^+ consumption (decreased pH) in the pH range of 1.0 to 6.2. White and Claassen (1980) related the variation of Si concentration with pH to the capacity of H^+ in replacing or exchanging $H_4SiO_4^\circ{}_{(aq)}$ with different acidity levels. The initial stages of weathering are characterized by exchange of aqueous H^+ for cations adsorbed on the surface of the glass particles (Dahlgren et al., 1993). This results in formation of a cation-depleted leached zone at the glass surface composed of structurally bonded Si and Al. The cation enrichment/depletion proceeds concomitantly with desilication of the glass (Dahlgren et al., 1993).

Opal Phytoliths

Opal phytoliths are silica bodies with characteristic shapes and sizes that are deposited in or secreted by plants (Witty and Knox, 1964; Simpson and Volcani, 1981; Tomkeieff, 1983). They typically have shapes and sizes characteristic of the parent plant material (Witty, 1962). Different terms have been used to describe opal phytolith bodies. These include biogenic opal (Drees et al., 1989) opaline phytoliths (Yeck and Gray, 1972; Pease and Anderson, 1969), plant opal (Jones and Beavers, 1963), grass phytoliths (Twiss et al., 1969), biolith (Jones and Hay, 1975), and phytolitharien (Baker, 1960).

Most authors agree on the cycle by which opal phytoliths form. The cycle begins with $H_4SiO_{4(aq)}$ in the soil solution, and as this absorbed by plants, opaline Si is deposited in the epidermal tissues of leaves and needles (Bartoli and Wilding, 1980; Jones and Handreck, 1967; Geis, 1973; Yeck and Gray, 1972; Jones and Milne, 1963). Deposition occurs mainly when plants absorb more Si than they require and are unable to excrete the excess (Esau, 1953). In general, Si deposition in tissues increases with the amount of water absorbed by a plant (Lanning et al., 1958). The silica is returned to soil, almost entirely as opal, by fallen leaves and needles (Bartoli and Wilding, 1980; Jones and Handreck, 1967). Opaline Si particles are released into soil through decomposition of the plant tissues (Geis, 1973; Bartoli and Wilding, 1980; Jones and Handreck, 1967). The opaline particles released form an important pool of $H_4SiO_4^{\circ}{}_{(aq)}$ for subsequent cycles (Jones and Handreck, 1967).

Several recent papers have dealt with specific mineralogical properties of opal phytoliths. Petrographic microscope techniques and X-ray diffraction analyses have been applied for studying these properties. In general, plant opal is optically isotropic, with

refractive index ranging from 1.41 to 1.48, specific gravity ranging from 1.5 to 2.3, and transmitted color from colorless to black to opaque (Wilding and Drees, 1971, 1974; Lanning et al., 1958). Their darkness depends on the organic C pigmentation occluded within the opal (Jones and Beavers, 1963; Wilding and Drees, 1974).

Opal phytoliths show numerous morphological features reflecting the nature of the dominant plant species in the soil. Twiss et al. (1969) observed different forms of plant phytoliths derived from grass leaves of different species. The forms were circular, rectangular, elliptical, saddle-shaped, variations of cross and dumbbells, and elongated rods. Wilding and Drees (1974), on the other hand, found the spheres, cups and scrolled or convoluted sheet forms to be the most distinctive phytoliths derived from deciduous tree leaves.

The size of Phytolith bodies, from grass vegetation, has been observed to be in the range of sand and silt (Witty, 1962; Bartoli and Wilding, 1980; Twiss et al., 1969). However, Norgren (1973) reported that most of the plant opal in plants is essentially clay size. On the basis of X-ray diffraction spectra, low angle X-ray scattering with a very diffuse band centered at about 4.1 Å were observed with plant opal (Jones and Beavers, 1963; Jones and Milne, 1963; Lanning et al., 1958). The low angle scattering is presumably caused by the absence of long-range crystal order (Bartoli and Wilding, 1980).

Phytoliths consist of SiO_2 and 5 to 15 % H_2O with small quantities of Mg, Ca, Na, K, Mn, Fe, and Al impurities (Jones and Beavers, 1963) and organic C (Bartoli and Wilding, 1980; Jones and Milne, 1963). By completely destroying organic matter with nitric and perchloric acids and then washing the phytoliths successively with hydrochloric

acid and distilled water, phytoliths may become entirely pure opal, $SiO_2.nH_2O$, (Jones and Handreck, 1967). The plant opal has a highly disordered or near amorphous structure (Jones and Segnit, 1971).

Plant opal phytoliths are common features in soils formed under a variety of vegetative soil ecosystems. Soils developed under extended periods of grass vegetation commonly contain 5 to 10 times more plant opal than those formed under forested environment (Jones et al., 1964; Wilding and Drees, 1971; Norgren, 1973). It is estimated that about 160,000 kg ha^{-1} of plant opal is produced of soil under 5,800 years of grass vegetation (Witty, 1962). Opal phytoliths have been found in soils derived from volcanic materials (Mizota et al., 1982). Norgren (1973) estimated that opal phytoliths were formed at a rate of 112 kg ha^{-1} yr^{-1} in the Walla Walla silt loam soils. This high formation rate was attributed to the large amount of readily weatherable volcanic-silica parent material from which these soils developed. Phytoliths in the Walla Walla silt loam constitute a significant portion of amorphous clays (Norgren, 1973). A better knowledge of the chemical and physical characteristics of plant opal and its behavior in soils will help us understand the biogeochemical cycling of Si in soils, pedogensis, and opal as a source of soluble Si in soils (Bartoli and Wilding, 1980).

The stability and *in situ* solubility of biogenic Si-components are not well known. Dissolution rate is one method of determining the stability of plant opal in soils (Bartoli and Wilding, 1980). The weathering rate of opal phytoliths is intermediate between amorphous Si, which weathers rapidly, and quartz (Eq. [6], Tan, 1993)

Quartz < crystobalite < opal phytoliths < amorphous silica. Eq. [6]

The solubility of opal phytoliths ranges from 0.5 to 10 mg Si L^{-1}, depending on its source and chemical properties (Wilding et al., 1979; Bartoli and Wilding, 1980). Solubility of opal phytoliths is about 3 to 5 times lower than amorphous Si and 3 to 10 times more than quartz (Bartoli and Wilding, 1980). Many factors influence the dissolution of opal phytoliths. These include its physical and chemical properties such as surface area, water content, density, Al content, and surrounding temperature (Bartoli and Wilding, 1980).

Bartoli and Wilding (1980) found a close positive relationship association between phytolith surface area and dissolution. However, an inverse association occurs between Al content and respective surface area-dissolution. They reasoned the reduction of Si dissolution by Al is due either to Al chemisorption to Si surface which, causes the latter to be less reactive, or to the reduction of surface area due to a coagulative effect of Al during Si synthesis.

A positive relationship between Si dissolution and moisture content was observed (Wilding et al., 1979). Phytoliths with lower water contents could be expected to have larger macro-molecular structural aggregate accompanied by lower surface areas and lower dissolution rates (Wilding et al., 1979; Bartoli and Wilding, 1980).

Increased temperature, on the other hand, accelerates Si dissolution by removing protective organic coatings such as humic acid, amides, and amines from the opal phytoliths (Wilding et al., 1967; Bartoli and Wilding, 1980).

Bartoli and Wilding (1980) studied the dissolution of opal phytoliths with pH. They concluded that dissolution of plant opal under natural conditions is independent of pH below 6. The dissolution rate of opal phytoliths may increase at pH above 9 (Witty, 1962)

Siliceous Pans Associated with Agricultural Practices

Pans are compacted, high density subsurface layers or horizons that have resulted from natural processes and/or operations related to agricultural production (Unger, 1979). They can restrict water movement and root penetration resulting in a negative influence on yield (Steinhardt and Franzmeier, 1979; Unger, 1979; McKeague and Sprout, 1975).

Amorphous Si, Fe, and Al minerals have been suggested as the binding agents leading to cementation of soil materials and pan formation (Wilson et al., 1996; Chartres, 1985; Steinhardt and Franzmeier, 1982). Silica as a cementing agent has been reported recently by many workers (Wilson et al., 1996; Chartres, 1990, 1985; Franzmeier et al., 1989; Smith and Daniels, 1989; Chadwick et al., 1989; Brown and Mahler, 1988; Milnes and Twidale, 1983). Several terms have been used to describe Si-enriched subsurface layers including Si-indurated (Singh and Gilkes, 1993), hard setting soils (Chartres et al., 1990), fragipan (Steinhardt and Franzmeier, 1979), silicate cemented (McKeague and Portz, 1980), Si-concentrated pan (Brown and Mahler, 1987), duripan (Flach et al., 1974), silcrete (Milnes and Twidale, 1983), and weak or incipient Si-cemented pans (Wilson et al., 1996; Chadwick et al., 1989). Silica-enriched pans differ in their hardness, thickness, and effect on potential crop yield, however, the main processes involved in their formation are similar. The occurrence of Si-enriched pans within different soil types and in various topographic localities is widespread and suggests a pedogenic origin. However, a genetic relationship between soil environment and Si-pan formation has not been clearly established. In general, Si weathering, leaching, and precipitation within a soil profile is thought to be responsible for cementation (Wilson et al., 1996; McKeague

and Cline, 1963b; Chadwick et al., 1987ab; Brown and Mahler, 1988; Chartres et al., 1990; Milnes and Twidale, 1983; Douglas et al., 1984; McKeague and Sprout, 1975).

Silica-enriched pans induced by cropping practices have been observed recently in the Palouse and Columbia plateau regions of the Pacific northwest (Brown and Mahler, 1987; Allmaras et al., 1982; Douglas et al., 1984). The bulk density of these pans is in the range of 1.3 Mg m^{-3} (Allmaras et al., 1982; Douglas et al., 1984), which is significantly lower than values commonly reported for fragipans. Allmaras et al. (1982) observed a high bulk density layer at a depth of 25 cm in his studies on Walla Walla silt loam soil. Douglas et al. (1984) claimed that Si accumulation may be associated with the highest bulk density and penetrometer load values observed in the Walla Walla silt loam soil. Physical analysis revealed low hydraulic conductivity at the same depth (Allmaras et al., 1982). Rickman and Klepper (1980) observed denitrification losses in a Walla Walla silt loam due to anaerobic conditions caused by a slowly permeable compacted horizon. Brown and Mahler (1988) observed a significant increase in water-soluble Si at a depth of 20 cm in the Palouse silt loam soil where a well-developed plow pan formed due to cropping activities.

During the process of Si-enriched pan formation, silicate minerals weather in the upper horizons and release their weathering products to the soil solution (Franzmeier et al., 1989; Chartres et al., 1990). Amorphous forms of Si can be dissolved rapidly under acidic soil environment (Beckwith and Reeve, 1963, 1964; Milnes and Twidale, 1983). Soils forming under volcanic materials are even more weatherable under acidic conditions (White and Claassen, 1980; Dahlgren et al., 1993; White, 1983; Mckeague and Sprout, 1975; Wilson et al, 1996; Chadwick et al., 1989). Silica-rich solution leached

downward and became perched over less permeable material (Franzmeier et al., 1989; Wilson et al., 1996; McKeague and Sprout, 1975). During the summer months, evaporation and utilization of water by plants promotes precipitation of amorphous Si (Kittrick, 1969; Chadwick et al., 1987ab; Chartres et al., 1990; Singh and Gilkes, 1993). Amorphous Si precipitates when Si concentration in solution reaches the range of 50 to 60 mg L^{-1} (McKeague and Cline, 1963b; Elgawhary and Lindsay, 1972; Williams et al., 1985; Williams and Crerar, 1985). In time, the precipitated Si forms bridges between adsorbing soil components that bond the particles near points of grain contact without filling the pore-space to a significant extent (Singh and Gilkes, 1993; Chadwick et al, 1987ab). Silica bridging between soil particles is responsible for the hardness and brittleness of theses pans.

SITE AND SOIL DESCRIPTIONS FOR THE STUDY AREA

The long-term residual management experiment plot was established in 1931 at the Columbia Basin Agricultural Research Center 15 km northeast of Pendleton, Oregon. (Fig. 1). This area is entirely within the Columbia Plateau physiographic province between the Cascade and Blue Mountains. The elevation is 455 m above sea level with slopes ranging from 0 to 5 %. The climate is semi-arid, characterized by cool, wet winters, and, hot, dry summers. The area receives, on average, 433 mm precipitation annually, with 70 % occurring between 1 September and 31 March (Table 1). The mean annual temperature is 10.2 °C, but ranges from a low of -0.6 °C in January to 38.2 °C in July. Potential water evaporation exceeds precipitation from March through October and reaches a maximum during the period from May through July (Table 2; Fig. 2).

The dominant native vegetation was bluebunch wheatgrass (*Agropyron spicatum*), Idaho fescue (*Festuca idahoensis*), and sandberg blue grass, *Poa secunda* (Robinson, 1961). Downybrome (*Bromus tectorum* L.) was an early invader after land was first cultivated in the mid 1880's. A wheat-fallow cropping system with nitrogen-fertilizer application has been practiced since 1931 (Rasmussen and Parton, 1994).

The experimental plot is located on the Walla Walla silt loam soil series (coarse silty, mixed, mesic typic Haploxeroll). The soil is formed in loess deposits, and it is the dominant soil series in the region. It is characterized by remarkable uniformity of floury texture throughout, soft consistence, and absence of definite structure (Douglas, 1956). Typically, the surface horizon is a grayish brown silt loam about 20 cm thick. The subsoil is lighter in color ranging from brown and pale brown silt loam about 100 cm thick or more. The series has an accumulation of diffuse calcium carbonate underlying

the soil substratum at 115 cm or deeper. Commonly with this series, the basaltic bed rock is found at a depth of 180 cm or more (Douglas, 1956). Detailed morphological descriptions of the soil cores collected for this study, along with particle-size analyses for all treatments is given in Appendix 1. Permeability of this series is moderately high with effective rooting zone to a depth of 115 cm or more. Runoff is medium, and the hazard of water erosion is moderate (USDA and SCS, 1985).

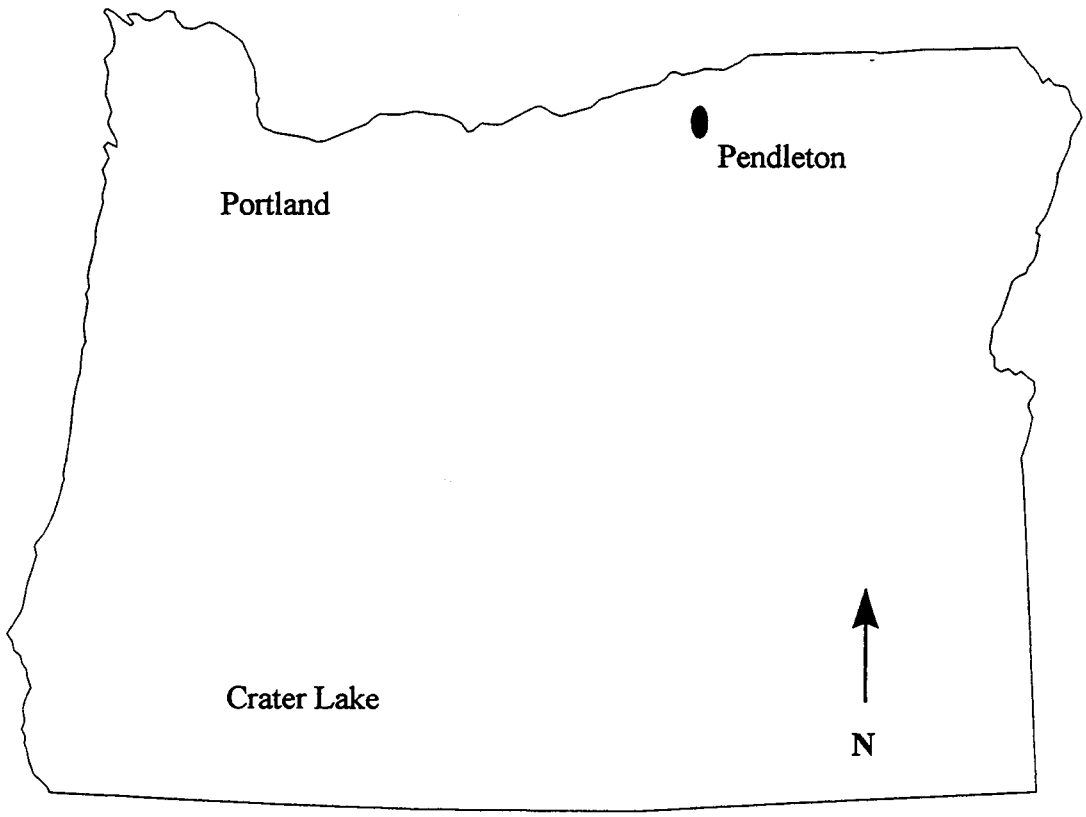

Figure 1. Location of the Columbia Basin Agricultural Research Center, Pendleton, Oregon.

Table 1. Monthly precipitation during the last 20-years at the Columbia Basin Agricultural Research Center.†

Crop yr.	Sept.	Oct.	Nov.	Dec.	Jan.	Feb.	Mar.	Apr.	May	Jun.	Jul.	Aug.	Total
	(mm)												
66-year avg.	18.3	33.3	50.8	52.07	48.8	38.1	43.4	38.9	37.3	32.0	9.1	12.7	414.8
1975-76	0	54.9	37.3	86.4	54.1	27.7	42.9	41.9	30.7	14.7	1.0	65.5	457.2
1976-77	11.2	13.5	11.9	15.0	22.9	14.5	43.7	11.7	43.2	7.9	3.0	56.1	254.5
1977-78	39.1	17.5	45.5	81.0	57.6	43.4	35.6	88.9	20.6	32.2	15.0	34.8	511.3
1978-79	40.9	0	42.7	57.9	33.3	39.1	44.2	46.2	29.2	4.6	3.0	52.8	340.0
1979-80	4.3	65.0	58.7	26.7	72.4	39.4	53.8	30.5	62.2	36.1	5.8	4.6	459.5
1980-81	31.5	75.2	46.0	50.0	32.0	58.7	58.4	32.8	58.4	53.8	10.2	0.5	508.0
1981-82	38.4	41.1	61.2	83.1	66.3	47.2	50.5	39.1	12.2	28.4	25.9	12.7	506.2
1982-83	42.7	68.1	37.1	68.3	41.4	75.4	99.1	31.2	52.8	48.8	25.4	17.3	607.6
1983-84	20.8	23.1	70.9	87.4	25.1	65.0	82.0	60.2	53.6	52.1	1.3	31.8	573.3
1984-85	24.9	30.0	87.1	49.8	17.5	37.8	33.8	16.5	22.6	36.1	1.3	24.9	382.3
1985-86	39.1	34.0	67.6	32.3	60.5	77.2	49.3	21.1	45.5	2.3	15.5	4.8	449.1
1986-87	47.5	23.1	86.6	24.1	52.8	33.3	47.0	21.1	41.4	15.7	11.9	1.5	406.1
1987-88	1.0	0	36.6	40.9	66.0	8.1	41.9	65.8	45.5	23.9	0	0	329.7
1988-89	10.2	2.0	92.7	27.9	72.6	39.4	74.9	49.3	55.6	8.4	3.8	30.2	467.1
1989-90	6.1	25.4	41.9	12.4	36.3	16.0	48.0	45.0	54.4	17.8	9.4	19.3	332.0
1990-91	0	34.8	43.9	30.0	29.2	21.8	43.4	25.7	120.1	56.4	3.8	6.1	415.3
1991-92	0.8	22.6	106.2	24.6	24.4	34.0	21.6	32.8	5.1	22.9	44.2	19.8	358.9
1992-93	14.7	43.2	66.3	33.0	61.7	26.4	58.9	67.8	40.1	51.1	11.9	66.0	541.3
1993-94	0	7.6	12.4	48.5	60.5	42.4	13.2	30.0	73.2	19.1	8.4	1.8	317.0
1994-95	19.3	36.6	95.8	46.5	69.9	29.2	59.7	74.2	39.6	43.9	5.6	10.4	530.6
1995-96	23.6	34.3	74.9	60.2	70.9	62.2	37.8						
20-year avg. ‡	19.6	30.9	57.4	46.2	47.8	38.9	50.0	41.6	45.2	28.7	10.4	22.9	439.9

† By Wilkins et al. (1996).
‡ Year 1995-96 is not included in 20-year mean figures.

Table 2. Average monthly precipitation and Class A pan evaporation at the Columbia Basin Agricultural Research Center during the last 20-years (1975-1995)

Month	Precipitation	Evaporation
	(mm)	
Sept.	19.6	174.8
Oct.	30.9	94.2
Nov.	57.4	00.0
Dec.	46.2	00.0
Jan.	47.8	00.0
Feb.	38.9	00.0
Mar.	50.0	76.7
Apr.	41.6	124.5
May	45.2	167.4
Jun.	28.7	221.8
Jul.	10.4	294.6
Aug.	22.9	266.0
Total	439.9	2102.7

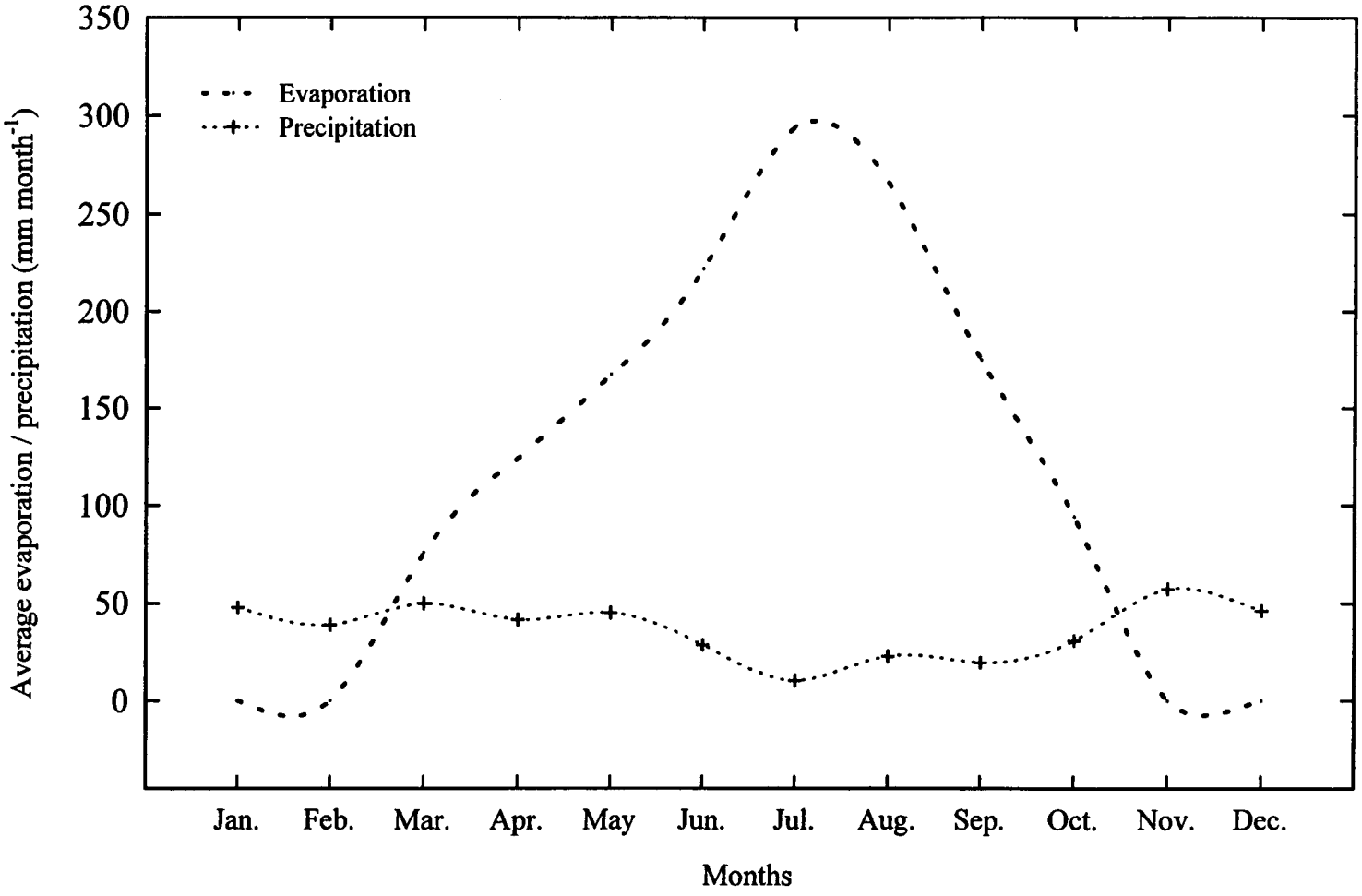

Figure 2. Average monthly evaporation and precipitation for Pendleton Agriculture Rsearch Center. Oregon (1971-1995).

TREATMENTS AND SAMPLING

Intact core samples were collected during the fallow season (6/95) from the long-term crop residue management plots located at the Columbia Basin Agricultural Research Center, Pendleton, Oregon. The plots have received different nitrogen fertilizer rates and crop residues for the last sixty years (Table 3). The strawy manure for the SM treatment consists of decomposed straw and manure obtained from a local ranch feedlot. The strawy manure is applied in late March.

Winter wheat (*Triticum aestivum* L.) is grown in a rotation fallow manner. The plots are plowed to 20 cm deep and smoothed with a field cultivator and tine harrow. Ammonium-based granular fertilizer was used for the first 40 years. Anhydrous ammonia has been used for the last 24 years. Nitrogen fertilizer is applied in October of the cropping year, 5 to 15 days prior wheat seeding. Anhydrous ammonia is injected in the gaseous or liquid form 20 to 25 cm below the soil surface. Wheat is seeded in early October and harvested in mid-July. Herbicides are used to control weeds during the cropping cycle. Wheat stubble is left undisturbed over winter. Weeds are controlled by tillage with a rod weeder, an implement with a horizontal rotating rod operated 5 to 7 cm deep, during the fallow cropping cycle. This is repeated three to four times between April and October to affect moisture conservation.

Soil cores were obtained with a power-operated hydraulic probe mounted on a four-wheel drive truck. The sampling tube that extracts the core from the ground had a diameter of 6 cm and a length of 120 cm. No compaction was observed during collection of cores. Drying of the soil core was reduced, by covering the intact cores with a plastic

film. The soil cores were sectioned with a knife at 2.5-cm-depth increments to 50 cm, and at 10-cm intervals thereafter. Soil samples were placed in paper bags lined with polyethylene to ensure moisture retention prior to analyses.

Table 3. Long-term residue management treatments.

Symbol	Description of management†	N addition‡		Total N applied for 64 years¶
		Ammonium	Ammonia	
		1931-1966	1967-present	
		--------- kg ha^{-1} yr^{-1} ---------		-------- kg ha^{-1} --------
C	Straw incorporated into soil (control)	0	0	0
SM	Straw plus 22 Mg ha^{-1} of strawy manure incorporated into soil	111§	111	3220
N-45	Straw incorporated into soil	34	45	1287
N-90	Straw incorporated into soil	34	90	1962

† All treatments moldboard plowed at the same depth.
‡ Organic N form was applied for SM treatment.
§ 56 kg ha^{-1} yr^{-1} of N was applied during 1942 to 1951, and no manure applied from 1943 to 1947.
¶ Only during cropping years.

METHODS AND MATERIALS

Physical Determinations

Soil Strength

Soil strength was determined in the field using a recording cone penetrometer (30-degree and a 10-mm diameter). Readings in bars (0.1 MPa) were recorded directly from the electronic display attached to the penetrometer. Six replicate penetrometer readings at 3.5 cm increments to a depth of 52.5 cm were used to calculate the mean soil strength for each treatment.

Bulk Density

The air-dried soil samples were oven dried at 105 °C until constant weights were reached. Oven-dried sample weights were recorded. Bulk density (ρ_b) was calculated based on Eq. [7]. Where r = 6 cm, and L = 2.5 cm.

$$\rho_b = m_s / \{\pi r^2 \times L\}. \ (Mg\ m^{-3}) \qquad \text{Eq. [7]}$$

Particle-Size Analysis

Air-dried soil samples were crushed and passed through < 2 mm sieve. Gravimetric water contents were determined by oven drying the samples at 105 °C for 24 h. Ten gram samples of air-dried soil were transferred into 250 mL plastic bottles. The samples were dispersed in a solution containing 10 mL of 5% sodium hexametaphosphate and 200 mL of distilled water by shaking for 12 h. The sand fraction was separated using a 53 μm sieve and transferred into tared empty glass beakers. The

sand fraction was oven dried at 105 °C. The volume of the suspension containing the silt and clay fractions was brought to 1 L with distilled water and was allowed to stand at 20 °C for several hours. The silt and clay fractions were then suspended by mixing and allowed to settle for 288 s., at which point a 20 mL aliquot was withdrawn from a depth of 10 cm using a vacuum pipette. The contents, containing fine and medium silt fractions, were transferred into pre-weighed vials and oven dried at 105 °C. After 8 h., a 20 mL aliquot of the clay fraction was collected and oven dried at 105 °C. The coarse silt fraction was calculated using Eq. [8] (Day, 1965; Green, 1981).

$$\% \text{ coarse silt} = 100 - (\% \text{ sand} + \% \text{ clay} + \% \text{ fine silt} + \% \text{ medium silt}). \quad \text{Eq. [8]}$$

Soil Core Descriptions

Soil color, texture, structure, consistence, roots, pores, pH, carbonates, and horizon boundaries were described (Appendix. 1) using the guidelines in the USDA Soil Survey staff (1993).

Soil Chemical Analyses

Soil pH

Soil pH values were measured in 0.01 *M* $CaCl_2$. Ten grams of air-dry soil was mixed with 10 mL of 0.01 *M* $CaCl_2$. The pH value of the 1:1 slurry was measured with a combination electrode connected to a digital pH meter.

Exchangeable H^+

A ten gram sample of air-dried soil was mixed with 20 mL of 0.5 *N* barium chloride ($BaCl_2$-$2H_2O$)-0.2 *N* triethanolamine (TEA) buffer solution and shaken for 30 min. The aqueous solution was separated from the soil by filtration through a No. 1 Whatman filter paper. The soil was leached with three additional 50 mL aliquots of $BaCl_2$ replacement solution. Two drops of greencresol and 10 drops of mixed indicator were added to the combined filtrates. The filtrate was titrated with 0.17 *M* HCl solution to a faint pink end point (A mL). A blank endpoint (B mL) was determined using 50 mL of buffer solution. The exchangeable hydrogen in cmol(+) kg^{-1} of each soil sample was calculated according to Eq. [9] (Thomas, 1982)

$$\text{Exchangeable } H^+ \text{ (cmol(+) kg}^{-1}\text{)} = \text{(B-A) x 0.17}M\text{ HCl / 10 g soil.} \qquad \text{Eq. [9]}$$

Water-Soluble Silica

Five grams of air-dried soil was placed in a 50 mL polyethylene centrifuge tube with 20 mL of de-ionized water. The suspension was shaken at room temperature (22 °C) for 2 h. The supernatant was separated by centrifugation at 788 x *g* for 30 min. Water-soluble silica was determined by a modified blue silicomolybdous acid

method by Weaver et al. (1968) as follows. A 50 μL aliquot of supernatant was transferred into plastic test tubes using an automatic pipette. The solution was diluted with 2 mL de-ionized H_2O. One milliliter of 2 *M* H_2SO_4 and 2 mL of 0.3 *M* ammonium paramolybdate tetrahydrate solution were added, respectively. The solution was shaken for 2 min. One milliliter of 20% tartaric acid and 0.2 mL of the ascorbic acid reducing agent were added. The solution was allowed to stand until a blue color developed. Water-soluble Si was measured at 820 nm using a diode array spectrophotometer equipped with an autosampler. The final concentration was reported in units of mg Si kg^{-1} soil.

Amorphous Silica

Ten milliliters of 0.5 *M* KOH was added to 0.50 g of soil sample in a polyethylene test tube. The soil suspension was heated to 85 °C and continuously mixed for 10 min., then centrifuged at 788 x *g* for 30 min. Twenty microliter aliquots of the supernatant were transferred into plastic tubes. The solution was diluted to a volume of 5 mL with de-ionized water and 0.5 mL 2 *M* H_2SO_4 and 1 mL of ammonium paramolybdate tetrahydrate solution were added, respectively. After 2 min. of shaking, 0.5 mL of 20 % tartaric acid and 0.1 mL of the ascorbic acid reducing agent were added. Silica was determined at a wavelength of 820 nm (Weaver et al., 1968) and reported as mg Si kg^{-1} soil.

Soil Mineralogical Analyses

X-ray Diffraction

The clay fractions were subjected to x-ray diffraction (XRD) analyses after Mg- and K-saturation, Mg-glycolation, and heat treatment at 110 °C. Air dried soil was crushed and transferred into a beaker and 500 mL of de-ionized water was added. The soil samples were dispersed by stirring in a blender followed by 3 min. of ultra-sonic probe dispersion. Samples were settled for 8-10 min. to isolate the (< 15 μm) soil fraction. The suspensions were centrifuged at 115 x *g* for 6 min. to separate the clay fraction (< 2 μm). The clay fraction was flocculated by washing three times with 0.5 *N* $MgCl_2$. Excess salt was removed by rinsing the clay three times with distilled water. The suspension was centrifuged at 1085 x *g* for 10 min. The clay fractions were Mg-saturated by adding 20 mL 1 *N* $MgCl_2$ to the settled clay fraction in polyethylene centrifuge tube. The clay suspension was shaken for 10 min. and then centrifuged at 12,062 x *g* for 10 min. Excess salt was removed by rinsing with deionized water. The last three steps were repeated for three times. A portion of the clay was smoothly smeared onto a glass slide using a micro spatula (Theisen and Harward, 1962). The specimens were placed in a desiccator at 54% R.H. (relative humidity). The clay fractions remaining in the centrifuge tubes were then saturated with 1 *N* KCl using the same procedure used for the $MgCl_2$ solution. The samples were step scanned using an automatic Philips 3100G diffractometer with a focusing monochromometer (Cu Kα radiation) at angles from 2° to 14° or 34° and (0.02°/step, /second). The digital XRD patterns were interpreted with the aid of JADE analytical software. Clay minerals were identified based on the criteria used by Glasmann and Simonson (1985).

Scanning Electron Microscopy

Undisturbed fresh-fracture surfaces of soil specimens were obtained from the soil core and mounted on aluminum stubs using Duco cement. Non-essential surfaces of the specimens were painted with colloidal carbon to reduce charging. The specimens were coated with 20 nm of 60/40 wt % Au/Pd alloy in a vacuum evaporator at 1 x 10^{-5} Torr. Images were recorded on a Polaroid 55 positive/negative 10 x 12.5 cm format film using an AMR 1000 SEM equipped with Kevex X-ray elemental analyzer.

Electron Microprobe Analysis

Soil samples of 1 cm^2 were impregnated with resin under vacuum. Impregnated soil samples were allowed to air dry for several days. The solidified samples were polished using lap wheels impregnated with 600 Grit, 3 μm, 1 μm aluminum, 1 μm diamond, and 15 mμ rings respectively. The samples were coated with carbon and analyzed under 15 kV accelerating voltage and 30.1 μA beam current using SX-50 Cameca probe. A counting time of 10 sec (peak) and 5 sec (each side of background) was used for all elements.

Soil Thin Sections

Undisturbed soil peds of approximately 3 cm^2 were impregnated with polyester resin. Prior to resin impregnation, water in the samples was replaced by acetone. The peds were allowed to stand in a hood for several days. After the initial solidification, they were hardened by oven drying at 45 °C. Soil thin sections were prepared by Spectrum Petrographics, Inc. The thin sections were examined with a petrographic light

microscope under plane polarized and crossed polarized light. The micromorphological terminology of FitzPatrick (1993) and Brewer and Sleeman (1988) was used to describe the prominent features observed in thin sections.

RESULTS AND DISCUSSION

Physical Properties

Bulk density and penetrometer load values were similar for all treatments (Fig. 3 and 4, respectively). Bulk densities reached maximal values (1.2 to 1.3 Mg m^{-3}) at a depth 20 to 25 cm (Fig. 3). Penetrometer load measurements increased rapidly and reached maximal values of 1.7 to 2.2 MPa at a depth 20 to 30-cm (Fig. 4) then decrease thereafter. Treatment N-90 has relatively lower maximal penetrometer values than the other treatments. Maximal bulk density values obtained in this study are significantly lower than fragipans, which typically have bulk densities ranging from 1.6 to 2.1 Mg m^{-3} (Lindbo and Veneman, 1993). However, our maximal bulk density measurements are higher than values of some till-derived pans of the Olympic peninsula reported by Wilson et al. (1996). The increase in bulk density at the 20 to 25 cm depth is consistent with the formation of a pressure pan due to plowing (Allmaras et al., 1982; Douglas et al., 1984).

Penetrometer load values (1.7 to 2.2 MPa) are higher than one would expect based on the bulk density values (Douglas et al., 1984). Although bulk density is only moderately higher in the zone below the plow layer (20 to 25 cm, Fig. 3), soil strength measured by penetrometer values, is quite high (Fig. 4). Data from other pan-related studies indicates that maximal penetrometer load values of the Walla Walla silt loam soil can not be attributed to the presence of a pressure pan alone (Allmaras et al., 1982). Francis and Kladivko (1989) reported penetrometer loads of less than 1.0 MPa and bulk density of 1.3 Mg m^{-3} at depths of 20 to 30 cm for a Mollisol under long-term moldboard

tillage. In another study, Bauder et al. (1981) found penetrometer load values of 1.4 MPa and bulk density of 1.2 Mg m^{-3} at the zone of 20 to 30 cm of a Mollisols under moldboard tillage.

Clay percentages for the Walla Walla silt loam decrease linearly from a depth of 0 to 40 cm for all treatments (Fig. 5). The same trend has been reported by Norgren (1973) and Douglas (1956) for the Walla Walla soil series. The highest clay abundance occurs in the Ap layers of the profiles. Clay percentage declines as the penetrometer resistance readings reach their maximal values. Obviously, the high soil strength is unrelated to clay accumulation. Particle size analysis results in Appendix 1 show that all four treatments had similar and uniform silt loam texture throughout the profile, indicating that all four sites were similar prior to cultivation.

Pikul and Allmaras (1986) measured organic C content in these Walla Walla silt loam soils and found low values with no significant accumulation at the plow zone. These soils contain about 0.8 to 1.8 % of organic C for the first 40 cm depth (Pikul and Allmaras, 1986). This implies that the observed high strength zones are not cemented by illuviation of metal-humus complexes. The above statements do not offer conconclusive evidence, but suggest the presence of a kind of cementing substance in the 20 to 30 cm-zone.

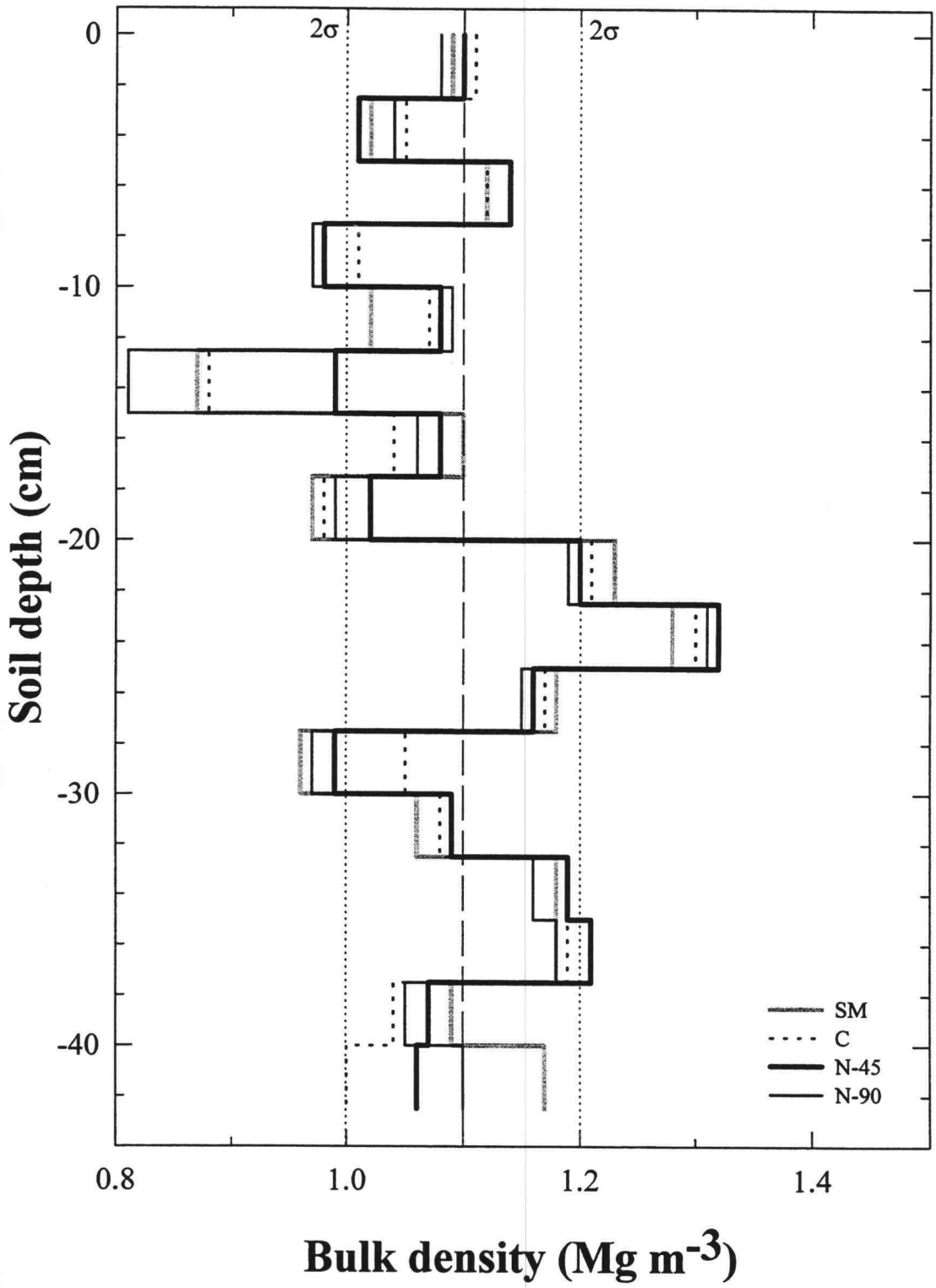

Figure 3. Bulk density as a function of depth with 2σ confidence intervals.

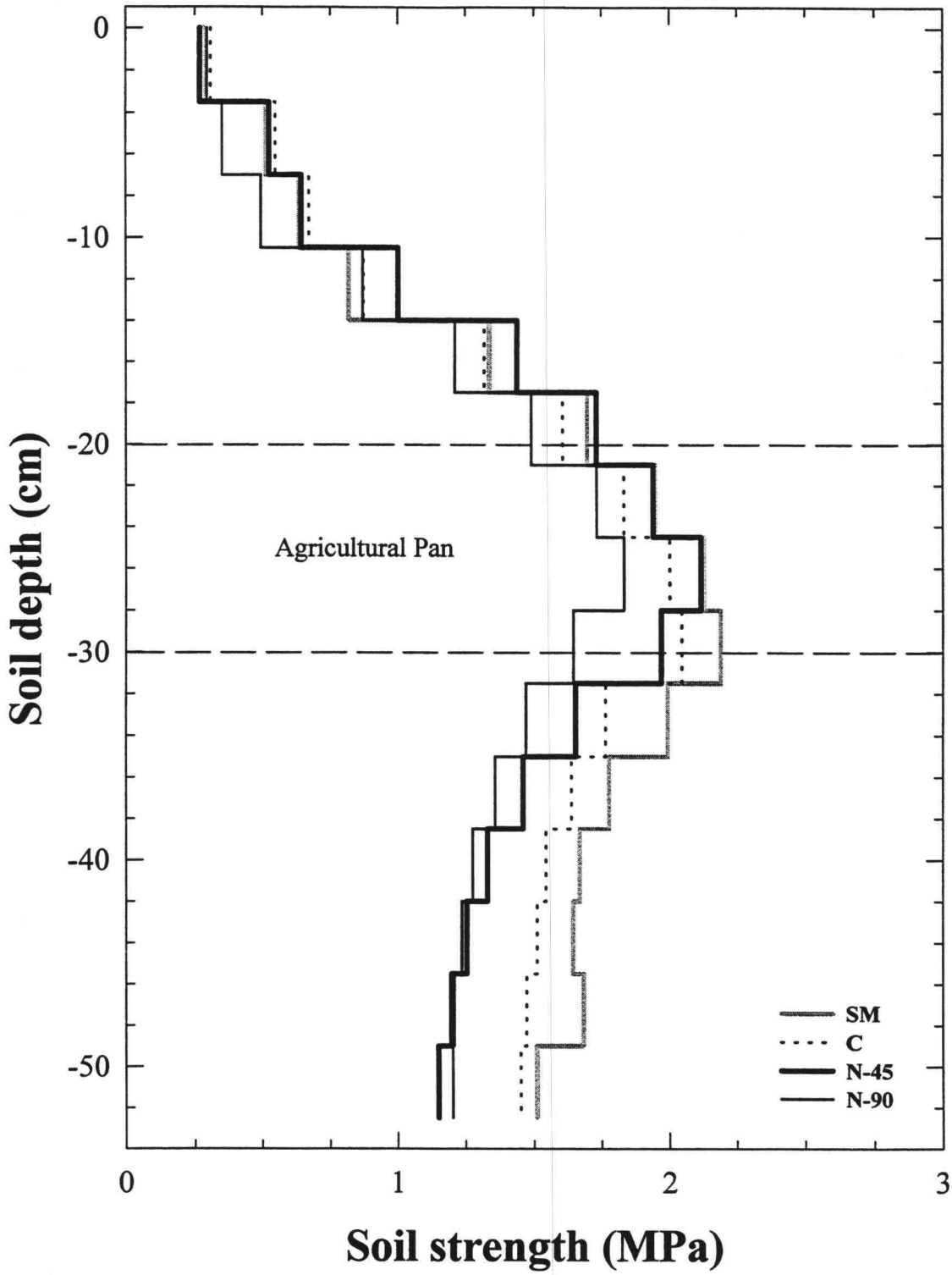

Figure 4. Penetrometer load values (soil strength) as a function of depth.

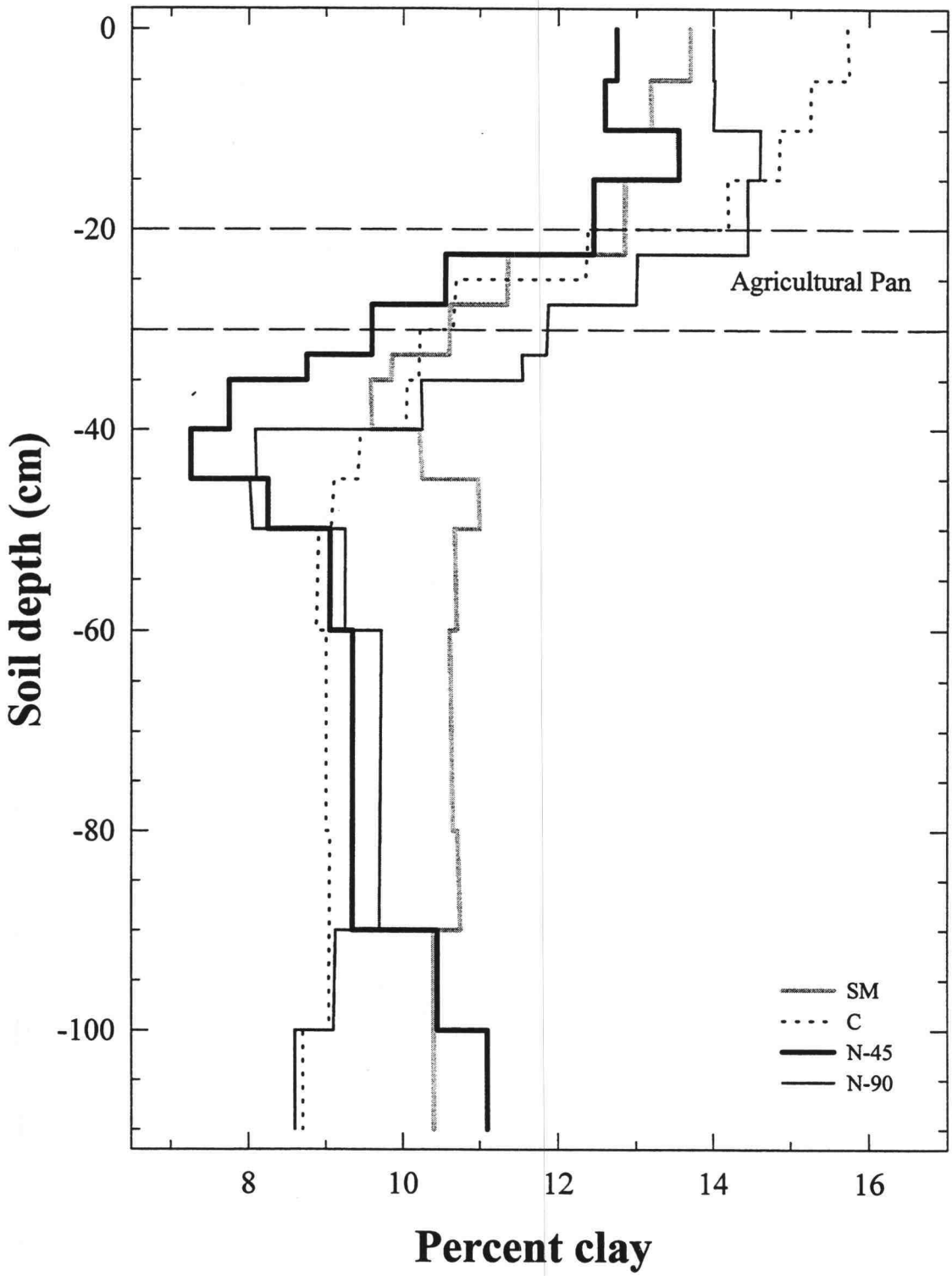

Figure 5. Clay percentage as a function of depth.

X-ray Diffraction

X-ray diffraction analyses of the clay fraction (< 2 μm) show the presence of crystalline vermiculite, kaolinite, illite, smectite, chlorite, and chlorite intergrade. A diffuse broad X-ray diffraction band centered at approximately 3.3 Å suggests the presence of amorphous Si in all of the management treatments (Appendix. 2). Similar clay fraction components were detected by Dudas (1973) for a Meadowood profile developed under Mt. Mazama ash. Representative XRD patterns with depth are shown in Figure 6. No major differences in the qualitative nature of the clay mineral assemblages were detected with depth among the treatments. The C3 horizon, however, is enriched in smectite and kaolinite relative to other horizons (Fig. 6). The similarity in clay mineralogy with depth suggests that the profiles are not stratified with respect to clay mineral assemblages, even though the Ap horizon is slightly enriched in total clay (Fig. 5). The Ap and AC horizons clays are dominated by mica and amorphous material, while kaolinite, smectite and choloritic intergrades as minor impurities (Fig 6ac). The C1 and C3 horizons are more smectitic but contain less amorphous material (Fig. 6de)

Figure 6. Representative X-ray diffraction patterns for the N-45 management plot: (a) Ap horizon; (b) Si-enriched zone (30-35 cm); (c) AC horizon; (d) C1 horizon; and, (e) C3 horizon. [Clay specimens were analyzed using: (1) Mg-ethylene glycolation; (2) Mg-54% R.H.; (3) K-54% R.H.; and, (4) K-110 ^{o}C].

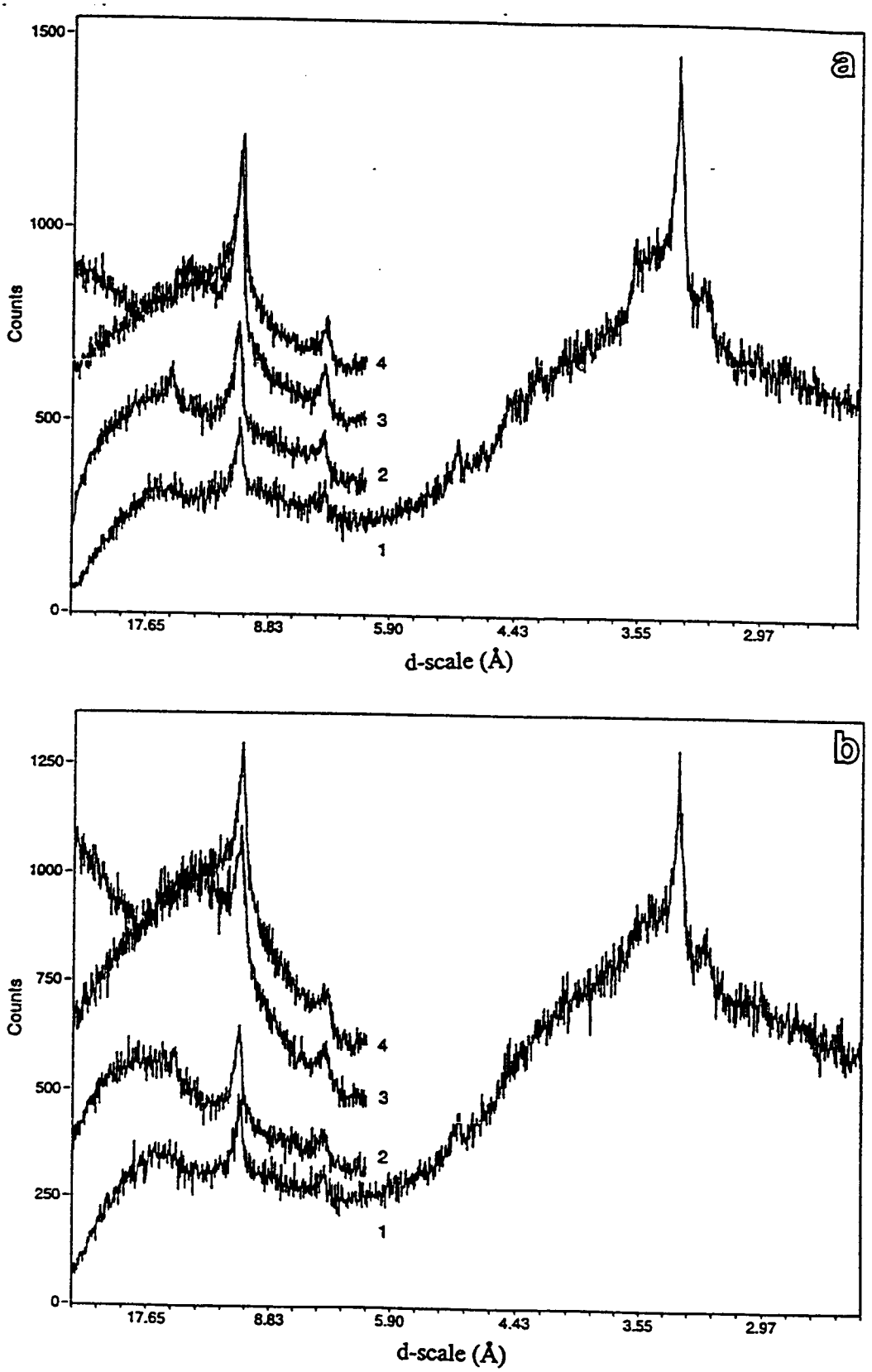
a
1500
1000
500
0
Counts
4
3
2
1
17.65
8.83
5.90
4.43
3.55
2.97
d-scale (Å)
b
1250
1000
750
500
250
0
Counts
4
3
2
1
17.65
8.83
5.90
4.43
3.55
2.97
d-scale (Å)

Figure 6.

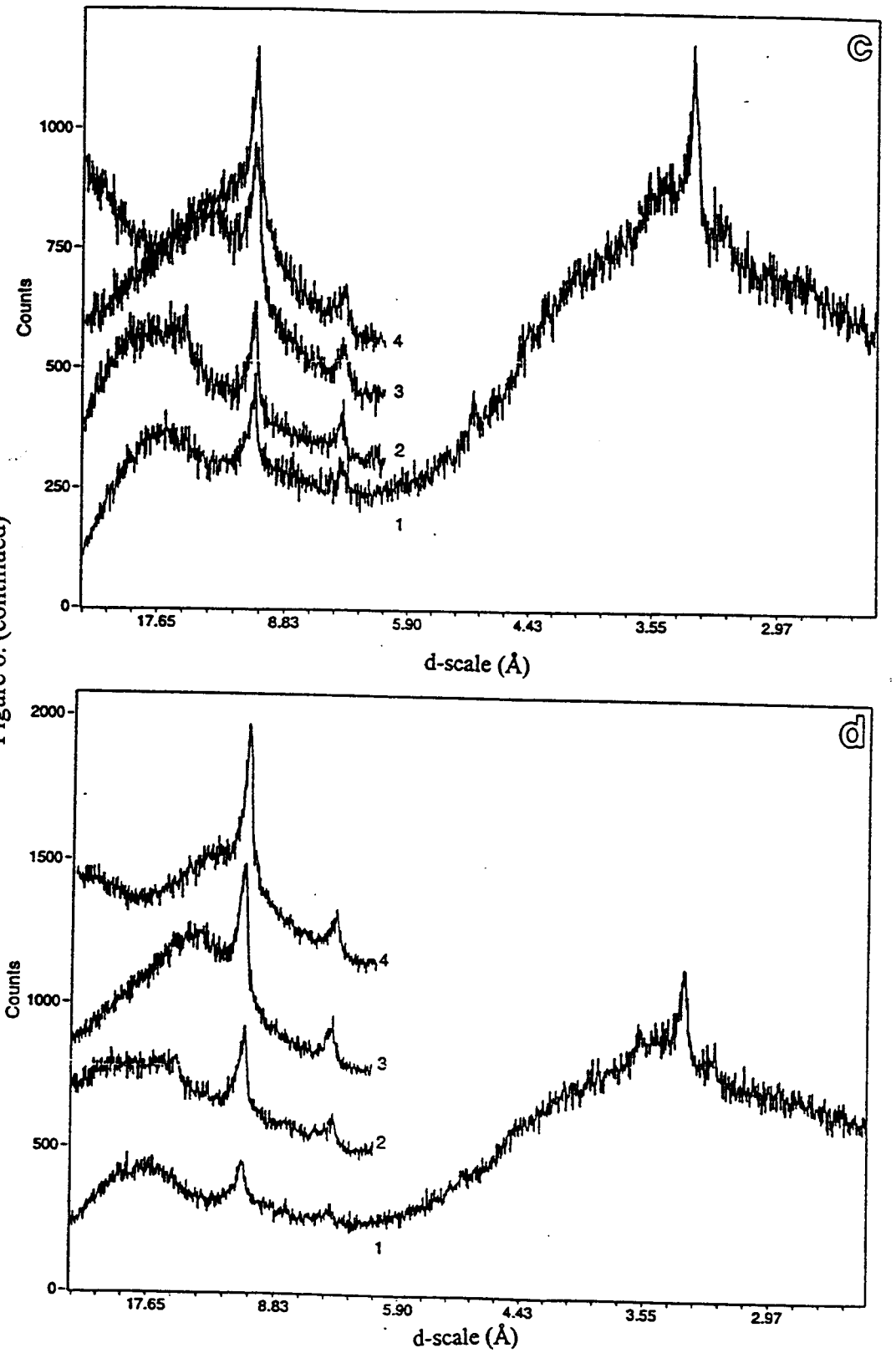

Figure 6. (continued)

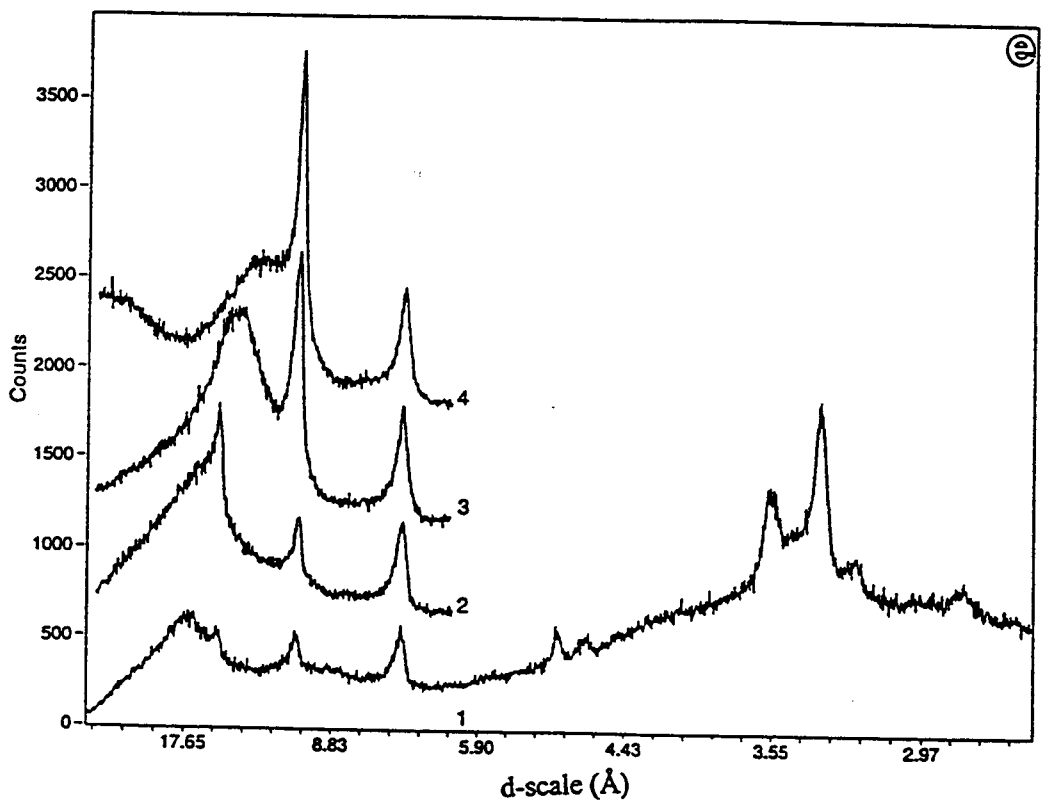

Figure 6. (continued)

Amorphous Silica

Amorphous Si concentrations, as determined by extraction with KOH, were greatest in the upper 20 cm of the soil profile for all management treatments (Fig. 7). Below 20 cm the concentrations of amorphous Si declines rapidly and reaches a more or less constant values with depth. The subsoil (< 30 cm) concentrations of amorphous Si is approximately 50 % less then the surface horizons. Treatment SM shows a relative increase in amorphous Si at depth 35 to 48 cm. Based on the data in Figure 7, the accumulated amount of amorphous Si in the profile can be estimated by integrating the concentration to a depth of 1 m (1×10^5 kg ha^{-1}).

An estimate of the amount of amorphous Si produced by the production of wheat phytoliths was obtained for each treatment, using average straw yield values (Table 4). Wheat straw contains 45 g SiO_2 kg^{-1} dry wt (Kowalski and Davies, 1982), while grain contains only 0.1 g SiO_2 kg^{-1} dry wt (Lanning and Eleuterius, 1992). An estimate of the average phytolith SiO_2 produced by the treatments can be obtained from the above values. Approximately 280 kg ha^{-1} yr^{-1} of amorphous wheat phytolith SiO_2 is produced during the cropping cycle. At this rate, the estimated cumulative production of amorphous phytolith Si is 8,900 kg Si ha^{-1} for the 64-years cropping period (Table 4). The estimated cumulative amount of amorphous Si constitutes only 9 % of the total (1×10^5 kg ha^{-1}) measured amorphous Si (Figure 7). This suggests most of the amorphous Si in the surface horizons originated from sources other than wheat vegetation.

Table. 4. Cumulative amorphous phytolith Si in straw yield after 64-years of wheat cultivation.

Treatment	Straw yield†	Amorphous phytolith Si	Cumulative Amorphous phytolith Si‡
	---------- kg ha^{-1} yr^{-1} ----------		---------- kg ha^{-1} ----------
C	4748	212	6784
SM	7520	338	10816
N-45	6128	274	8768
N-90	6428	288	9216

† Based on Rasmussen and Parton (1994).
‡ Only during cropping years.

Agricultural Soil Acidity

Soil pH and exchangeable acidity are indirect measures of the amount of biogeochemical weathering that has taken place. Soil pH values measured in the plow layer for treatments N-45 and N-90 are lower than for the control (Fig. 8). This dramatic shift in pH after fertilization is attributed to the nitrification of applied N fertilizer (Eq. 1). Similar observations have been reported by Brown and Mahler, 1988; and Douglas et al., 1984. Allmaras et al. (1982) reported that NH_4^+ fertilization reduced soil pH values to depths as great as 60 cm.

Soil pH of treatment N-45 was slightly lower in the upper 20 cm when compared to treatment N-90, although the latter had been treated with higher rates of N fertilizer. This unexpected result may be due to natural soil variability or to a higher native organic matter content for treatment N-45 prior the experiment (Rassmusen, 1996, Personal communication). Treatment SM yielded the highest soil pH (Fig. 8). Although the nitrogen application rate of treatment SM exceeded both treatments N-45 and N-90 (Table. 3), the addition of "basic" cations in the strawy manure appears to counteract acidification produced by nitrification. Soil pH for all treatments converge near neutrality at a depth of 1 m consistent with the presence of $CaCO_{3(s)}$.

Exchangeable acidity distributions presented in Figure 9 are consistent with the amount of N added except for the SM treatment. Total exchangeable acidification increased with N application rate. Treatments N-45 and N-90 have become more acidic on the surface with a sharp transition in acidity to the more alkaline subsoil material below. Exchangeable acidity values of the plow layer for treatment N-90 were slightly higher than those of N-45. This is directly attributable to the rate of N applied (Table. 3).

Exchangeable acidity for treatment C is lower in the Ap zone than those of N-45 and N-90 treatments. The SM treatment contains components of acidity and alkalinity which makes it difficult to explain its exchangeable acidity distributions.

Protons produced by nitrification of N applied appear to not be neutralized by the H^+ balancing system, i.e. the amount of H^+ added and removed from the soil-plant system. As a result the protons displaced exchangeable bases and increased exchangeable acidity in the surface horizons. The displaced bases may then be leached as companion cations to NO_3^-. Addition of anhydrous ammonia fertilizer increases the release of cations from the Ap layer of the Walla Walla soil (Douglas, 1984). Cation leaching was also observed with Canadian soils acidified by anhydrous NH_3 application (Bouman et al., 1995). A proton balance for 64 years of N fertilization was constructed by estimating the change in exchangeable acidity relative to the C treatment, Zero-N (Table 5). It was assumed that acidification was confined to the upper 1 m depth and no significant amount of H^+ was lost from the soil by leaching. The maximum possible proton production from nitrification (i.e., 1 mol H^+ mol^{-1} N) is 135, 184, and 230 kmol H^+ ha^{-1} for the N-45, N-90, and SM treatments, respectively. (The amounts of N in shoots/straw were returned to the soil and thus do not need to be accounted for in terms of the proton balance). Acidification due to "basic" cation removal in grain was estimated to be 6, 7, and 10 kmol ha^{-1} for N-45, N-90, and SM treatments respectively. Actual proton production (measured acidification, Fig. 9) for N-45 and N-90 N treated soils compared well with the predicted acidification values (Table 5). The predicted acidification for SM treatment, however, was much higher than the measured one. "Basic" cations derived from the 22 Mg ha^{-1} yr^{-1} straw application may counteract acidification from N fertilization.

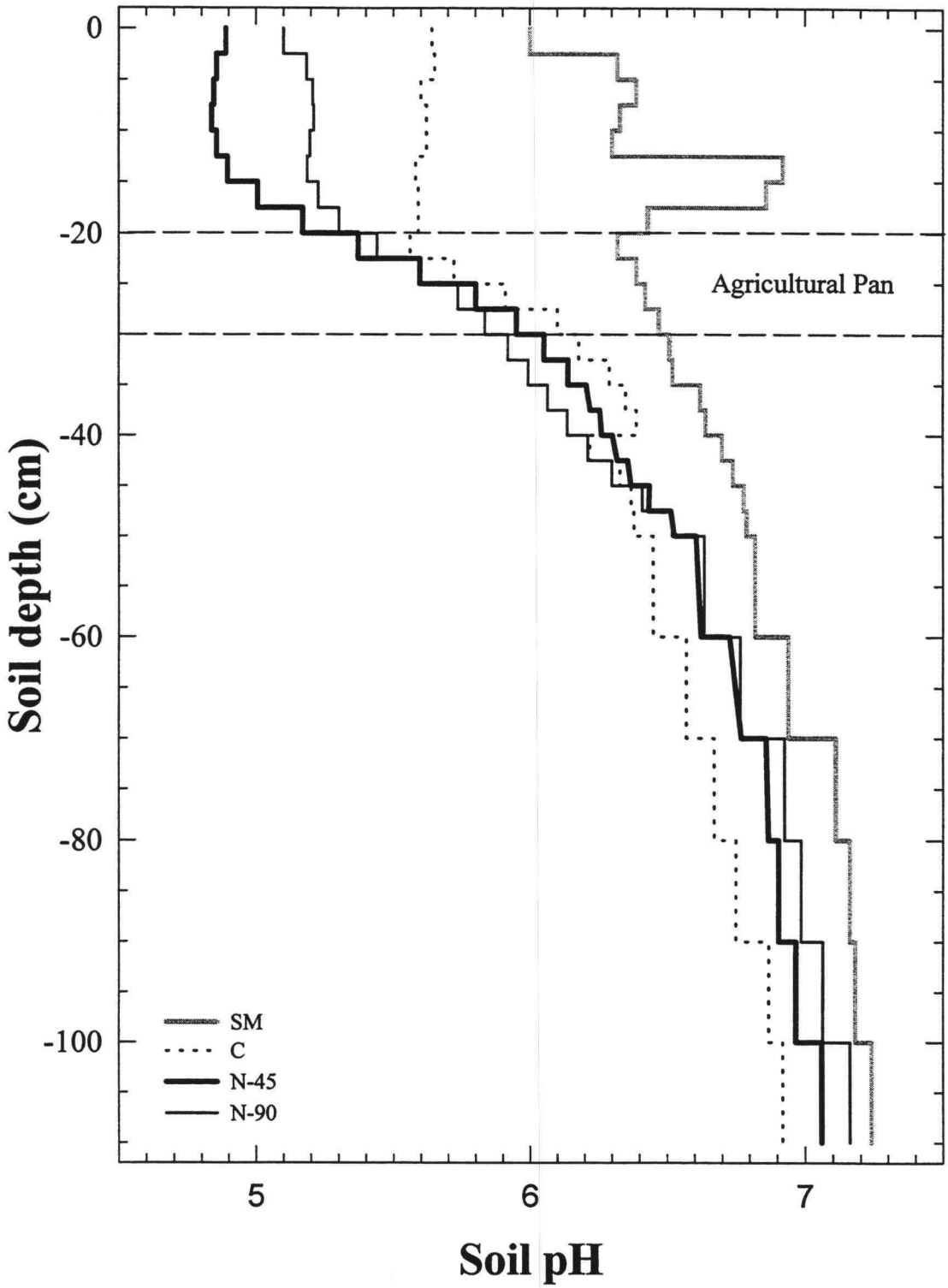

Figure 8. Soil pH values as a function of depth.

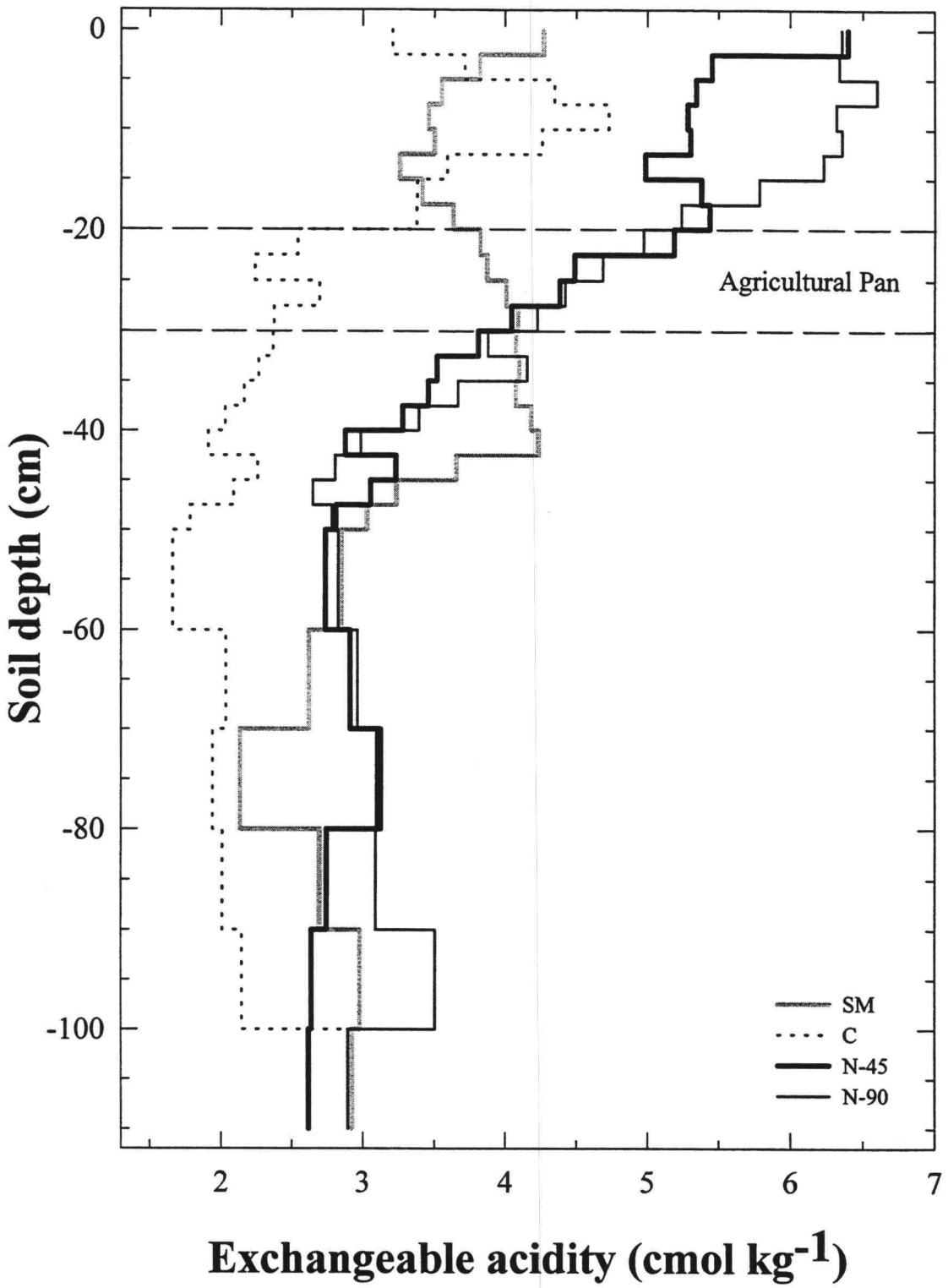

Figure 9. Exchangeable acidity by depth for treatments.

Table 5. Proton budget for N-45, N-90, and SM treatments receiving N fertilizer for 64 years.

	N-45	N-90	SM
	---------- kmol H^+ ha^{-1} ----------		
Potential acidification† (a)	135	184	230
Protons neutralized by plant uptake of NO_3^-‡ (b)	35	51	81
Excess base export§ (c)	6	7	10
Predicted acidification (a + c -b)	106	140	159
Measured acidification¶	132	167	92

† Potential acidification was estimated assuming that all N fertilizer was oxidized to NO_3^-, with production of 1 mol H mol^{-1} N.

‡ Estimated, based on Rasmussen and Parton (1994) data, as the difference between fertilized and the C treatment (zero-N).

§ Calculated based on grain yield provided by Rasmussen and Parton (1994) and on "basic cations" (K, Mg, Na, and Ca) content in wheat grain estimated by McGrath (1985) and Troeh and Thompson (1993).

¶ Were expressed on an area basis (i.e., kmol H^+ ha^{-1}) using bulk density values to convert from gravimetric units.

Water-Soluble Silica

The concentrations of water-soluble silica (Si_w) are at their lowest values in the Ap horizons for treatments N-45 and N-90 (Fig. 10). Soluble Si concentrations of N-90 is even lower than Si_w concentrations of N-45. The SM treatment has the highest Si_w concentrations in the Ap layer. Water-soluble Si concentrations for treatments SM, N-45, and N-90 reach maximum values within the depth range of 20 to 45 cm. The maximum Si_w values for these treatments are below the Ap and within the agricultural-compacted pans (Fig. 10). Moreover, the maximum Si_w zones occur just below the horizons with the greatest amorphous Si concentrations (Fig. 7). Treatment C has a relatively constant Si_w distribution and lacks an apparent maxima in Si_w concentration.

Variation in Si_w distributions for the various treatments is due to the type of agricultural management applied into the plots (Table 3). This is because the parent material of all plots is a uniform loess deposit with a similar particle size distribution (Appendix 1), qualitative and quantitative clay mineralogy (Fig. 6), and distributions of amorphous Si (Fig. 7).

The amount of N fertilizer applied and the addition of strawy manure as the major agricultural field practices appear to influence Si_w distributions in the Walla Walla silt loam soil. Surface acidification of the Ap horizons for treatments N-45 and N-90 (Fig. 8; Fig. 9) enhances pedogeochemical weathering of silicate materials found in these soils. The N-90 treatment has the lowest Si_w concentration in the Ap layer. Possible explanations for these observations include: (i) the long periods of intensive weathering due to high N application may have caused more Si_w to be released into soil solution where it is then leached into subsurface horizons. Although the experimental site is

located in a region characterized by potential net annual moisture deficit, the possibility of Si leaching in years with above-average precipitation can not ruled out, or when rainfall distribution is such that large amounts come in short periods. Bouman et al. (1995) reported N leaching beyond 150-cm depth on soils (south Canada) characterized by mean annual precipitation of only of 355 mm, and potential evaporation of 635 mm. Campbell et al. (1993) have conclusively shown this to be the case under even more arid conditions at Swift Current in Saskatchewan; and/or, (ii) much of the released Si_w by weathering may be absorbed by wheat on the higher yielding N-90 treatment plot. The highest Si_w concentrations found with the SM treatment, in the Ap layer, is likely due to the added strawy manure which contributed to the total Si_w measured.

The annual Si_w released into soil solution was estimated by integrating the values for water soluble Si in Figure 10 to 1 m. Values of 11, 12, 9, and 13 kg Si_w ha^{-1} yr^{-1} for the C, N-45, N-90, and SM, respectively were obtained. The average of the annual estimated Si_w represents only 0.7 % of the total solid forms of amorphous Si. This observation suggests the presence of a large pool of amorphous Si which can be weathered to soluble Si_w under appropriate soil environmental conditions.

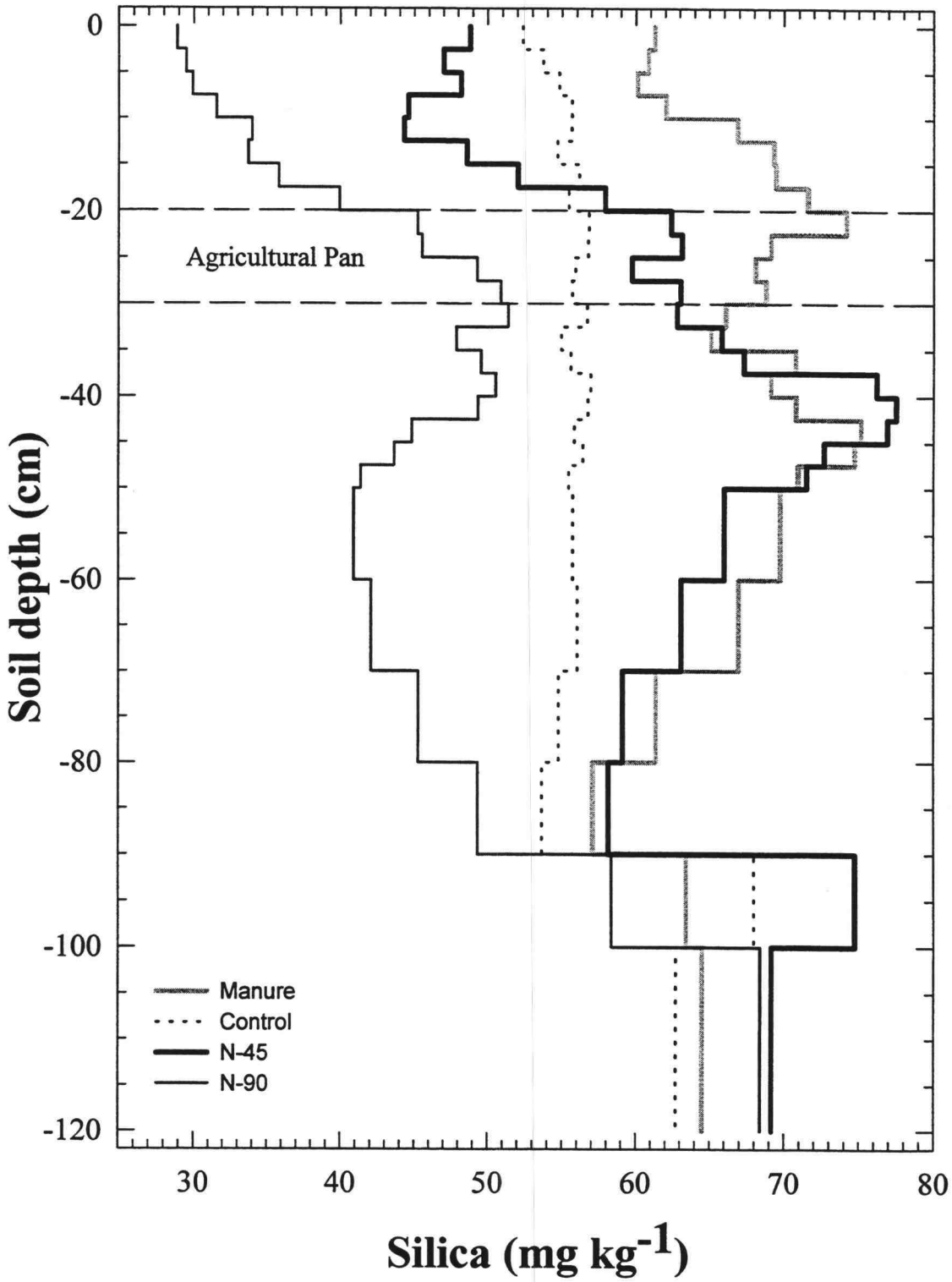

Figure 10. Water-soluble Si concentration as a function of depth.

Silica-Enriched Pan Micromorphology

A close examination of soil peds from the maximum Si_w zone by a combination of optical and electron optical techniques revealed the occurrence of high density soil fabric with a well packed Si-enriched silty matrix (Fig. 11b). The silt particles of this layer are coated with silicate gel-like materials. This material appears to coat the pore-space between the soil grains. The same phenomenon was observed within the maximal Si_w zone of the SM treatment. Layers above and below the Si-enriched zone were less dense and characterized by loose fabric and the absence of Si coatings (Fig. 11ac, respectively). These data implicate Si_w as a potential cementing agent in these soils. Weathering of the Ap amorphous Si pool (Fig. 7) is the likely source of Si_w which results in the Si-enrichment of the subsurface horizons. Accumulation and precipitation of weathered amorphous Si appears to take place at zones below the Ap layer (20 to 45 cm deep).

A comparison of soil fabric in terms of density and extent of packing was made between samples from the zone of maximal Si_w accumulation and the control. Treatment C has loose fabric and absence of a detectable Si-coated matrix (Fig. 12c) compared to the SM and N-45 treatments, respectively (Fig. 12ab).

Highly resolved images of the maximum Si_w concentrated zones show the occurrence of a web-like network with narrow bridges of silicate materials formed between soil grains (Fig. 13). Wilson et al. (1996) found a thin web-like network of amorphous aluminosilicate cements in pan-affected soils of the Olympic Peninsula, Washington. The silicate features observed in the Walla Walla soil are characterized as weakly developed or incipient cements (Fig. 13ab). The features are generally very thin

(< 0.25 μm) and are difficult to resolve during microanalysis due to sample topography, associated with clays, and the occurrence of other silicate materials. Loose fabric and absence of detectable Si bridges in the C treatment (Fig. 14abc) correlate well with the low Si_w concentrations measured relative to the N-45 and SM treatments (Fig. 10). No obvious differences in the X-ray diffraction traces between the Si-enriched zone (Fig. 6b) and the surface and subsoil horizons were found (Fig. 6acde). This suggests that an amorphous Si is the mineral solid responsible for the formation of bridges or coatings in the Si-enriched zones, rather than a well-ordered, mineral phase. Physical measurements, including penetrometer load and bulk density, may not be sensitive enough to detect the differences in strength in the weakly Si-cement features. More sensitive techniques, for example, Vane shear resistance may help identify the variability in strength produced between treatments.

The degree of visible porosity observed in soil thin sections for S-enriched horizons was compared to adjacent layers. Few fine irregular pores and dense peds were observed in the Si-enriched layer (Fig. 15b). The layer has a low saturated hydraulic conductivity of approximately 2×10^{-7} m s^{-1} (Douglas et al., 1984). Precipitated Si appears to fill the large voids, leading to lower values of the total porosity and hydraulic conductivity (Fig. 15b). Pikul and Allmaras (1986) reasoned the low hydraulic conductivity found in some Walla Walla soils in the long-term residue plots was a result of Si coatings on mineral grains.

Visible porosity was higher in both layers adjacent to the Si-enriched layer (Fig. 15ac). The surface Ap layer has more large pore at the expense of the small pore porosity (Fig. 15a). This is due to the loose fabric created soil moisture conservation tillage

practices. Surface tillage practices preferentially create large pores (Mark et al. 1990). Layers below the Si cemented zone contained more medium pore-space (Fig. 15c).

Figure 11. Scanning electron photomicrographs depicting the variation in fabric of different layers within N-45 management treatment: (ac) lower fabric density with loose silt particles of layers above (Ap 18.5-21 cm) and below (C2 50-52.5 cm) the Si-enriched layer respectively; and, (b) Si-enriched layer at AC(27.5-30 cm) with high density silty fabric coated by gel-like Si materials.

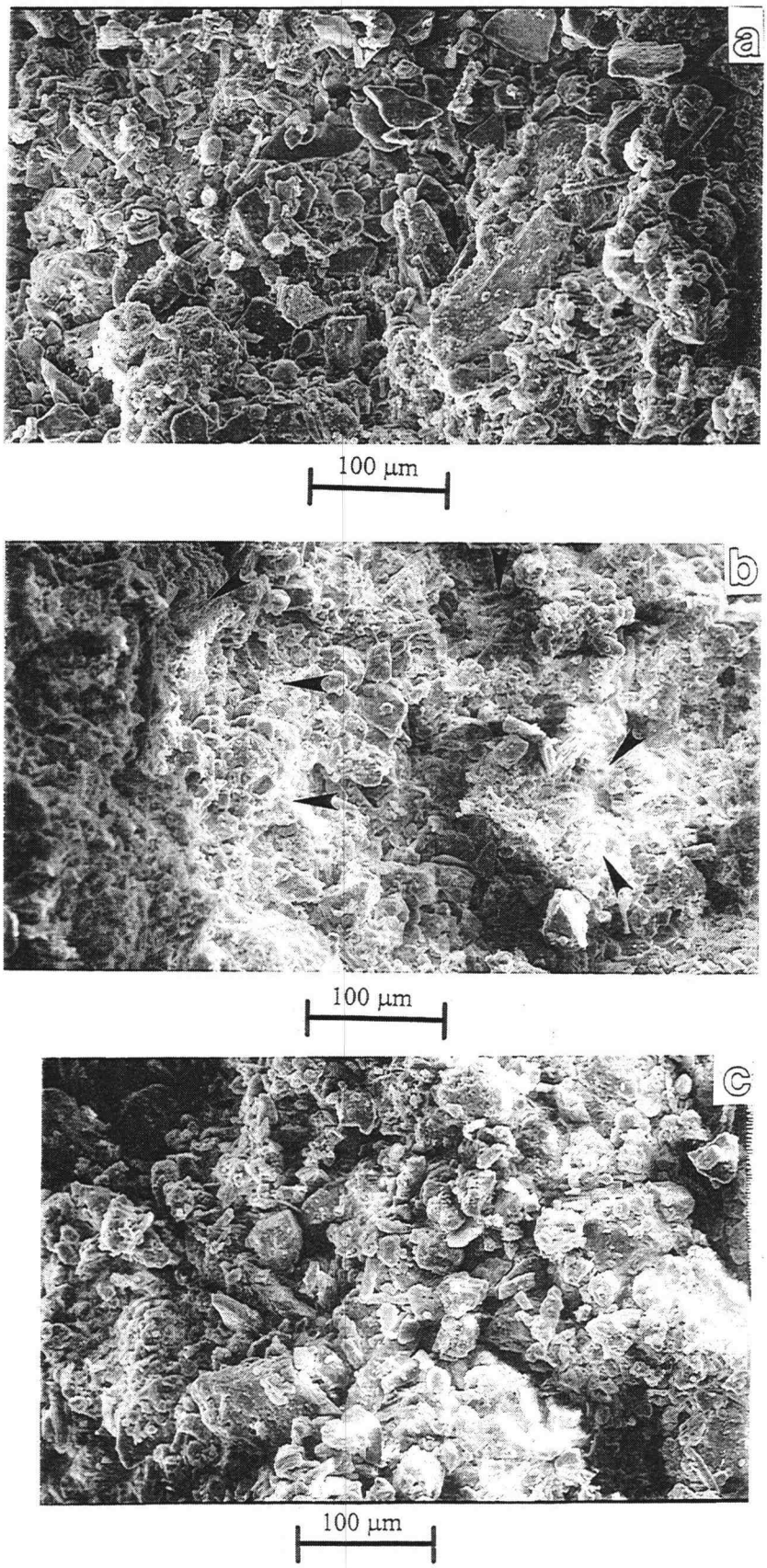

Figure 11.

Figure 12. Scanning electron photomicrographs showing fabric variability among treatments: (ab) high density fabric with well packed and Si-enriched silty matrix of treatments SM at AC (33-35.5 cm) and N-45 at C1 (40-42.5 cm); and, (c) loose fabric and absence of detectable Si-coated matrix of the C at AC (27-29.5 cm).

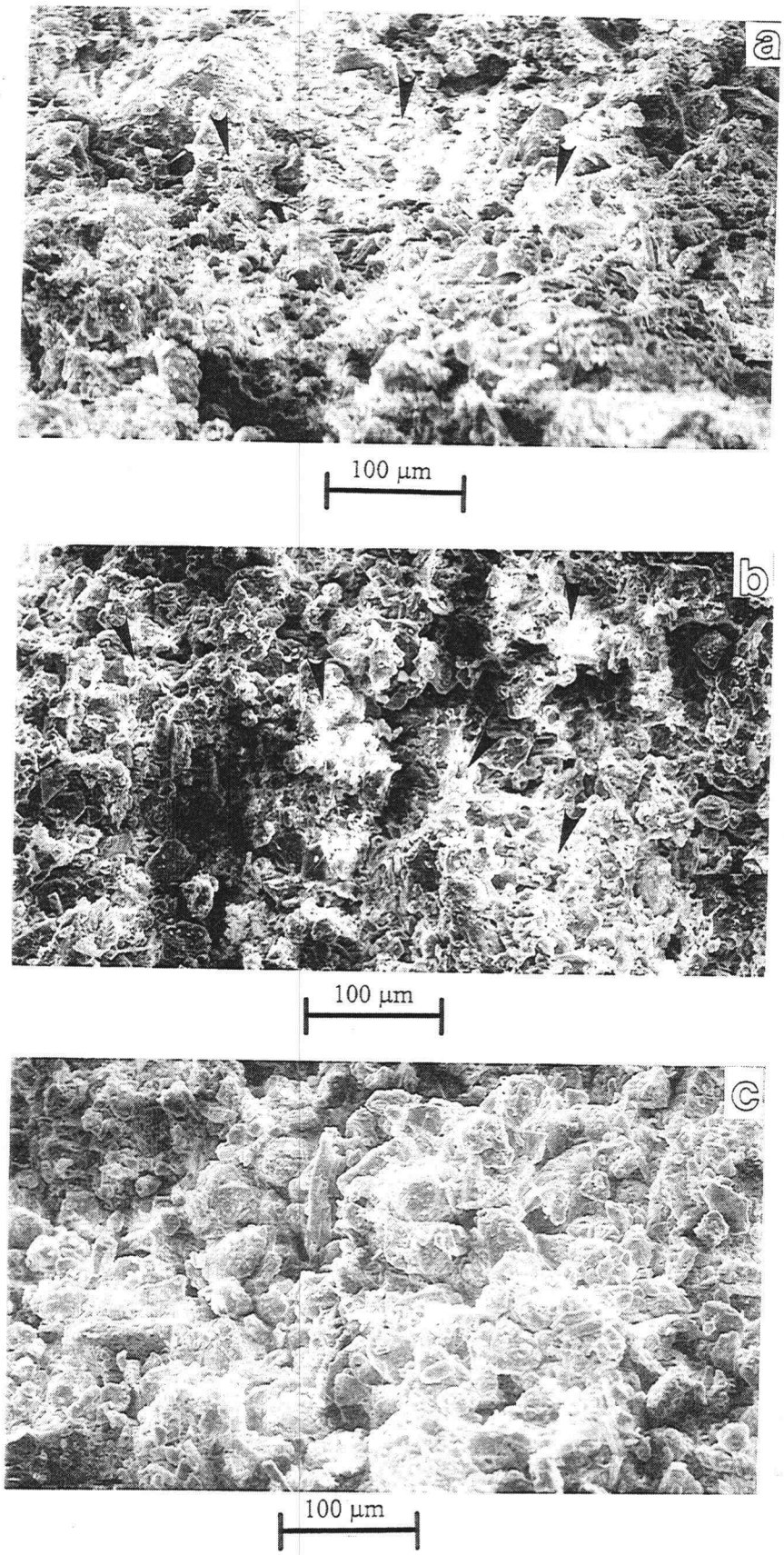

Figure 12.

Figure 13. Weakly-cemented grain bridging by pedogenic Si as observed by scanning electron photomicrographs: (a) silty grains bridged by narrow amorphous forms of Si material (SM [AC (33-33.5 cm)]); (b) incipient accumulation of web-like network of clay mantled by amorphous Si. Gel forms small ridges on adjacent grains suggesting dehydration of gel coat (N-45 [C1 (40-42.5 cm)]); and, (c) Si-cemented bridge between opal phytolith and the adjacent soil grains (SM [AC (33-33.5 cm)]).

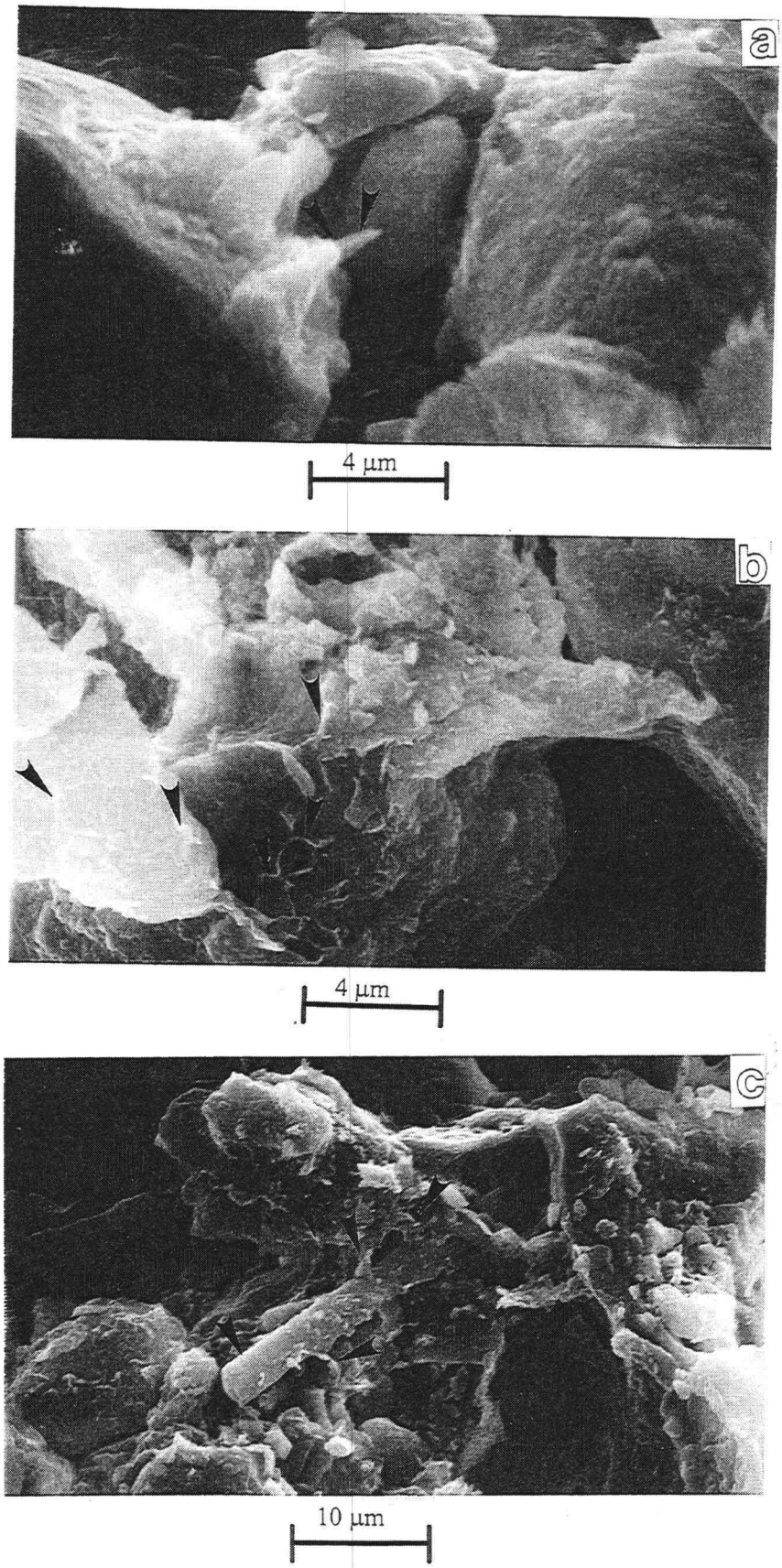

Figure 13.

Figure 14abc. Representative scanning electron photomicrographs for management treatment C showing absence of detectable Si bridges or cementation features.

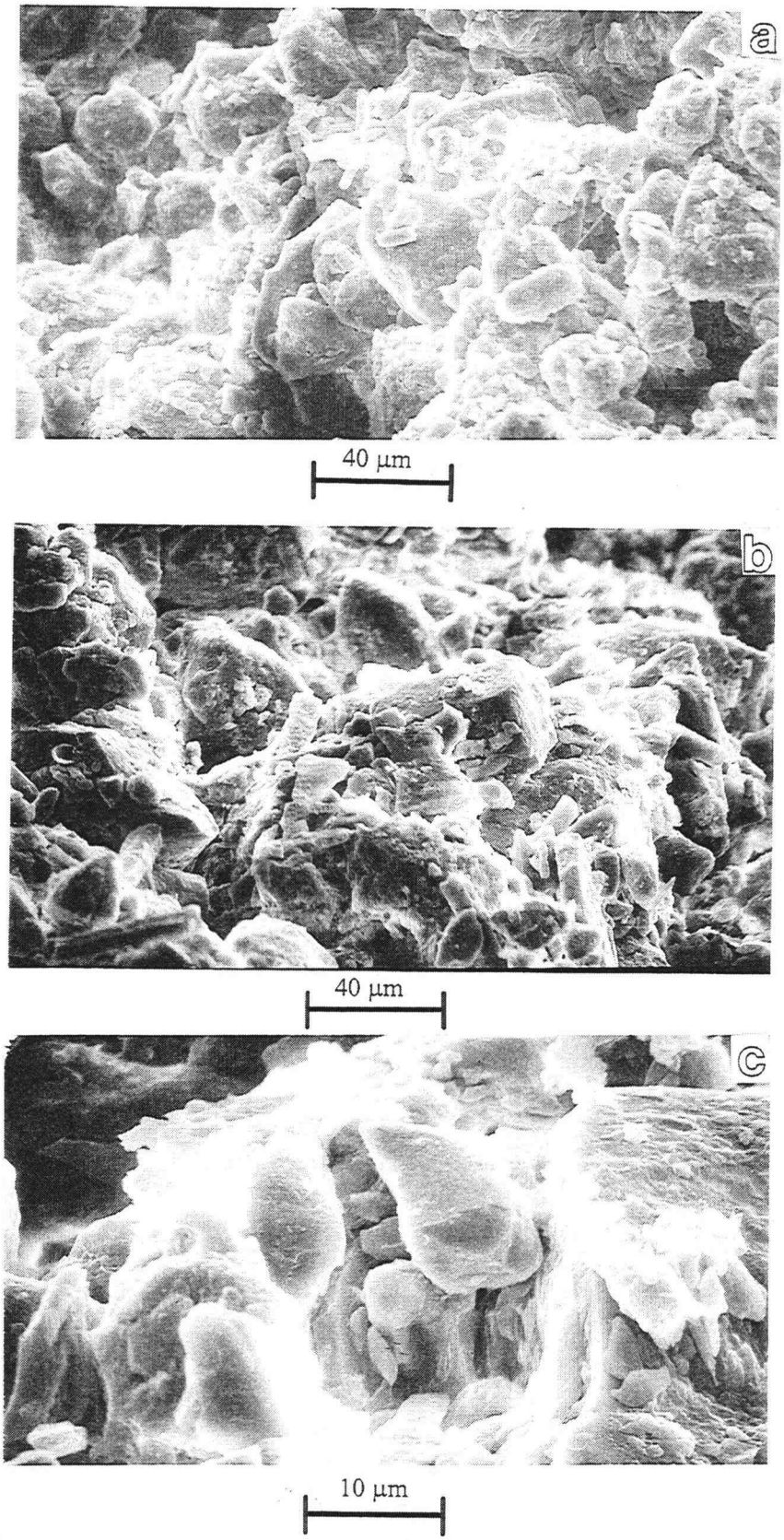

Figure 14abc.

Figure 15. Comparison of porosity in three adjacent soil layers of the SM treatment: (a) many large irregular pores in the Ap (15 cm); (b) closed packed fabric showing dense peds with few fine irregular pores in the Si enriched zone C1 (39 cm); and, (c) numerous small irregular peds and abundant spherical and subrounded irregular pores of the Bw (55 cm) horizon below the Si-enriched layer. Photo taken under crossed polarized light with quartz plate to accent porosity (pores appear pink in color).

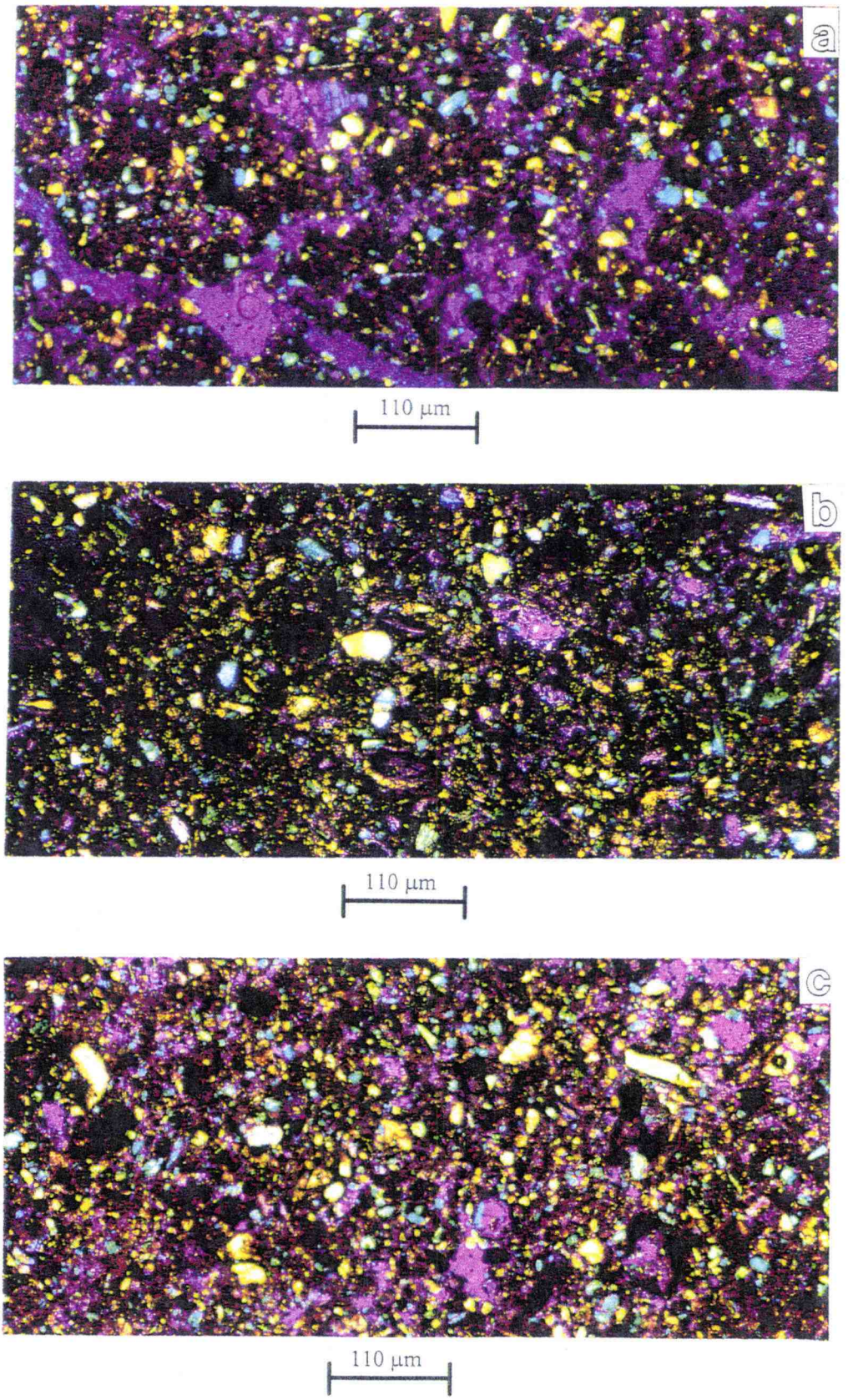

Figure 15.

Sources of Readily Weatherable Silica

Scanning electron microscopy and soil petrographic analysis for all treatments indicate the presence of significant amounts of volcanic materials, such as glass shards (Fig. 16ab, 17a) and pumice (Fig. 17b). The average concentration of SiO_2 in the Walla Walla volcanic glass samples is approximately 73.9 % (Table. 6), indicating a rhyolitic ash source. Non-colored rhyolitic glasses are classified by total SiO_2 contents of 70 to 100 % (Shoji et al., 1975). The Si : Al ratio of the glass is 5.3. The glass was concentrated in the Ap horizons rather than in subsurface layers. Opal phytoliths were also observed to be concentrated in the Ap horizons of these soils (Fig. 16c, 17c). Significant accumulations of volcanic glass and opal phytoliths in the Ap horizon may be the reason for relative maximum in clay content measured in the surface horizons (Fig. 5). Dingus (1973) found 9.5 % clay in the 0-15 cm depth of a Walla Walla soil series sampled at Tollgate in Umatilla county (30 km away from the study area). Phytoliths may comprised a significant portion of amorphous clays in Ap layers of Walla Walla silt loam soils (Norgren, 1973). Furthermore, the abundance of volcanic glass and plant opal in the Ap horizons explains the high concentration of amorphous Si measured for these horizons (Fig. 7). Hydrolysis of volcanic glass is probably the main source of Si_w

(Fig. 10). Weathering of volcanic glass is responsible for the genesis of Si-pans of the Olympic peninsula, Washington (Wilson et al., 1996). Chadwick et al. (1989) provides convincing evidence showing that weathering of volcanic materials is the major source for Si which results cementation in the Holocene soils in northern Monitor valley, Nevada.

Weathering of volcanic glass materials in the Ap horizon may promote cementation of the subsurface horizons in the Walla Walla silt loam soils. Five lines of evidence support this hypothesis: (i) abundance of volcanic components in these soils; (ii) laboratory data which show that Si is rapidly released from volcanic glass at low soil pH (White and Claassen, 1980); (iii) lower thermodynamic stability of volcanic compounds than most alumino-silicate minerals of similar composition (Lindsay, 1979); (iv) activation energies for the dissolution of volcanic minerals are about one-half those for feldspars with similar chemical composition (White, 1983); and, (v) many other soil minerals are not weathered rapidly in the present arid to semi arid environment (Flach, 1969).

Surface acidification enhances the pedogeochmical weathering of volcanic materials (White and Claassen, 1980). Hydrogen ions, derived from nitrification of N fertilizer, exchange with the surface bound cations on the glass. Removal of these cations weakens the glass and increases its porosity, making it more susceptible to dissolution and desilication (Dahlgren et al., 1993). Many vesicular volcanic materials (pumice) were observed in these soils (Fig. 12a). Increasing vesicularity results in a greater surface area exposed to chemical weathering (Dahlgren et al., 1993).

The average chemical composition of the Walla Walla soil volcanic glass is very similar to the those from Mt. Mazama and Mt. St. Helens tephras measured by Westgate and Gorten (1981) and King (1986) (Table. 7). Walla Walla glass composition, however, is more dominated by the Mazama than St. Helens tephra. This implies the

glasses in the parent material of Walla Walla soil are mainly derived from the eruption of Mt. Mazama, 6600 years ago. Minor amounts of ash (< 3mm) from the 1980 Mt. St. Helens eruption fell on the study area (Douglas, 1997, personal communication).

Figure 16. Scanning electron photomicrographs showing representative views of the major sources of weatherable amorphous silicate materials: (a) fragment of volcanic material surrounded by silt size soil particles; (b) fragment of volcanic shard; and, (c) representative opal phytoliths.

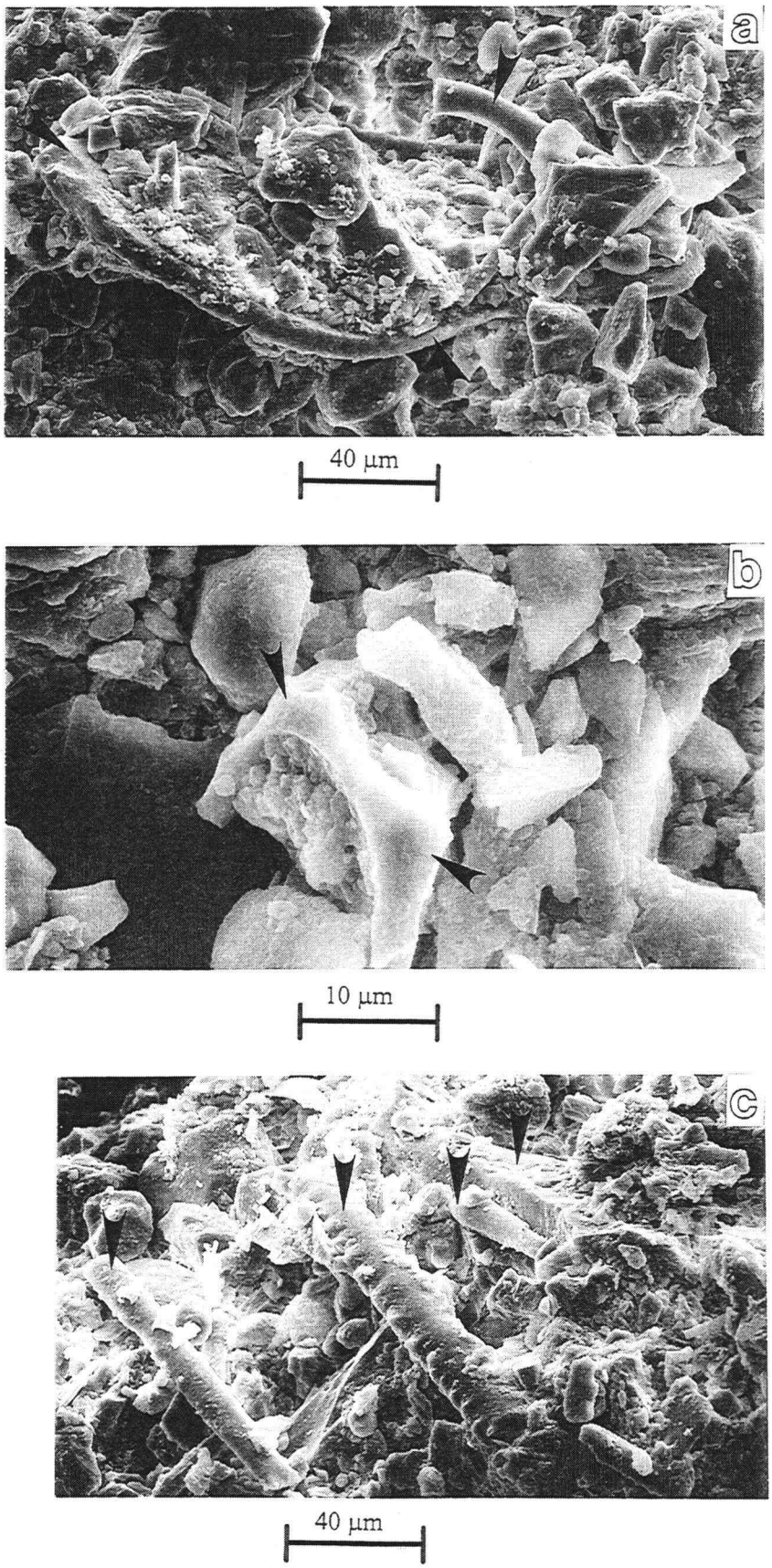

Figure 16.

Figure 17. Soil thin sections showing sources of readily weatherable Si under plain polarized light: (a) hydrated volcanic pumice with vesicles; (b) volcanic shard with sharp bladed edges embedded in silty matrix; and, (c) opal phytoliths in a silty matrix.

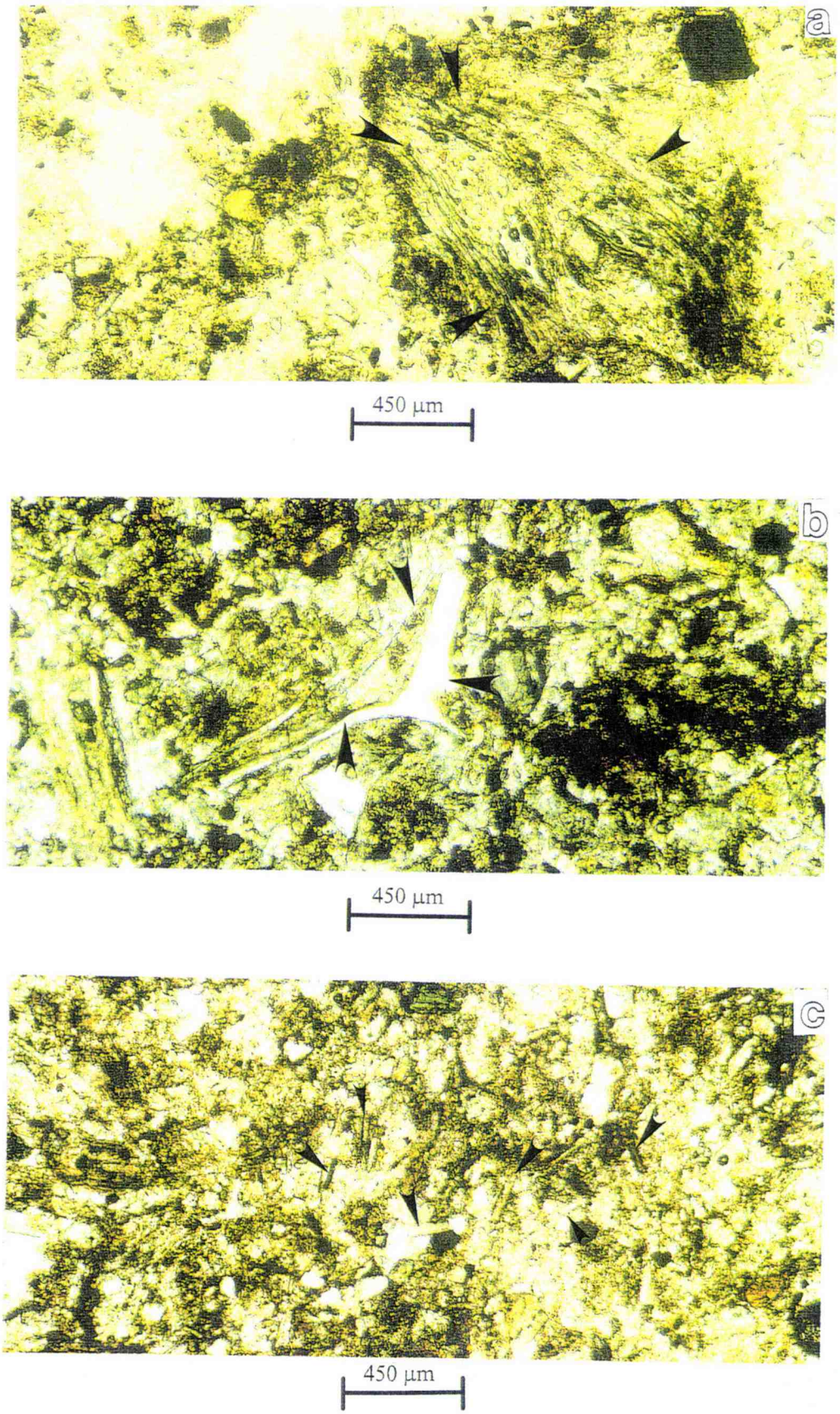

Figure 17.

Table 6. Glass composition of Walla Walla soil as determined by electron microprobe analysis.

	(%)											
	Na_2O	MgO	Al_2O_3	SiO_2	PO_3	K_2O	CaO	TiO_2	CrO	MnO	FeO	Total
	2.91	0.46	14.28	74.76	0.07	2.46	1.53	0.45	0.002	0.08	1.98	98.99
	1.72	0.47	14.51	73.87	0.07	2.64	1.56	0.42	0.002	0.06	1.94	97.28
	4.15	0.47	14.58	73.43	0.07	2.78	1.53	0.40	0.008	0.05	1.87	99.34
	3.01	0.54	14.29	71.19	0.07	2.62	1.71	0.38	0.002	0.03	1.96	95.81
	2.81	0.54	14.63	72.91	0.08	2.67	1.51	0.41	0.002	0.06	1.90	97.52
	2.86	0.46	14.39	73.27	0.06	2.71	1.62	0.41	0.002	0.05	1.97	97.79
	3.05	0.45	14.66	73.93	0.06	2.59	1.56	0.41	0.015	0.04	1.79	98.53
	3.27	0.48	14.50	73.22	0.07	2.58	1.64	0.40	0.035	0.08	1.90	98.17
	3.11	0.61	14.65	73.07	0.07	2.62	1.74	0.46	0.002	0.08	2.07	98.48
	4.05	0.58	14.84	73.81	0.11	2.74	1.75	0.47	0.043	0.04	2.06	100.50
	2.99	0.47	14.13	73.11	0.02	2.73	1.56	0.48	0.015	0.06	1.86	97.41
	2.11	0.47	14.27	73.59	0.07	2.72	1.67	0.41	0.002	0.09	1.97	97.35
	3.71	0.33	13.97	75.93	0.04	2.19	1.67	0.16	0.005	0.03	1.17	99.21
	3.32	0.34	14.16	76.09	0.06	2.15	1.69	0.16	0.061	0.02	1.20	99.24
	4.10	0.16	13.42	74.75	0.05	2.25	1.06	0.15	0.025	0.04	0.94	96.95
	3.93	0.40	12.36	76.64	0.06	2.51	0.97	0.14	0.018	0.01	1.19	98.22
	2.61	0.44	14.67	73.09	0.08	2.25	1.36	0.40	0.002	0.02	1.77	96.69
	1.24	0.43	14.63	73.87	0.04	2.30	1.54	0.42	0.020	0.08	1.94	96.51
Avg.	3.05	0.45	14.27	73.92	0.06	2.53	1.54	0.36	0.014	0.05	1.75	98.00
SD	0.80	0.10	0.58	1.31	0.02	0.21	0.21	0.12	0.017	0.02	0.36	1.19
1 σ counting statistics												
	0.086	0.020	0.064	0.149	0.028	0.033	0.029	0.022	0.023	0.023	0.057	
Detection limits												
	0.02	0.0082	0.01	0.015	0.014	0.0064	0.0076	0.011	0.023	0.015	0.016	

Table 7. Comparison of the average glass composition of Mt. Mazama and St. Helens ash to the glass component of the Walla Walla soil.

	Mazama†	Mazama‡	St. Helens‡	St. Helens†	St. Helens†	Walla Walla
	(%)					
SiO_2	72.58 ± 0.31	72.59 ± 1.63	74.94 ± 0.19	75.07 ± 1.80	75.04 ± 0.36	73.92 ± 1.31
TiO_2	0.48 ± 0.03	0.50 ± 0.03	0.17 ± 0.02	0.08 ± 0.03	0.16 ± 0.01	0.36 ± 0.12
Al_2O_3	14.40 ± 0.16	14.36 ± 0.34	14.48 ± 0.15	13.91 ± 0.34	14.34 ± 0.20	14.27 ± 0.58
FeO	2.11 ± 0.08	1.92 ± 0.12	1.41 ± 0.05	1.18 ± 0.10	1.38 ± 0.04	1.75 ± 0.36
MnO	0.04 ± 0.00	0.05 ± 0.07	0.03 ± 0.00	0.04 ± 0.05	0.02 ± 0.00	0.05 ± 0.02
MgO	0.56 ± 0.08	0.42 ± 0.13	0.49 ± 0.08	0.35 ± 0.05	0.52 ± 0.07	0.45 ± 0.10
CaO	1.66 ± 0.10	1.39 ± 0.07	1.85 ± 0.06	1.58 ± 0.04	1.85 ± 0.06	1.54 ± 0.21
Na_2O	5.18 ± 0.20	5.35 ± 0.54	4.44 ± 0.21	3.31 ± 1.97	4.37 ± 0.27	3.05 ± 0.80
K_2O	2.70 ± 0.11	2.80 ± 0.12	2.03 ± 0.08	2.32 ± 0.26	2.09 ± 0.05	2.53 ± 0.21
CrO						0.01 ± 0.02
PO_3						0.06 ± 0.02
Total	99.71	99.38	99.84	97.84	99.77	99.00
n§	98	6	14	6	11	27

† Westgate and Gorton (1981).
‡ King (1986).
§ n = number of analysis.

More evidence on the origin of Walla Walla volcanic glass was provided by the examination of elemental ratio plots. These plots were constructed using the data in Table 5 (Fig. 18abcd). Most of the chemical analyzes for the Walla Walla glasses are within the composition range of that of Mazama and St. Helens glass. Moreover, examination of Figure 18d suggests that many of the glass particles in Walla Walla soils are derived from Mt. Mazama tephara. Glass specimens which can be traced to Mount St. Helens tephra are chemically distinct by having lower K composition (Westgate et al., 1970).

Solubility of biogenic opal is higher than many soil minerals such as quartz and crystobalite (Tan, 1993; Drees et al., 1989). The solubility of biogenic opal, however, is less than that of volcanic materials (Drees et al., 1989). Weathering of biogenic opal contributes only small quantities of Si that causes cementation of Holocene soils in Nevada (Chadwick et al., 1989). He reported that volcanic glass dissolution is the major source of Si cementation in these soils. The weathering rate of plant opal is low or nil in dry cool regions (Witty, 1962). Some plant opal is observed to be very resistant to dissolution and relatively unweathered in soils. Wilding (1967), for example, determined an age of 13000 years, using carbon dating, for plant opal in some arid grass land soils.

Formation of biogenic opal is common in many soils derived from volcanic materials (Mizota et al., 1982). The occurrence of highly weatherable volcanic sources, combined with grass vegetation promotes the formation of biogenic opal in the Walla Walla soil. The genesis of biogenic opal is even higher in soils developed under young volcanic tephras where sources of soluble Si are present (Lowe, 1986). This is found to be the case in the Walla Walla soil, which developed under young Mazama tephra.

Plant opal found in this study originated from wheat and native grass species which grow in the area. Micromorphology of most plant opal assemblages examined are similar to the Idaho fescue and bluebunch wheatgrass phytoliths observed by Norgren (1973) and Witty (1962). This is most likely the result of the resistance of opal phytolith to weathering and consequently their relatively long half-life in semi-arid environments. The majority of the sand-size phytolith observed were either spiny elongated (Fig. 19a), spiny with pavement elongated (Fig. 19b), or smoothly elongated (Fig. 14c) (after, Twiss et al., 1969).

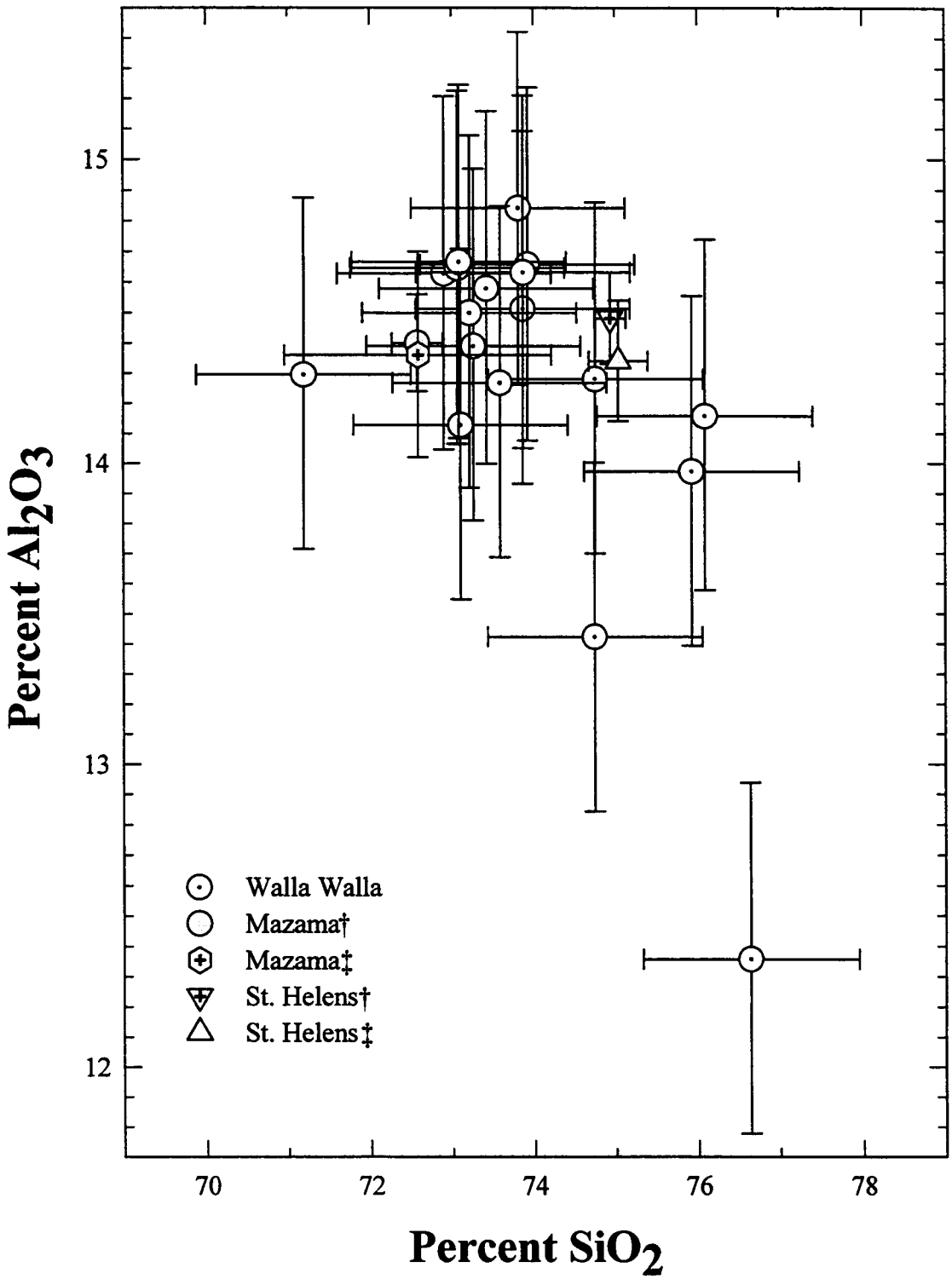

Figure 18a. Percent of Si *vs.* Al oxides in a Walla Walla glass specimen compared with Mazama and St. Helens tephra. Horizontal and vertical lines represent 2σ error bars.

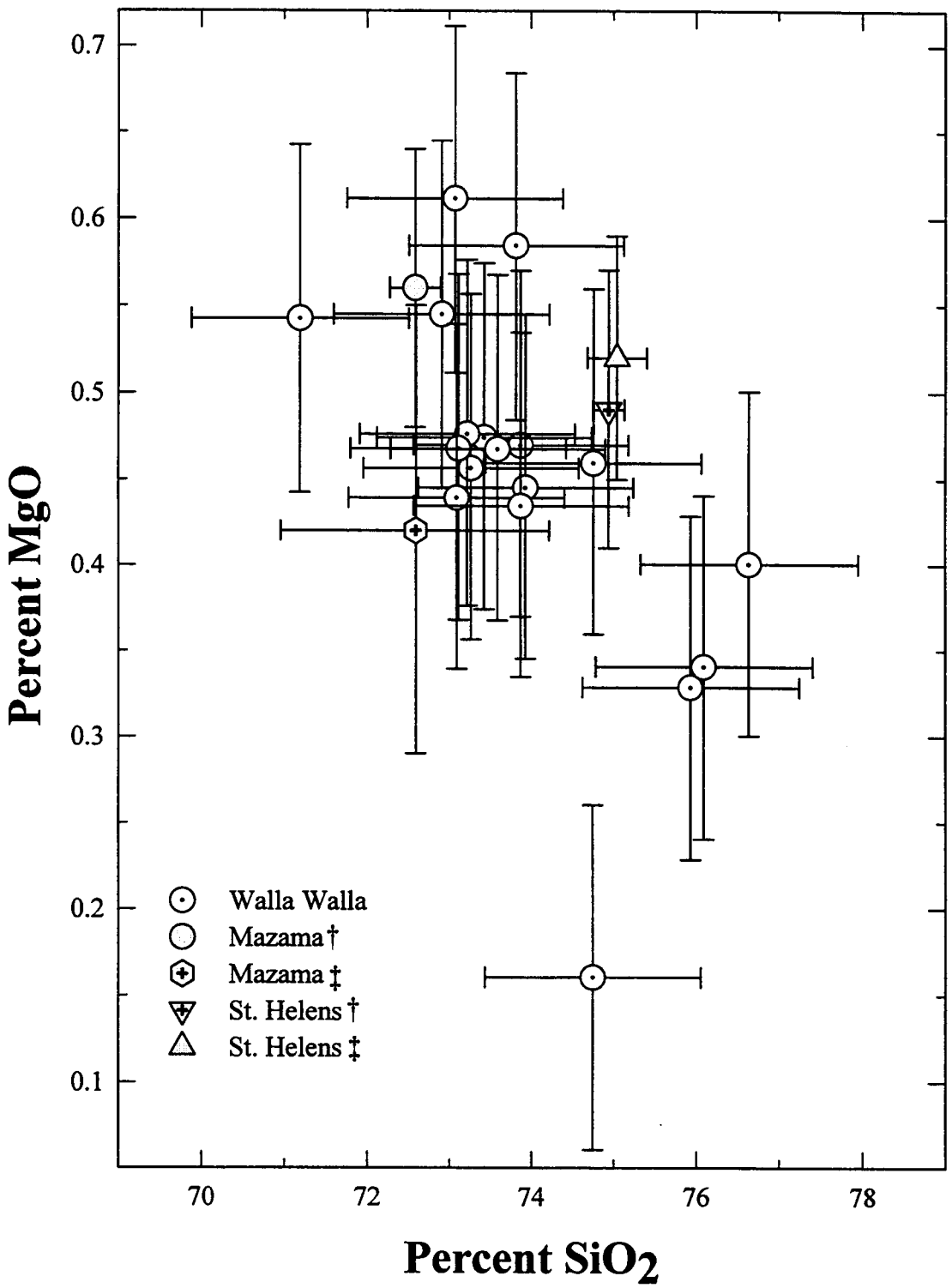

Figure 18b. Percent of Si *vs.* Mg oxides in a Walla Walla glass specimen compared to Mazama and St. Helens tephra. Horizontal and vertical lines represent 2σ erorr bars.

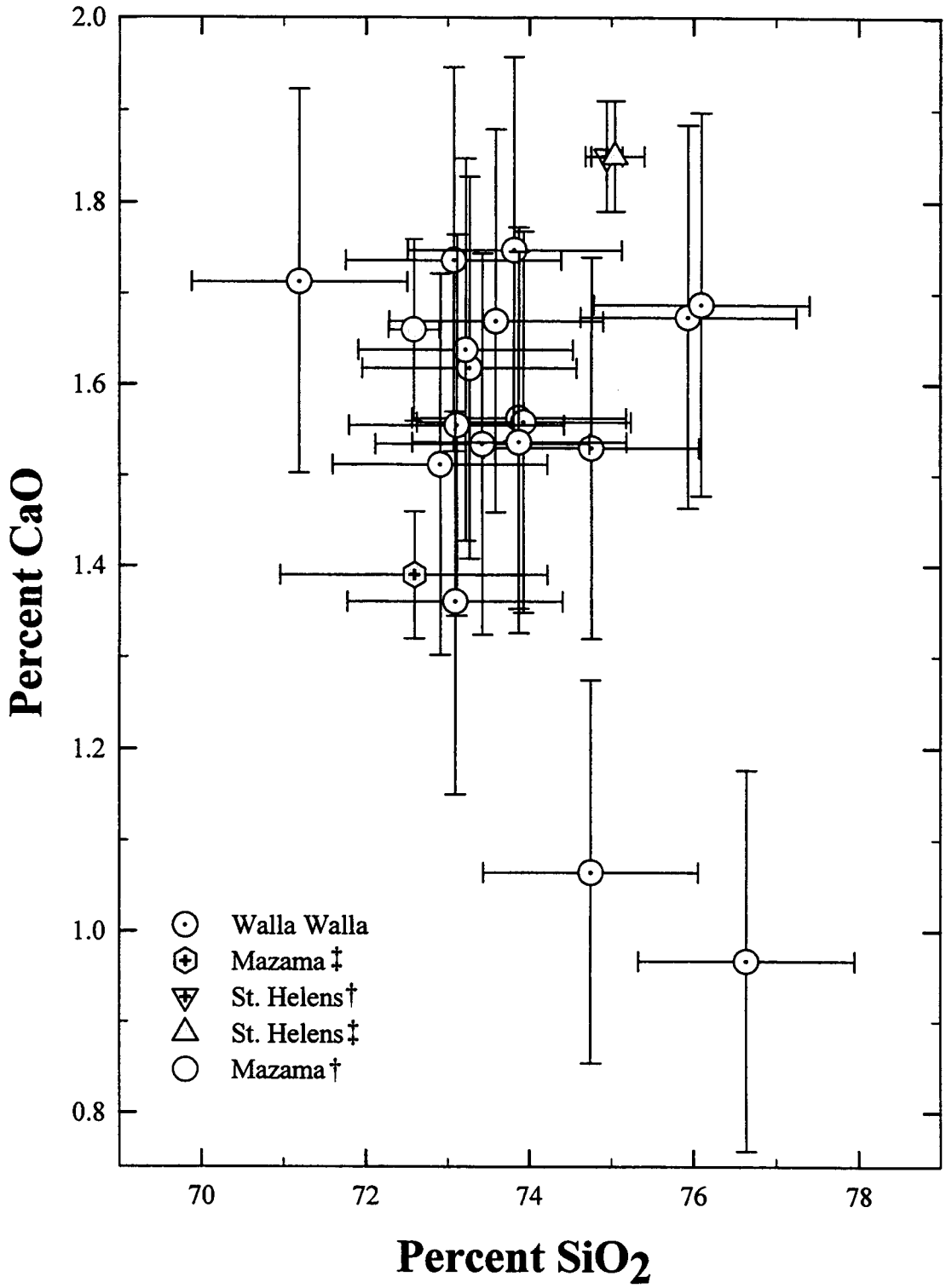

Figure 18c. Percent of Si *vs.* Ca oxides in a Walla Walla glass specimen compared with Mazama and St. Helens tephra. Horizontal and vertical lines represent 2σ error bars.

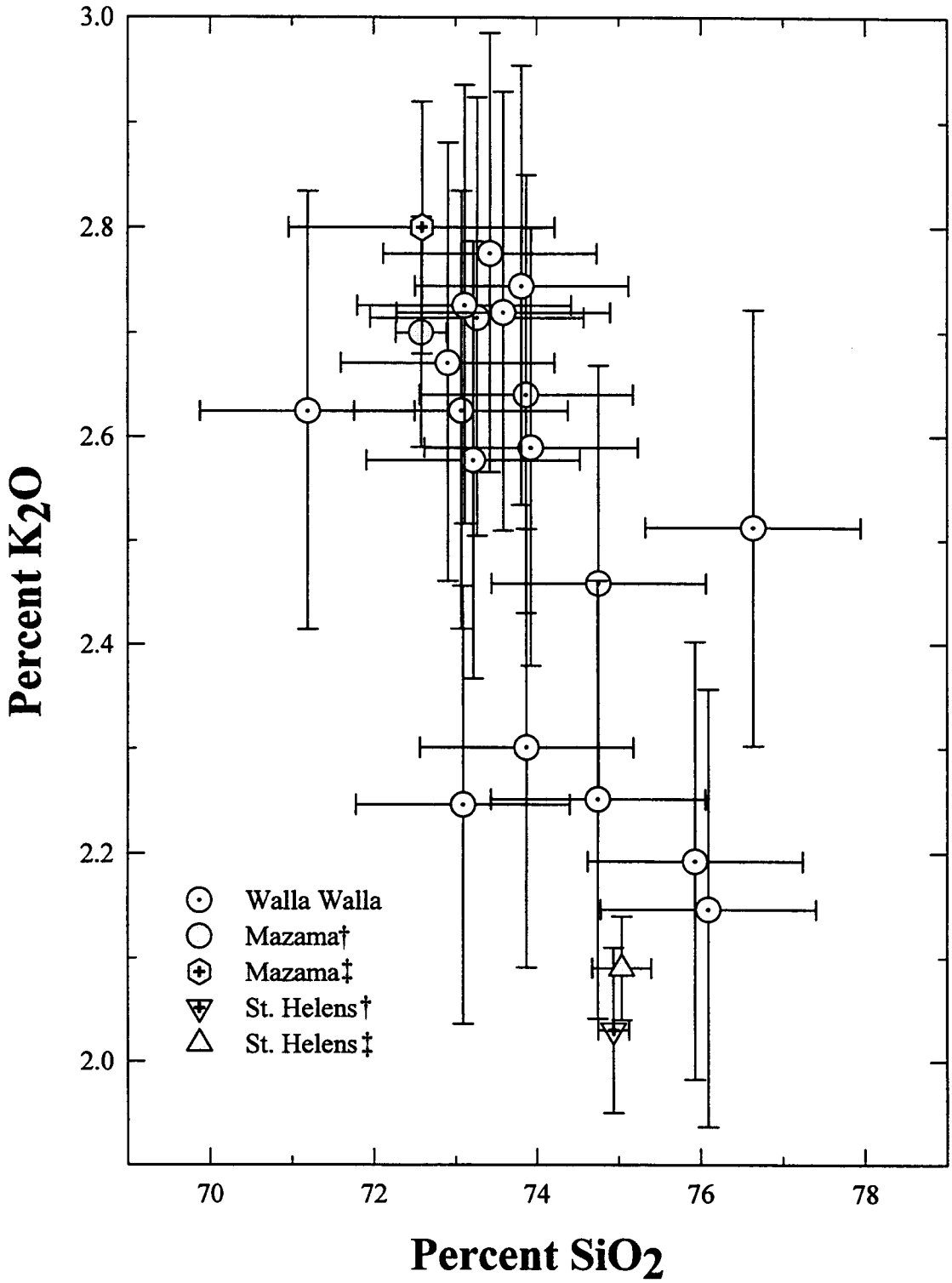

Figure 18d. Percent of Si *vs.* K oxides a Walla Walla glass specimen compared with Mazama and St. Helens tephra. Horizontal and vertical lines represent 2σ erorr bars.

Figure 19. Scanning electron photomicrographs of varied forms of opal phytoliths: (a) spiny elongated; (b) spiny elongated with pavement; and, (c) smoothly elongated.

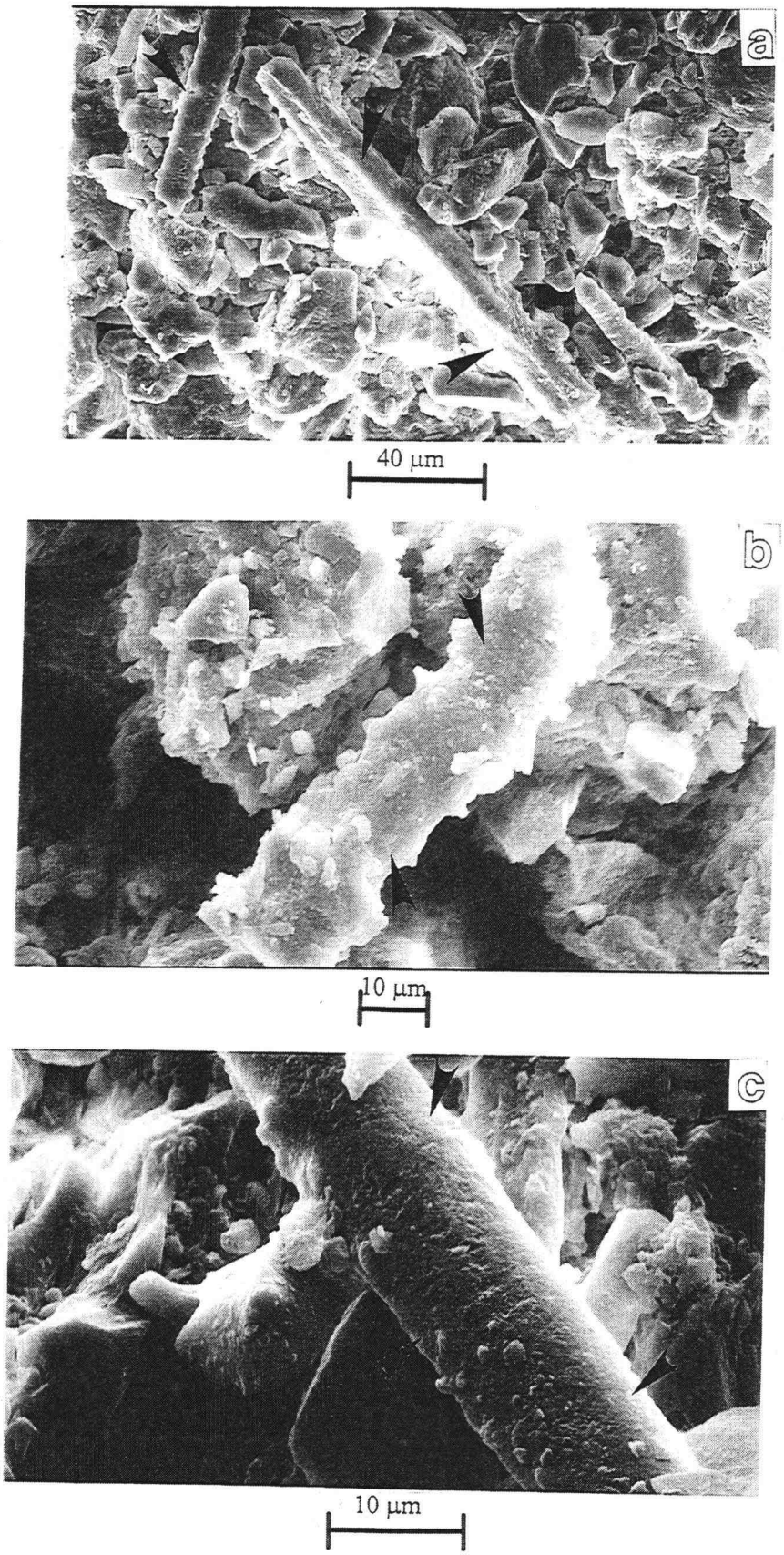

Figure 19.

Genesis of Silica-Enriched Pan

The designation "Si-enriched pan" is used to describe the harden dense horizon just below the depth of plowing. Several chemical, physical, and mineralogical evidence point to Si as the principal cementing agent. Agricultural practices have partially influenced the formation of the Si-enriched pans, by creating conditions of low permeability and high bulk density immediately below the amorphous Si-enriched plow zone. Silica leached from the Ap layer precipitates both within and just below the agricultural-compacted zone, forming microscopic bridges between grains. Thus, the genesis of weakly developed Si-pans has three components: (i) weathering of Si-rich materials, primarily those of volcanic ash and opal phytoliths due acidification of the surface soils; (ii) plowing and compaction due to tillage practices; and, (iii) evaporation of Si_w rich soil solution at the structural boundary between the plowed surface soil and unplowed soil.

During the process of Si-enriched pan formation, pedogeochemical weathering of amorphous silicate compounds takes place, especially during the moist period (Fig. 20). Volcanic glass, clay-size volcanic dust, pumice, and opal phytoliths are readily weatherable source of soluble Si. The clay-size volcanic dust is the most susceptible to weathering due to its large surface area and small particle size (Fig. 20). The rate of pedogeochemical weathering is enhanced by production of agricultural acidity. Nitrogen fertilization and "basic" cation uptake are the major agricultural processes contributing to acidity. Biologically-produced H^+ attacks the silicate mineral bonds (Fig. 21a). As a result, $H_4SiO_{4(aq)}$ (Si_w) and cations are released into soil solution. This pedogeochemical weathering of silicate materials can be represented simply by Eq. [7].

$$\text{Amorphous Al and Si Oxides} + H^{+}_{(aq)} \rightleftharpoons \text{Secondary minerals} + \text{Cations}_{(aq)} + H_4SiO_{4(aq)}; \quad \text{Eq. [7]}$$

Water-soluble Si (Si_w) is either taken up by crop or leached into subsurface horizons (Fig. 20; Fig. 21b). During the summer fallow season, high evaporation rates result in the upward movement of Si_w via capillary flow (Fig. 20c). Climate data obtained for the area show that annual evaporation of soil moisture exceeds precipitation (Table 2; Fig 2). Robert and Ekin (1984) reported a net evaporative loss of water from the Walla Walla soil of 3 to 5 cm during the fallow summer season. Once the soil solution, containing elevated concentrations of Si_w, reaches the boundary between the Ap layer and the subsoil, further upward movement of water takes place in the vapor phase (Fig. 21c). This is due to the high content of large pores in Ap layer. As a result, most of the evaporation takes place at or below the boundary of the plow zone, where Si_w accumulation occurs (Fig. 21c). As the soil dries, Si_w increasingly diffuses into smaller pores where it is adsorbed and then precipitated onto silicate or sesquioxide mineral surfaces (Fig. 21d). With further drying SiO_2 polymers are formed. These eventually form bridges between soil particles at points of grain contact (Fig. 21d).

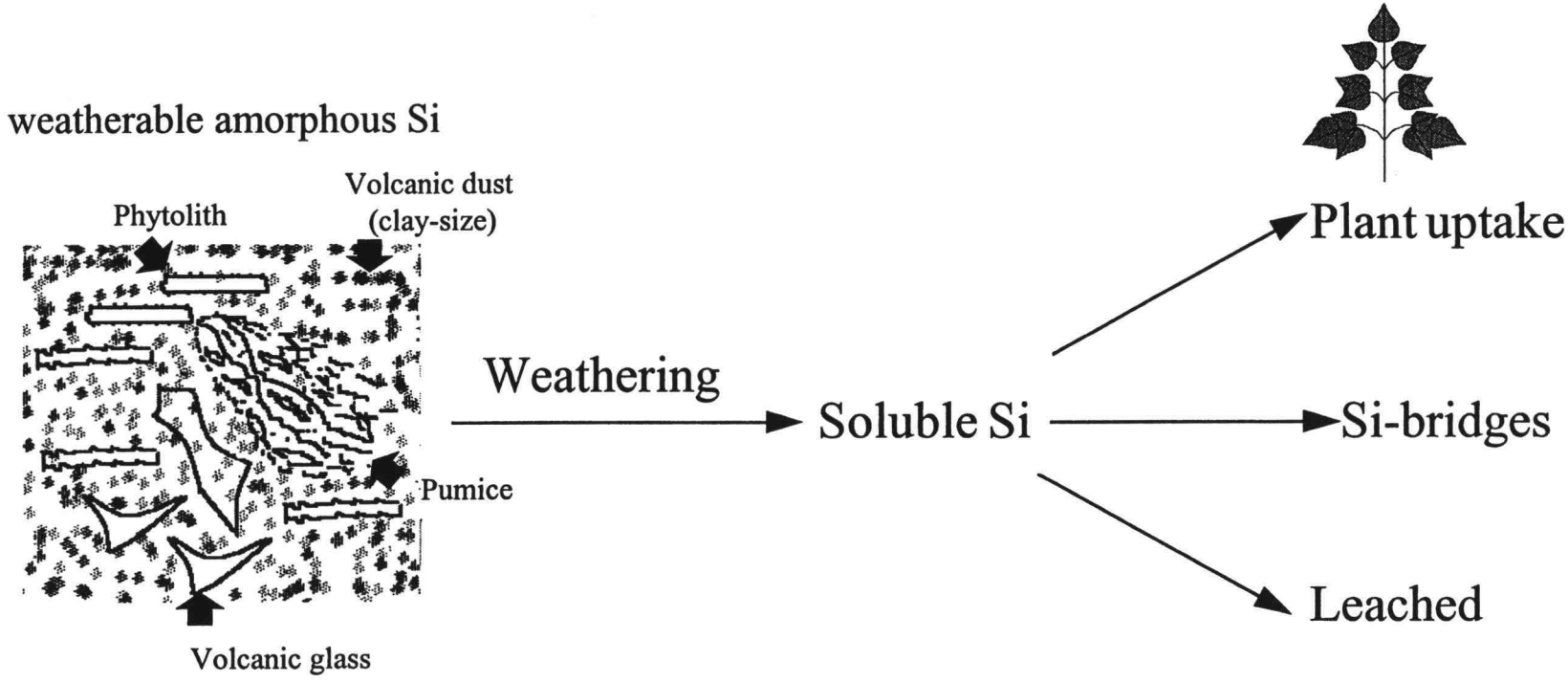

Figure 20. Possible sinks of soluble Si resulting from the weathering of amorphous silicate materials.

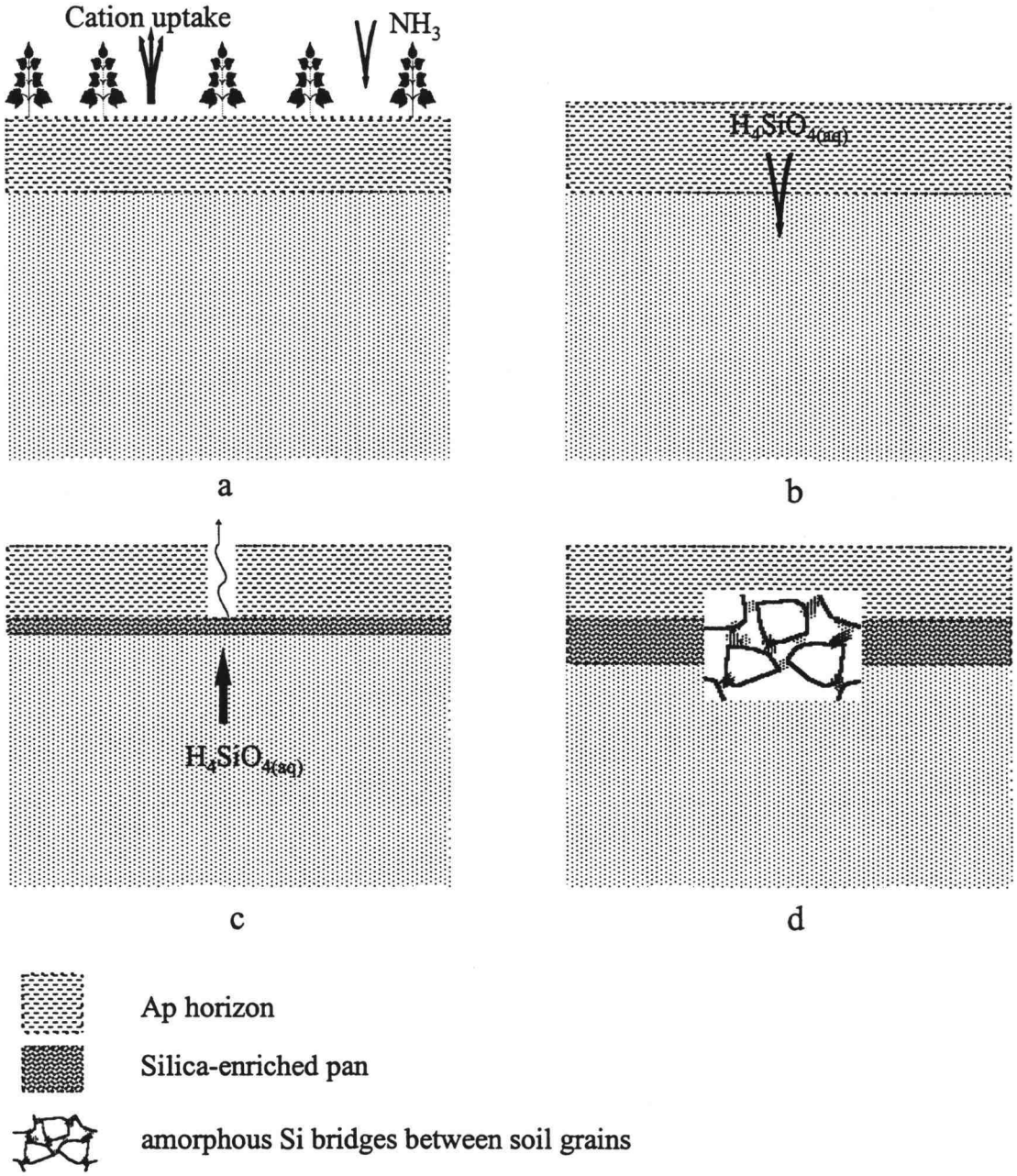

Figure 21. A model illustrating the formation of Si-enriched pan in the Walla Walla silt loam soil: (a) N fertilization and cation uptake as the major sources of agricultural surface acidification; (b) silicate materials weather under acidic conditions releasing $H_4SiO_{4\,(aq)}$ which leaches into subsurface layers during winter and early spring; (c) high evaporation during summer/fallow season enhances upward movement of aqueous Si; and, (d) Soluble Si precipitates as $SiO_{2(s,\,am)}$ on further drying forming bridges across soil grains.

CONCLUSIONS

Agricultural management practices, parent material mineralogy, and cycles of wetting and drying are important factors affecting Si cementation in the Walla Walla silt loam soil. Silica cements are derived from the weathering of volcanic glass, pumice, clay-size volcanic dust, and biogenic opal that are concentrated in the Ap horizons of the Walla Walla soil. The abundance of highly weatherable silicate material in the Ap horizons acts as a pool for Si that causes cementation in subsurface horizons.

Field crop practices, acting in concert with pedogenic processes, accelerate formation of weakly developed amorphous Si-cements. Acidification, tillage, traffic compaction, and additions of the strawy manure are the major agricultural practices enhancing amorphous Si-cement development. Acidification due to N application enhances Si cementation through accelerated weathering of readily-soluble Si sources within the Ap horizons. Addition of the strawy manure provides a significant amount of amorphous Si that is available for the cementation process. Tillage appears to enhance Si accumulation and precipitation by altering the normal cycle of water movement through the soil horizons. Evaporation of soil moisture takes place at the boundary between the Ap and subsoil. This process of evaporative concentration of water-soluble Si results in the formation of hardened Si-enriched pan.

Optical microscopic techniques served as important tools for the exploration of the physical characteristics of the weakly Si-pans. Bridges, coatings, and web-like networks of amorphous Si formed between soil grain contacts. These Si features, however, were very thin and appeared to be in their early stage of development. Bulk

density and penetrometer load techniques were not sensitive enough to detect the differences in strength produced by the incipient amorphous Si-cements among the management treatments.

A detailed study of the relationship of Si cycle to the formation of Si-enriched pans is strongly suggested. This will help us understand the behavior of Si as a cementing agent in these soils in relation to the wheat-fallow agricultural practices. In addition, this will guide us in managing these soils in long-term soil conservation programs.

Deep tillage appears to be a short-term solution to the problem of pan formation. Our observations and proposed mechanism suggest that pans should reform after a number of years. This is consistent with anecdotal accounts regarding "deep ripping" and the formation of pans. Pockets of restricted drainage, believed to result from pans, seem to reappear a few years after field has been deep tilled.

Minimum tillage practices may serve to ameliorate the formation of Si-enriched pans. The maintenance of soil carbon in surface horizons under minimum tillage may result in disruption of Si cementation.

BIBLIOGRAPHY

Adams, F. 1984. Crop response to lime in southern United States. p. 211-265. *In* F. Adams (ed.) soil acidity and liming. 2nd ed. Agron. Monogr. 12. ASA, CSSA, and SSSA, Madison, WI.

Alexander, G.B., W.M. Heston, and R.K. Iler. 1954. The solubility of amorphous silica in water. J. Phys. Chem. 58:453-455.

Allmaras, R.R., K. Ward, C.L. Douglas, and L.G.Ekin. 1982. Long-term cultivation effects on hydraulic properties of a Walla Walla silt loam. soil Tillage Res. 2:256-279.

Baker, G. 1960. Phtolitharien. Aust. J. Sci. 22:392-393.

Bartoli, F., and L.P. Wilding. 1980. Dissolution of biogenic opal as a function of its physical and chemical properties. Soil Sci. Am. J. 44:873-878.

Bauder, J.W., G.W. Randall, and J.B. Swan. 1981. Effect of four continuous tillage systems on mechanical impedance of a clay loam soil. Soil Sci. Soc. Am. J. 45:802-806.

Beckwith, R.S., and R. Reeve. 1963. Studies on soluble silica in soils: I. The sorption of silicic acid by soils and minerals. Aust. J. Soil Res. 1:157-168.

Beckwith, R.S., and R. Reeve. 1964. Studies on soluble silica in soils: II. The release of monosilicic acid from soils. Aust. J. Soil Res. 2:33-45.

Bolan, N.S., M.J. Hedley, and R.E. White. 1991. Processes of soil acidification during nitrogen cycling with emphasis on legume based pastures. Plant Soil. 134:53-63.

Bouman, O.T., D. Curtin, C.A. Compbell, V.O. Biederbeck, and H. Ukrainetz. 1995. Soil acidification from long-term use of anhydrous ammonia and urea. Soil. Soc. Am. J. 59:1488-1494.

Breemen, V.N., J. Mulder, and C.T. Driscoll. 1983. Acidification and alkalinization of soils: Hydrogen ion transfer, chemical reaction equations. Plant Soil. 75:283-308.

Brewer, R., and J.R. Sleeman. 1988. Soil structure and fabric. CSIRO. Australia.

Brown, T.H., and R.L. Mahler. 1987. Sorption of silica in a northern Idaho Palouse silt loam. Soil Sci. 144:181-189.

Brown, T.H., and R.L. Mahler. 1988. Relationship between soluble silica and plow pans in Palouse silt loam soils. Soil Sci. 145:359-364.

Campbell, C.A., R.P. Zentner, F. Selles, and O.U. Akinremi. 1993. Nitrate leaching as influenced by fertilization in the brown soil zone. Can. J. Soil. 73:387-397.

Chadwick, O.A., D.M. Hendricks, and W.D. Nettleten. 1987a. Silica in duric soils: I. A depositional model. Soil Sci. Soc. Am. J. 51:975-982.

Chadwick, O.A., D.M. Hendricks, and W.D. Nettleten. 1987b. Silica in duric soils: II. Mineralogy. Soil Sci. Soc. Am. J. 51:982-985.

Chadwick, O.A., D.M. Hendricks, and W.D. Nettleton. 1989. Silicification of Holocene soils in northern Monitor valley, Nevada. Soil Sci. Am. J. 53:158-164.

Chartres, C.J. 1985. A preliminary investigation of hardpan horizons in north-west south Wales. Aust. J. Soil Res. 23:325-337.

Chartres, C.J., J.M. Kirby, and M. Raupach. 1990. Poorly ordered silica and aluminosilicates as temporary cementing agents in hard-setting soils. Soil Sci. Soc. Am. J. 54:1060-1067.

Day, P.R. 1965. Particle fractionation and particle-size analysis. p. 545-567. *In* C. A. Black et al. (eds.) Methods of soil analysis, Part 1. 2nd ed. Agron. Monogr. 9. ASA and SSSA, Madison, WI.

Dahlgren, R., S. Shoji, and M. Nanzyo. 1993. Mineralogical characteristics of volcanic ash soils. Dev. Soil Sci. 21:101-143.

Dingus, D.D. 1973. The nature and properties of amorphous colloids formed from Mazama tephra. Ph.D. diss. Oregon State Univ., Corvallis.

Douglas, C.L., Jr. 1984. Silicic acid and oxidizable carbon movement in a Walla Walla silt loam as related to long-term residue and nitrogen application. Ph.D. diss. Oregon State Univ., Corvallis.

Douglas, J.F. 1956. Morphology and genesis of the Condon, Morrow, and Walla Walla series of the mid-Columbia basin, Oregon. Ph.D. diss. Oregon State Univ., Corvallis.

Douglas, C.L., Jr., R.R. Allmaras, and N.C. Roager, Jr. 1984. Silicic acid and carbon movement in a Walla Walla silt loam as related to long-term management. Soil Sci. Am. J. 48:156-162.

Drees, L.R., L.P. Wilding, N.E. Smeck, and A.L. Senkayi. 1989. Silica in soils: Quartz and disordered silica polymorphs. p. 913-974. *In* J.B. Dixon and S.B. Weed (eds.) Minerals in soil environment. 2nd ed. SSSA, Madison, WI.

Dudas, M.J. 1973. Mineralogy and trace element chemistry of Mazama ash soil. Ph.D. diss. Oregon State Univ., Corvallis.

Elgawhary, S.M., and W.L. Lindsay. 1972. Solubility of silica. Soil Sci. Soc. Amer. Proc. 36:439-442.

Esau, K. 1953. Plant Anatomy. John Wiley & Sons, NY.

Faure G. 1991. Principles and applications of inorganic geochemistry. Macmillan publishing company, Englewood Cliffs, NJ.

FitzPatrick, E.A. 1993. Soil microscopy and micromorphology. John Wiley & Sons Ltd., West Sussex, England.

Flach, K.W., W.D. Nettleton, L.H. Gile, and J.G. Cady. 1969. Pedocementation: Induration by silica, carbonates, and sesquioxides in the Quaternary. Soil Sci. 107:442-453.

Flach, K.W., W.D. Nettleton, and R.E. Nelson. 1974. The micromorphology of silica-cemented soil horizons in western north America. p. 714-729. *In* G.K. Rutherford (ed.) Soil microscopy. Brown & Martin Ltd., Kingston, Ontario.

Francis, J.L., and E.J. Kladivko. 1989. Soil strength properties under four tillage systems at three long-term study sites in Indiana. Soil Sci. Soc. Am. J. 53:1539-1545.

Franzmeier, D.P., L.D. Norton, and G.C. Steinhardt. 1989. Fragipan formation in loess of the Midwestern United States. p. 69-97. *In* N.E. Smeck and E.J. Ciolkosz (eds.) Fragipans: Their occurrence, classification, and genesis. SSSA. Madison, WI.

Geis, J.W. 1973. Biogenic silica in selected species of deciduous angiosperms. Soil Sci. 116:113-119.

Glasmann, J.R., and G.H. Simonson. 1985. Alteration of basalt in soils of western Oregon. Soil Sci. Soc. Am. J. 49:262-273.

Green, A.J. 1981. Particle-size analysis. p. 4-29. *In* J.A. McKeague (ed.) Manual on soil sampling and methods of analysis. Canadian Society of Soil Sci., Ottawa.

Jackson, M.L., and G.D. Sherman. 1953. Chemical weathering of minerals in soils. Advan. Agro. 5:219-318.

Jackson, T.L., and H.M. Reisenauer. 1984. Crops response to lime in the western United States. p. 333-347. *In* F. Adams (ed.) soil acidity and liming. 2nd ed. Agron. Monogr. 12. ASA, CSSA, and SSSA, Madison, WI.

Jones, J.B., and E.R. Segnit. 1971. The nature of opal: I. Nomenclature and constituent phases. J. geol. Soc. Aust. 18:57-68.

Jones, L.H.P., and A.A. Milne. 1963. Studies of silica in the oat plant: I. Chemical and physical properties of the silica. Plant and Soil. 18:207-220.

Jones L.H.P., and K.A. Handreck. 1965. The relation between the silica content of the diet and the excretion of silica by sheep. J. Agric. Sci. 65:129-134.

Jones, L.H.P., and K.A. Handreck. 1967. Silica in soils, plants, and animals. Adv. Agron. 19:107-149.

Jones, R.L., and A.H. Beavers. 1963. Some mineralogical and chemical properties of plant opal. Soil Sci. 96:375-379.

Jones, R.L., L.J. McKenzie, and A.H. Beavers. 1964. Opaline microfossils in some Michigan soils. Ohio J. Sci. 64:417-423.

Jones, R.L., and W.W. Hay. 1975. Bioliths. p. 481-496. *In* J.E. Gieseking (ed.) Soil components, Vol. 2, Inorganic components. Springer-Verlag New York Inc., Secaucus, NJ.

King, R.H. 1986. Weathering of Holocene airfall tephras in southern Canadian rockies. p. 239-264. *In* S.M. Colman, and D.P. Dethier (eds.) Rates of chemical weathering of rocks and minerals. Academic Press. NY.

Kittrick J.A. 1969. Soil minerals in the Al_2O_3-SiO_2-H_2O system and a theory of their formation. Clays and Clay Minerals. 17:157-167.

Kowalski, R., and G.F. Davis. 1982. Silica content of *Triticuma aestivum* L. in relation to humic acid concentrations in the soil. Plant and Soil. 68:139-141.

Krauskopf, K.B. 1956. Dissolution and precipitation of silica of silica at low temperatures. Geoch. Cosmoch. Acta. 10:1-26.

Lanning, F.C., B.W. Ponnaiya, and C.F. Crumption. 1958. The chemical nature of silica in plants. Plant Physiol. 33:339-343.

Lanning, F.C., and L.N. Eleuterius. 1992. Silica and ash in seeds of cultivated grains and native plants. Annals of Botany. 69:151-160.

Lindbo, D.L., and P.L.M. Veneman. 1993. Morphological and physical properties of selected fragipan soils in Massachusetts. Soil Sci. Soc. Am. J. 57:429-436.

Lindsay, W.L. 1979. Chemical equilibria in soils. John Wiley & Sons, NY.

Lowe, D.J. 1986. Controls on the rates of weathering and clay mineral genesis in airfall tephras: A review and NewZealand case study. p. 265-320. *In* S.M. Colman, and D.P. Dethier (eds.) Rates of chemical weathering of rocks and minerals. Academic Press. NY.

Mark, D.A., T.C. Kaspar, and R. Horten. 1990. Characterization of tillage and traffic effects on unconfined infiltration measurements. Soil Sci. Soc. Am. J. 54:837-840.

McGrath, S.P. 1985. The effects of increasing yield on the macro-and microelement concentrations and off takes in the grain of winter wheat. J. Sci. Food Agric. 36:1073-1083.

McKeague, J.A., and M.G. Cline. 1963a. Silica in soils. Adv. Agron. 15:339-397.

McKeague, J.A., and M.G. Cline. 1963b. II. The adsorption of monosilicic acid by soil and other substances. Can. J. Soil Sci. 43:83-96.

McKeague, J.A., and P.N. Sprout. 1975. Cemented subsoils (duric horizons) in some soils of British Columbia. Can. J. Soil Sci. 55:189-203.

McKeague, J.A., and R. Protz. 1980. Cement of duric horizons, micromorphology and energy dispersive analysis. Can. J. Soil Sci. 60:45-52.

Milnes, A.R., and C.R. Twidale. 1983. An overview of silicification in Cainozoic landscapes of arid central and southern Australia. Aust. J. Soil Res. 21:387-410.

Mizota, C., J.A. Carrasco, and K. Wada. 1982. Clay mineralogy and some chemical properties of Ap horizons of Ando soils used for paddy rice, Japan. Geoderma 27:225-237.

Norgren, J.A. 1973. Distribution, form and significance of plant opal in Oregon soils. Ph.D. diss. Oregon State Univ., Corvallis.

Pease, D.S., and J.U. Anderson. 1969. Opal phtoliths in *Bouteloua Eriopoda Torr.* roots and soils. Soil Sci. Soc. Am. Proc. 33:321-322.

Pierre, W.H., and W.L. Banwart. 1973. Excess-base and excess-base/nitrogen ratio of various crop species and parts of plants. Agron. J. 65:91-96.

Pikul, J.L.Jr., and R.R. Allmaras. 1986. Physical and chemical properties of Haploxeroll after 50 years of residue management. Soil Sci. Soc. Am. J. 50:214-219.

Rasmussen, P.E., and W.J. Parton. 1994. Long-term effects of residue management in wheat-fallow: I. input, yield, and soil organic matter. Soil Soc. Am. J. 58:523-530.

Raupach, M., and C.S. Piper. 1959. Interactions of silicate and phosphate in a lateritic soil. Aust. J. Agric. Res. 10:818-831.

Rickman, R.W., and B.L. Klepper. 1980. Wet season aeration problems beneath surface mulches in dryland winter wheat production. Agron. J. 72:733-736.

Robert, E.R., and L.G. Ekin. 1984. Effect of stubble management in a wheat-fallow rotation on water conservation and storage in eastern Oregon. Columbia Basin Agricultural Research. Special Report 713. p.30.

Robinson, R.H. Jr. 1961. The geography, morphology and environmental relationships of the Walla Walla soil series in Oregon. Ms. thesis. Oregon State Univ., Corvallis.

Shoji, S., Kobayashi, K.S. Yamada, and J. Masui. 1975. Chemical and mineralogical studies on volcanic ashes. I. Chemical composition of volcanic ashes and their classification. Soil Sci. Plant. Nutr. 21:311-318.

Simpson, T.L., and B.E. Volcani. 1981. Silicon and siliceous structures in biological systems. Springer-Verlag New York Inc., Secaucus, NJ.

Singh, B., and R.J. Gilkes. 1993. The recognition of amorphous silica in indurated soil profiles. Clay Minerals. 28:461-474.

Smith, B.R. and R.B. Daniels. 1989. Occurrence and characteristics of fragipans on the coastal plains of the southeastern United States. p. 33-42. *In* N.E.Smeck and E.J. Ciolkosz (eds.) Fragipans: Their occurrence, classification, and genesis. SSSA. Madison, WI.

Steinhardt, G.C., and D.P. Franzmeier. 1979. Chemical and mineralogical properties of fragipans of the Cincinnati catena. Soil Sci. Soc. Am. J. 43:1008-1013.

Steinhardt, G.C., D.P. Franzmeier, and L.D. Norton. 1982. Silica associated with fragipan and non-fragipan horizons. Soil Sci. Soc. Am. J. 46:656-657.

Stumm, W. 1992. Chemistry of the soil-water interface. John Wiley & Sons, NY.

Tan, K.H. 1993. Principles of soil chemistry. 2nd ed. Marcel Dekker, New York, NY.

Theisen, A.A. and M.E. Harward. 1962. A paste method for preparation of slides for clay mineral identification by x-ray diffraction. Soil Sci. Soc. Am. Proc. 26:90-91.

Thomas, G.W. 1982. Exchangeable cations. p. 159-165. *In* A.L. Pageet al. (ed.) Methods of Soil analysis. Part 2. 2nd ed. Agron. Monogr. 9. ASA and SSSA, Madison, WI.

Tomkeieff, S.I. 1983. Dictionary of petrology. John Wiley & Sons, NY.

Troeh, F.R., and L.M. Thompson. 1993. Soils and soil fertility. Oxford. NY.

Twiss, P.C., E. Suess, and R.M. Smith. 1969. Morphological classification of grass phytoliths. Soil Sci. Soc. Amer. Proc. 33:109-114.

Unger, P.W. 1979. Effects of deep tillage and profile modification on soil properties, root growth, and crop yields in the United States and Canada. Geoderma. 22:275-295.

USDA and SCS. 1985. Soil survey of Umatilla county area, Oregon. U.S. Print. Office, Washington, DC.

USDA soil survey staff. 1993. Soil survey manual. U.S. Print. Office, Washington, DC.

Wada, K., and A. Ingue. 1974. Adsorption of monomeric silica by volcanic ash soils. Soil Sci. Plant Nutr. (Tokyo) 20:5-15.

Weaver, R.M., J.K. Syers, and M.L. Jackson. 1968. Determination of silica in citrate-bi-car-bonate-dithionite extracts of soils. Soil Sci. Am. Proc. 32:497-501.

Westgate, J. A., D. G. Smith, and M. Tomlinson. 1970. Late Quaternary tephra layers in southwestern Canada. p. 13-34. *In* R.A. Smith and J.W. Smith (eds.) Early man and environments in North America. University of Calgary Archaeological Association, Student's Press, Calgary, Alberta.

Westgate, J. A., and M.P. Gorton. 1981. Correlation in tephra studies. p. 73-94. *In* S. Self. and R. S. J. Sparks (eds.) Tephra studies. Dordrecht, Netherlands.

White, A.F. 1983. Surface chemistry and dissolution kinetics of glassy rocks at 25 °C. Geochim. Cosmochim. Acta. 47:805-815.

White, A.F., and H.C. Claassen. 1980. Kinetic model for the short term dissolution of a rhyolitic glass. Chem. Geol. 28:91-109.

Wilding, L.P. 1967. Radiocarbon dating of biogenic opal. Science (Washington D.C.). 156:66-67.

Wilding, L.P., R.E. Brown, and N. Holowaychuk. 1967. Accessibility and properties of occluded carbon in biogenetic opal. Soil Sci. 103:56-61.

Wilding, L.P., and L.R. Drees. 1971. Biogenic opal in Ohio soils. Soil Sci. Soc. Am. Proc. 35:1004-1010.

Wilding, L.P., and L.R. Drees. 1974. Contribution of forest opal and associated crystalline phases to fine silt and clay fractions of soils. Clays and Clay Minerals 22:295-306.

Wilding, L.P., C.T. Hallmark, and N.E. Smeck. 1979. Dissolution and stability of biogenic opal. Soil. Sci. Soc. Am. J. 43:800-802.

Wilkins, D.E., R.W. Rickman, and D.J. Rydrych. 1996. p. 102. Columbia Basin Agric. Research. Oregon Agric. Expt. Station Special Report 961.

Williams, L.A., and D.K. Crerar. 1985. Silica diagenesis, II. General mechanisms. J. Sediment. Petrol. 55:312-321.

Williams, L.A., G.A. Parks, and D.K. Crerar. 1985. Silica diagenesis, I. Solubility controls. J. Sediment. Petrol. 55:301-311.

Wilson, M.A., R. Burt, T.M. Sobecki, R.J. Engel, and K. Hipple. 1996. Soil properties and genesis of pans in till-derived Andisols, Olympic Peninsula, Washington. Soil Soc. Am. J. 60:206-218.

Witty, J.E. 1962. Grass opal in some chestnut and forested soils of Wassco county, Oregon. Ms. thesis. Oregon State Univ., Corvallis.

Witty, J.E., and E.G. Knox. 1964. Grass opal in some chestnut and forested soils in north central Oregon. Soil Sci. Soc. Amer. Proc. 28:685-688.

Yeck, R.D., and F. Gray. 1972. Phytolith size characteristics between Udolls and Ustolls. Soil Sci. Soc. Amer. Proc. 36:639-641

APPENDICES

Appendix 1

Soil core descriptions with particles-size analyses for the treatment sites.

C

Horizon		Description
Ap -	0 to 20 cm	Very dark grayish brown (10YR 3/2) silt loam, dark grayish brown (10YR 4/2)dry; weak medium and coarse subangular blocks; slightly hard, very friable, slightly sticky, slightly plastic; many very fine and few fine roots; many very fine and fine and few medium tubular pores; moderately acid; abrupt wavy boundary.
AC -	20 to 29 cm	Very dark grayish brown (10YR 3/2) silt loam, dark grayish brown (10YR 4/2) dry; massive; slightly hard, very friable, slightly sticky, slightly plastic; many very fine and few fine roots; many very fine and few fine tubular pores; moderately acid; very hard thin layer in the first 5 cm of the horizon; clear smooth boundary.
C1 -	29 to 63 cm	Dark grayish brown (10YR 4/2) silt loam, grayish brown (10YR 5/2) dry; massive; slightly hard, very friable, slightly sticky, slightly plastic; common very fine roots; many very fine and common fine tubular pores; slightly acid; clear smooth boundary.
C2 -	63 to 79 cm	Dark yellowish brown (10YR 4/4) silt loam, yellowish brown (10YR 5/4) dry; massive; slightly hard, very friable, slightly sticky, slightly plastic; common very fine roots; many very fine and few fine tubular pores; neutral; clear smooth boundary.

Horizon		Description
C3 -	79 to 115 cm	Dark yellowish brown (10YR 4/4) silt loam, light yellowish brown (10YR 6/4) dry; massive; soft, very friable, slightly sticky, slightly plastic; common very fine roots; many fine and few medium tubular pores; neutral; clear smooth boundary.

Horizon	Sand (%)	C. silt (%)	M,F. silt (%)	Clay (%)
Ap	17.4	35.9	31.7	15.0
AC	20.0	36.2	33.1	10.7
C1	21.6	37.3	31.7	9.4
C2	16.9	41.0	32.7	9.4
C3	15.7	40.3	35.3	8.7

SM

Horizon		Description
Ap -	0 to 23 cm	Very dark grayish brown (10YR 3/2) silt loam, dark grayish brown (10YR 4/2) dry; weak fine and medium subangular blocky structure; slightly hard, very friable, slightly sticky, slightly plastic; many very fine and few fine roots; many very fine tubular pores; slightly acid; abrupt smooth boundary.
AC -	23 to 35 cm	Dark grayish brown (10YR 4/2) silt loam, grayish brown (10YR 5/2) dry; massive; slightly hard, very friable, slightly sticky, slightly plastic; many very fine and few fine roots; many very fine and few fine tubular pores; slightly acid; very hard thin layer in the first 5 cm of the horizon; clear smooth boundary.
C1 -	35 to 50 cm	Brown to dark brown(10YR 4/3) silt loam, brown (10YR 5/3) dry; massive; slightly hard, very friable, slightly sticky, slightly plastic; many very fine roots; many very fine and few fine tubular pores; neutral; clear smooth boundary.
Bw -	50 to 65 cm	Dark yellowish brown (10YR 4/4) silt loam, yellowish brown (10YR 5/4) dry; weak medium subangular blocky structure; slightly hard, very friable, slightly sticky, slightly plastic; many very fine roots; many very fine and common fine tubular pores; neutral; clear smooth boundary.

Horizon		Description
C3 -	65 to 81 cm	Brown to dark brown (10YR 4/3) silt loam, brown (10YR 5/3) dry; massive; slightly hard, very friable, slightly sticky, slightly plastic; many very fine roots; many very fine tubular pores; neutral; abrupt smooth boundary.
C4 -	81 to 95 cm	Dark yellowish brown (10YR 4/4) silt loam, light yellowish brown (10YR 6/4) dry; massive; slightly hard, very friable, slightly sticky, slightly plastic; common very fine roots; many very fine and few fine tubular pores; neutral; clear smooth boundary.
C5 -	95 to 115 cm	Brown to dark brown (10YR 4/3) silt loam, pale brown (10YR 6/3) dry; massive; slightly hard, very friable, slightly sticky, slightly plastic; few very fine roots; few very fine tubular pores; neutral.

Horizon	Sand (%)	C. silt (%)	M,F. silt (%)	Clay (%)
Ap	22.5	37.3	27.0	13.2
AC	27.6	32.9	29.2	10.2
C1	27.9	35.1	26.5	10.5
C2	16.9	41.0	32.7	9.4
Bw	21.1	38.3	30.4	10.2
C3	18.3	39.7	31.0	11.1
C4	16.6	40.5	32.5	10.4

N-45

Horizon		Description
Ap -	0 to 21 cm	Very dark grayish brown (10YR 3/2) silt loam, dark grayish brown (10YR 4/2) dry; weak medium subangular blocky structure; slightly hard, very friable, slightly sticky, slightly plastic; many very fine and few fine roots; many very fine tubular pores; very strongly acid; abrupt smooth boundary.
AC -	21 to 35 cm	Very dark grayish brown (10YR 3/2) silt loam, grayish brown (10YR 5/2) dry; massive; slightly hard, very friable, slightly sticky, slightly plastic; many very fine roots; many very fine and few fine tubular pores; moderately acid; very hard thin layer in the first 5 cm of the horizon; clear smooth boundary.
C1 -	35 to 49 cm	Dark grayish brown (10YR 4/2) silt loam, brown (10YR 5/3) dry; massive; slightly hard, very friable, slightly sticky, slightly plastic; many very fine roots; many very fine and fine tubular pores; slightly acid; clear smooth boundary.
C2 -	49 to 60 cm	Brown to dark brown (10YR 4/3) silt loam, brown (10YR 5/3) dry; massive; slightly hard, very friable, slightly sticky, slightly plastic; many very fine roots; many very fine and fine tubular pores; neutral; clear smooth boundary.
C3 -	60 to 88 cm	Brown to dark brown (10YR 4/3) silt loam, pale brown (10YR 6/3) dry; massive; slightly hard, very friable, slightly sticky, slightly plastic; many very fine roots; many very fine and fine with few medium tubular pores; neutral; clear smooth boundary.

Horizon		Description
C4 -	88 to 105 cm	Dark yellowish brown (10YR 4/4) silt loam, light yellowish brown (10YR 6/4) dry; massive; slightly hard, very friable, slightly sticky, slightly plastic; many very fine roots; many very fine and common fine tubular pores; neutral; calcium carbonates as few small strongly effervescent calcium carbonates concretions in the lower part of the horizon; clear smooth boundary.
Ck -	105 to 118 cm	Yellowish brown (10YR 5/4) silt loam, very pale brown (10YR 8/4) dry; weak very thin platy structure; slightly hard, loose, nonsticky, nonplastic; common very fine roots; many very fine and fine with common medium tubular pores; violently effervescent; slightly alkaline.

Horizon	Sand (%)	C. silt (%)	M,F. silt (%)	Clay (%)
Ap	19.0	35.2	33.1	12.7
AC	18.0	37.8	35.0	9.2
C1	18.9	39.6	34.3	7.2
C2	17.1	39.2	34.7	9.0
C3	11.6	46.2	32.4	9.8
C4	10.5	48.4	29.9	11.1

N-90

Horizon		Description
Ap -	0 to 23 cm	Very dark grayish brown (10YR 3/2) silt loam, dark grayish brown (10YR 4/2) dry; weak fine subangular blocky structure; slightly hard, very friable, slightly sticky, slightly plastic; many very fine and few fine roots; many very fine, common very fine, and few fine tubular pores; strongly acid; clear smooth boundary.
AC -	23 to 38 cm	Dark brown (10YR 3/3) silt loam, brown (10YR 5/3) dry; massive; slightly hard, very friable, slightly sticky, slightly plastic; many very fine roots; many very fine tubular pores; moderately acid; very hard thin layer in the first 5 cm of the horizon abrupt smooth boundary.
C1 -	38 to 46 cm	Dark brown (10YR 3/3) silt loam, brown(10YR 5/3) dry; massive; slightly hard, very friable, slightly sticky, slightly plastic; many very fine roots; many very fine tubular pores; slightly acid; abrupt smooth boundary.
C2 -	46 to 69 cm	Brown to dark brown (10YR 4/3) silt loam, brown (10YR 5/3) dry; massive; slightly hard, very friable, slightly sticky, slightly plastic; many very fine roots; many very fine and common fine tubular pores; neutral; abrupt smooth boundary.
C3 -	69 to 78 cm	Brown to dark brown (10YR 4/3) silt loam, pale brown (10YR 6/3) dry; massive; slightly hard, very friable, slightly sticky, slightly plastic; many very fine roots; many very fine and fine tubular pores; neutral; abrupt smooth boundary.

Horizon		Description
C4 -	78 to 108 cm	Dark yellowish brown (10YR 4/4) silt loam, light yellowish brown (10YR 6/4) dry; massive; slightly hard, very friable, slightly sticky, slightly plastic; common very fine roots; many very fine and fine tubular pores; neutral.
C5 -	108 to 118 cm	Dark yellowish brown (10YR 4/4) silt loam, very pale brown (10YR 7/4) dry; massive; slightly hard, loose, slightly sticky, nonplastic; common very fine roots; many very fine and fine with common medium tubular pores; strongly effervescent; neutral.

Horizon	Sand (%)	C. silt (%)	M,F. silt (%)	Clay (%)
Ap	24.3	33.6	27.9	14.2
AC	18.9	37.5	31.8	11.8
C1	19.2	38.4	34.3	8.1
C2	18.0	40.4	32.3	9.2
C3	15.6	42.6	32.2	9.61
C4	15.8	42.0	33.5	8.6

Appendix 2

X-ray diffraction traces for horizons of the C, SM, and N-90 treatments respectively.

Figure 1. X-ray diffraction patterns for the C treatment at (a) Ap horizon; (b) AC (20-25 cm) horizon; (c) AC (25-29 cm) horizon; (d) C1 horizon; and, (e) C2 horizon. [Clay specimens were analyzed using: (1) Mg-ethylene glycolation; (2) Mg-54% R.H.; (3) K-54% R.H.; and, (4) K-110 ^{o}C].

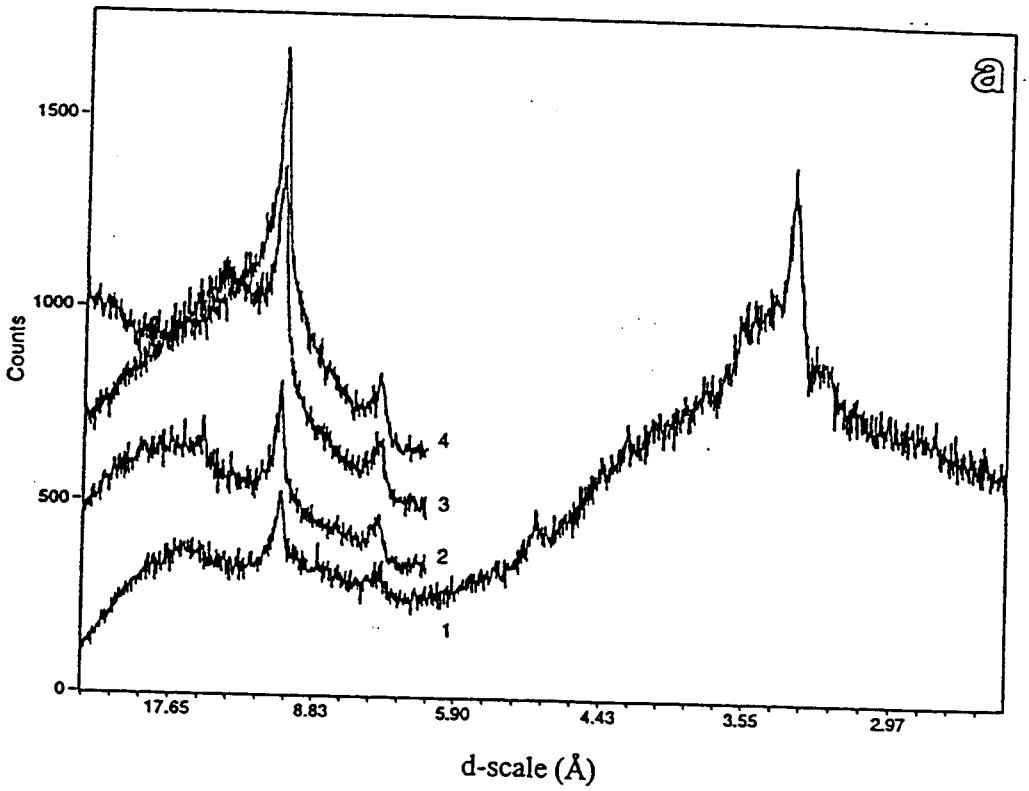
a
1500
1000
500
0
Counts
4
3
2
1
17.65
8.83
5.90
4.43
3.55
2.97
d-scale (Å)

Figure 1.

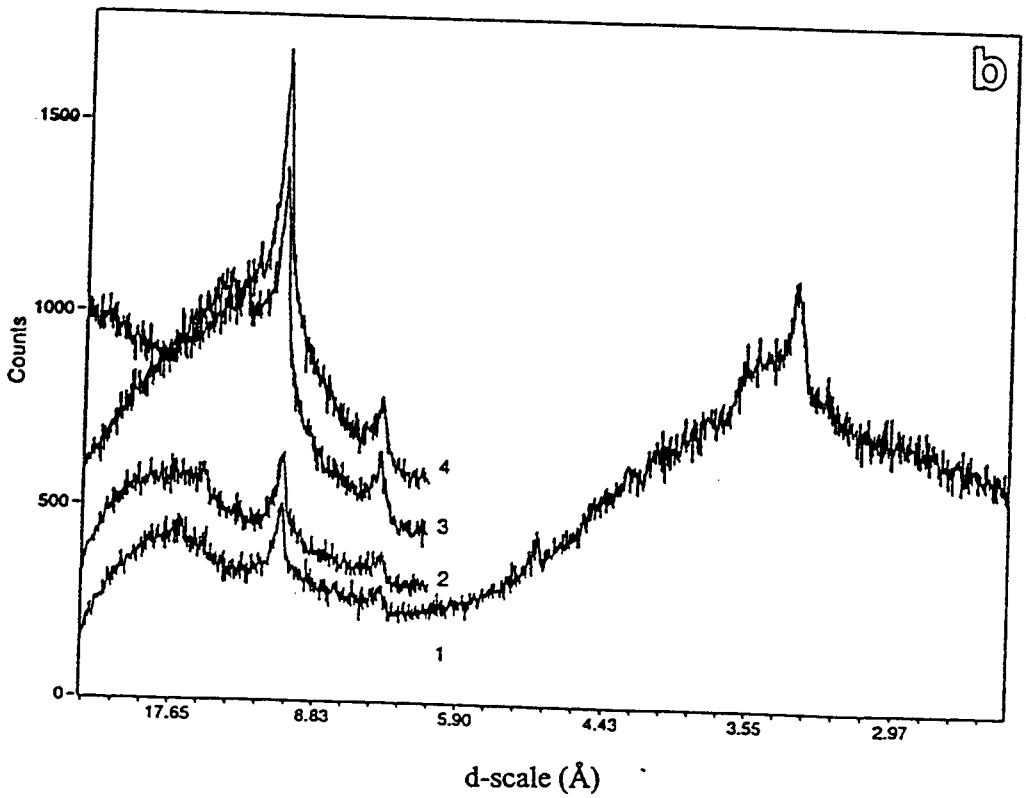
b
1500
1000
500
0
Counts
4
3
2
1
17.65
8.83
5.90
4.43
3.55
2.97
d-scale (Å)

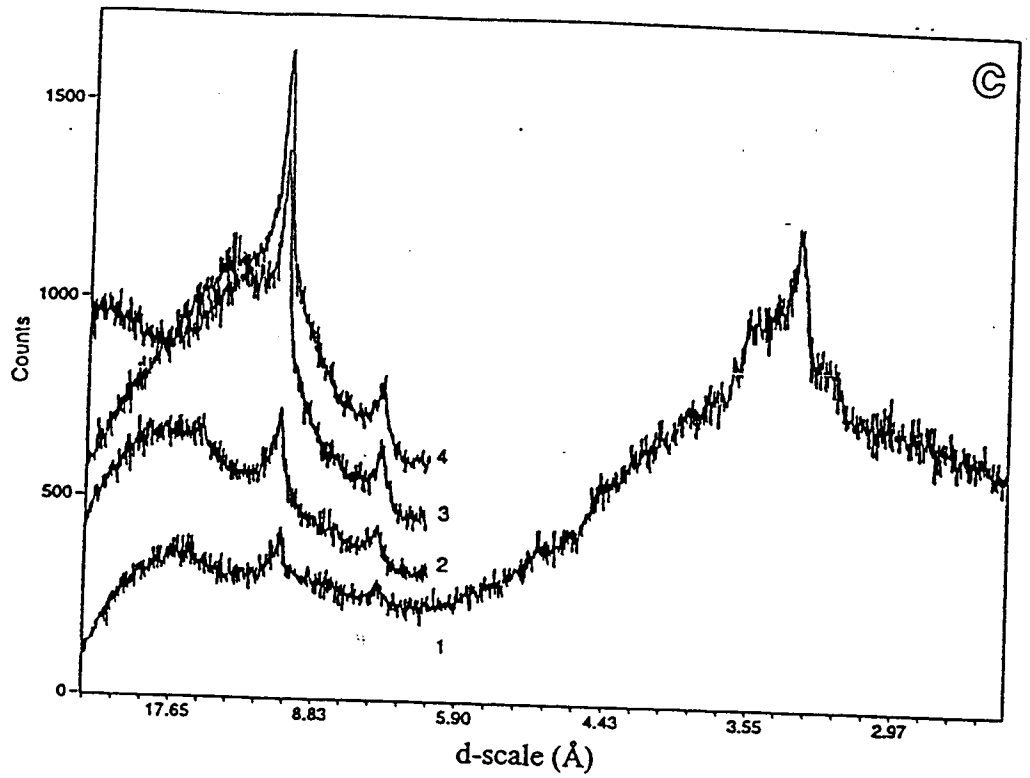

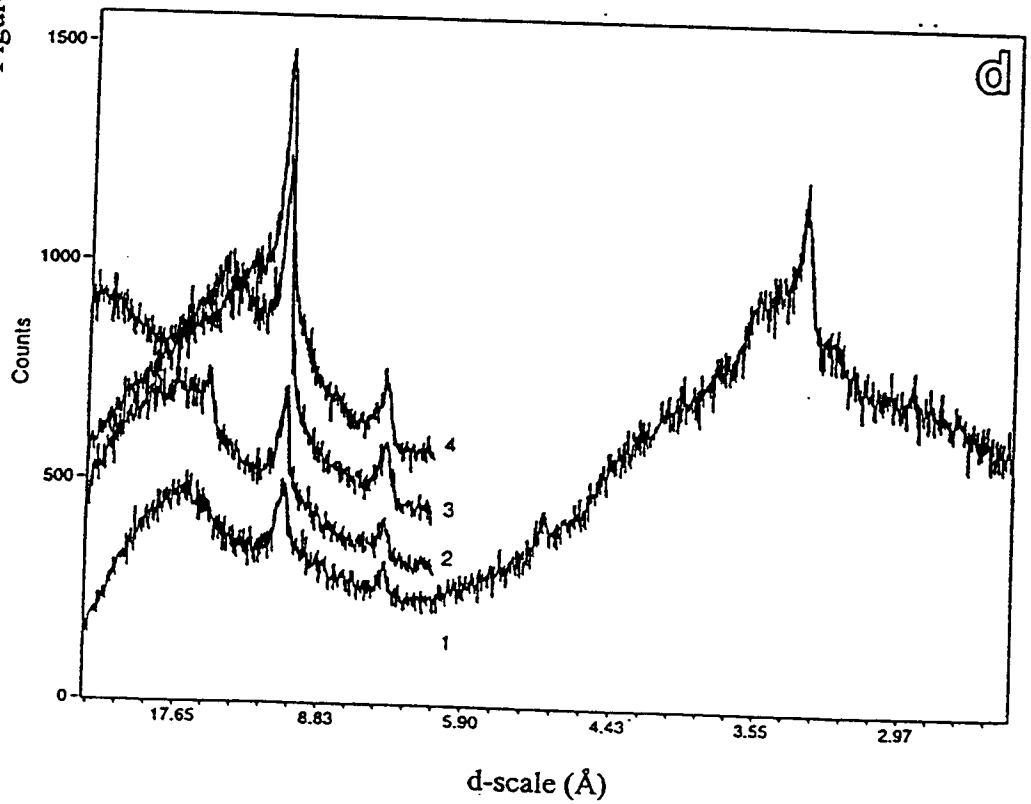

Figure 1. (continued)

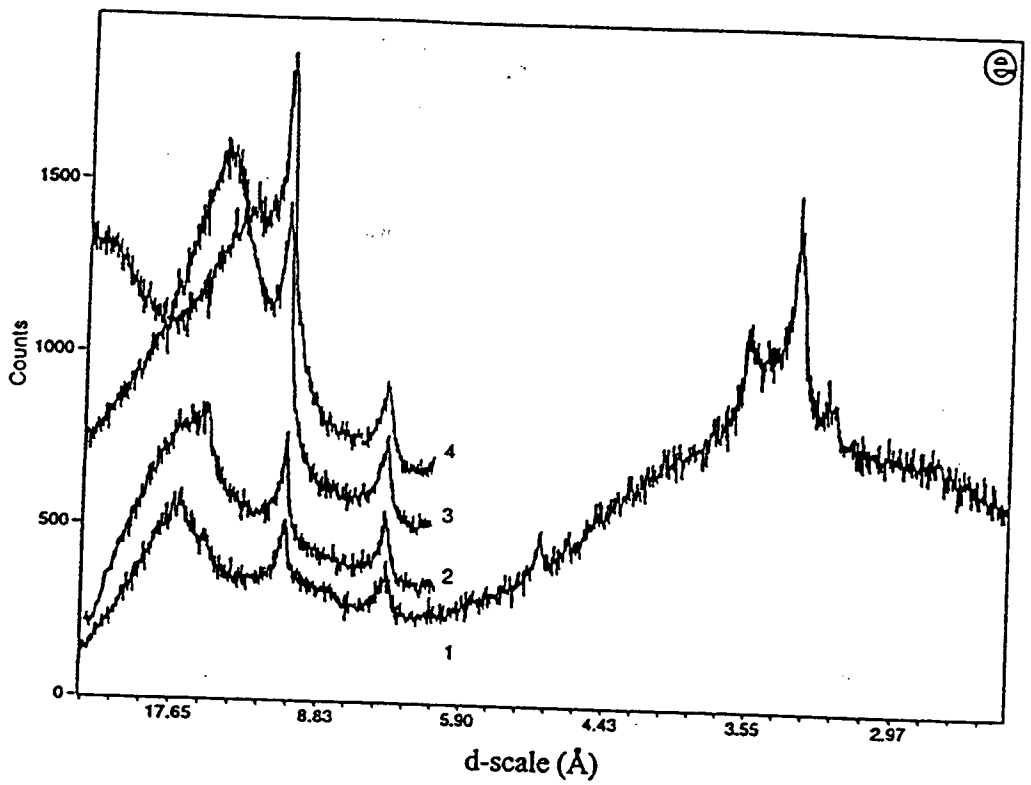

Figure 1. (continued)

Figure 2. X-ray diffraction patterns for SM treatment at (a) Ap horizon; (b) AC horizon; (c) Si-enriched zone (40-45 cm); (d) C1 horizon; and, (e) C3 horizon. [Clay specimens were analyzed using: (1) Mg-ethylene glycolation; (2) Mg-54% R.H.; (3) K-54% R.H.; and, (4) K-110 °C].

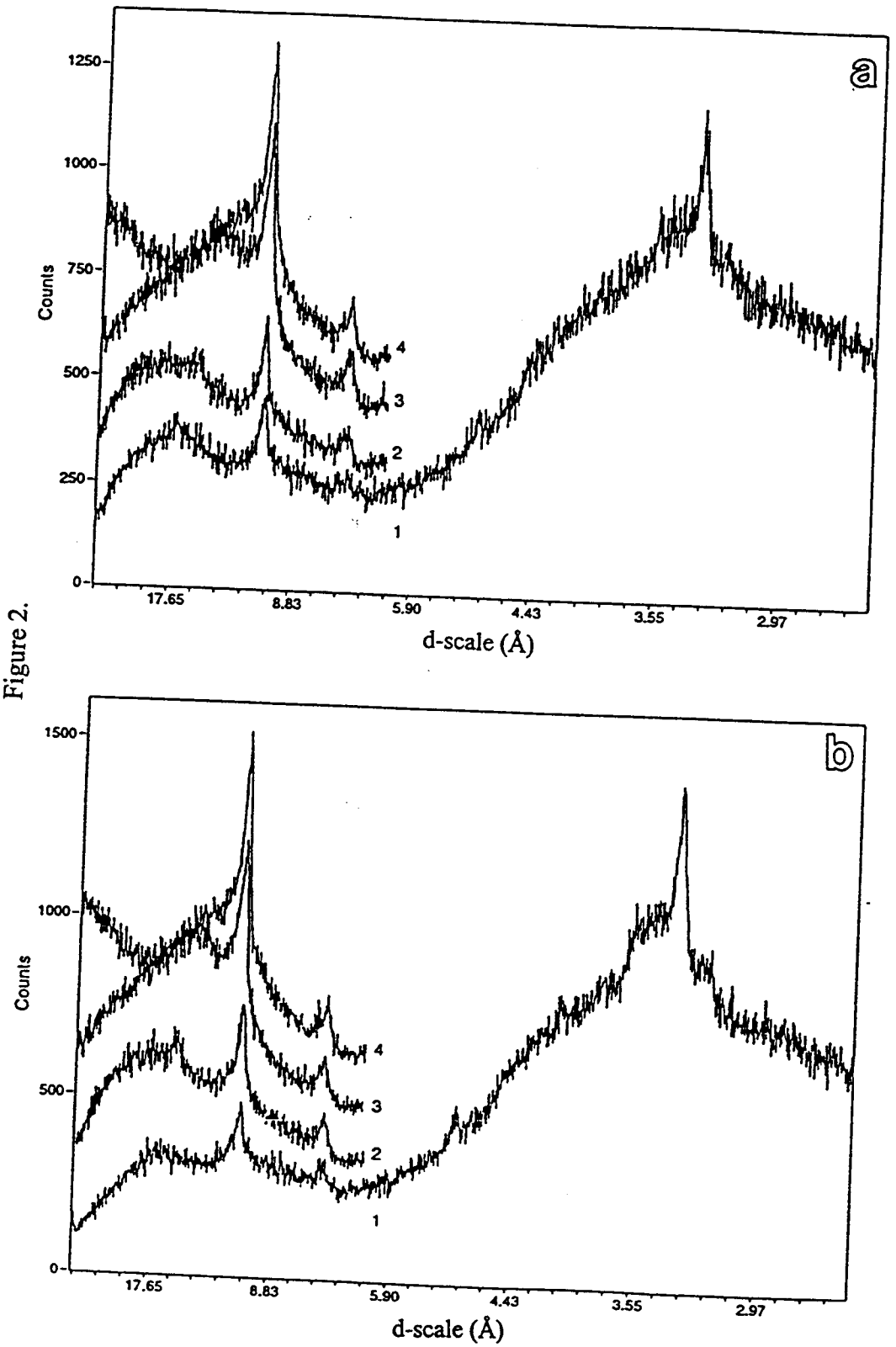
a
1250
1000
750
500
250
0
Counts
4
3
2
1
17.65
8.83
5.90
4.43
3.55
2.97
d-scale (Å)
b
1500
1000
500
0
Counts
4
3
2
1
17.65
8.83
5.90
4.43
3.55
2.97
d-scale (Å)

Figure 2.

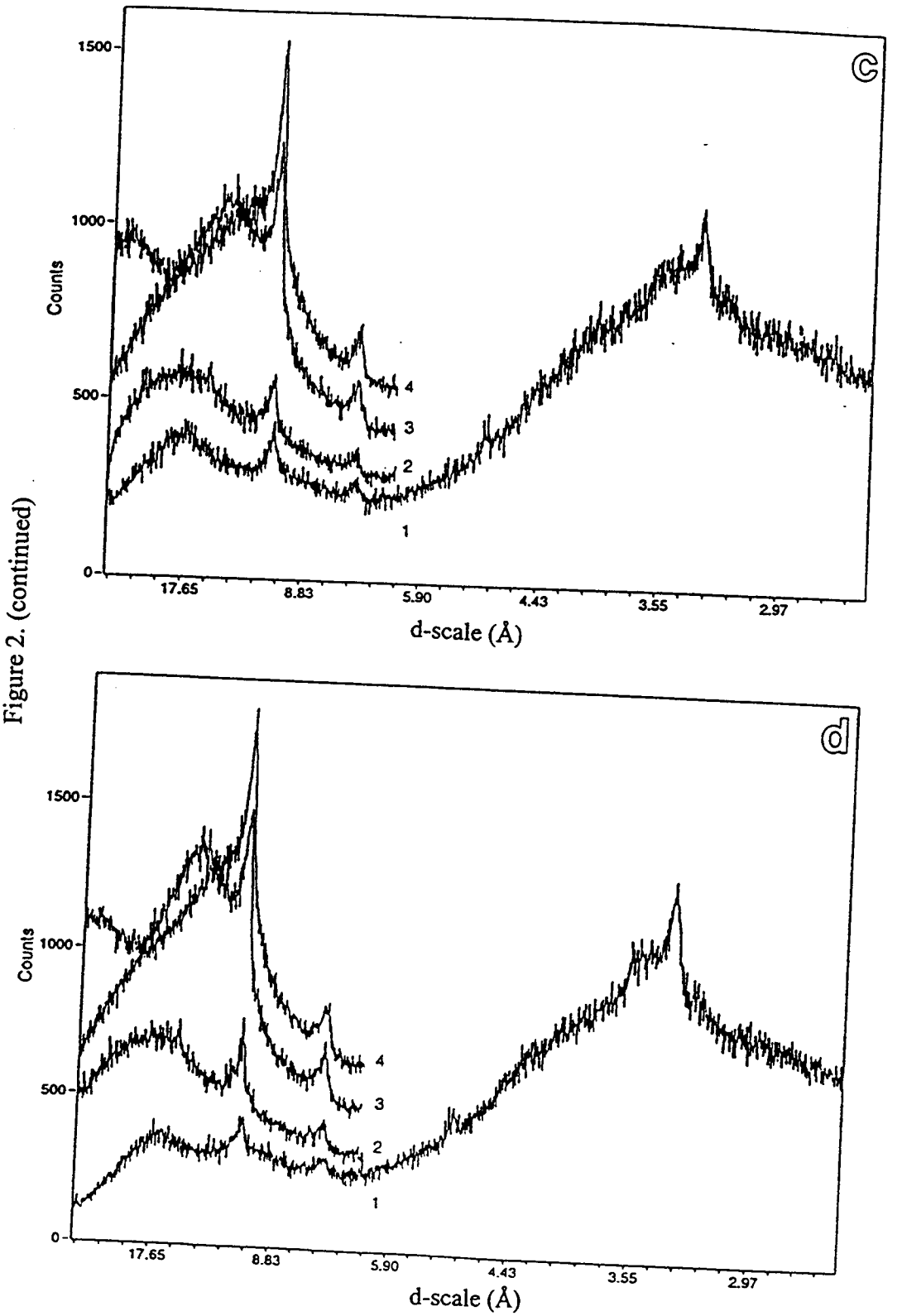

Figure 2. (continued)

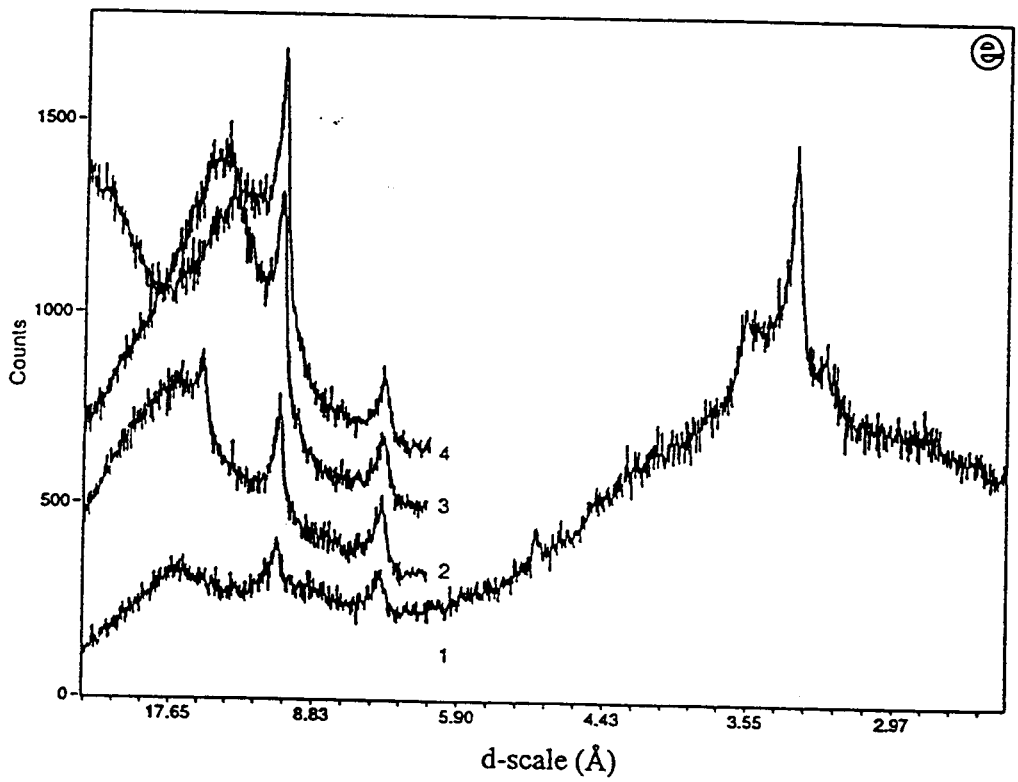

Figure 2. (continued)

Figure 3. X-ray diffraction patterns for N-90 treatment at (a) Ap horizon; (b) Maximum Si_w zone (25-30 cm); (c) AC horizon; (d) C1 horizon; and, (e) C3 horizon. [Clay specimens were analyzed using: (1) Mg-ethylene glycolation; (2) Mg-54% R.H.; (3) K-54% R.H.; and, (4) K-110 °C] .

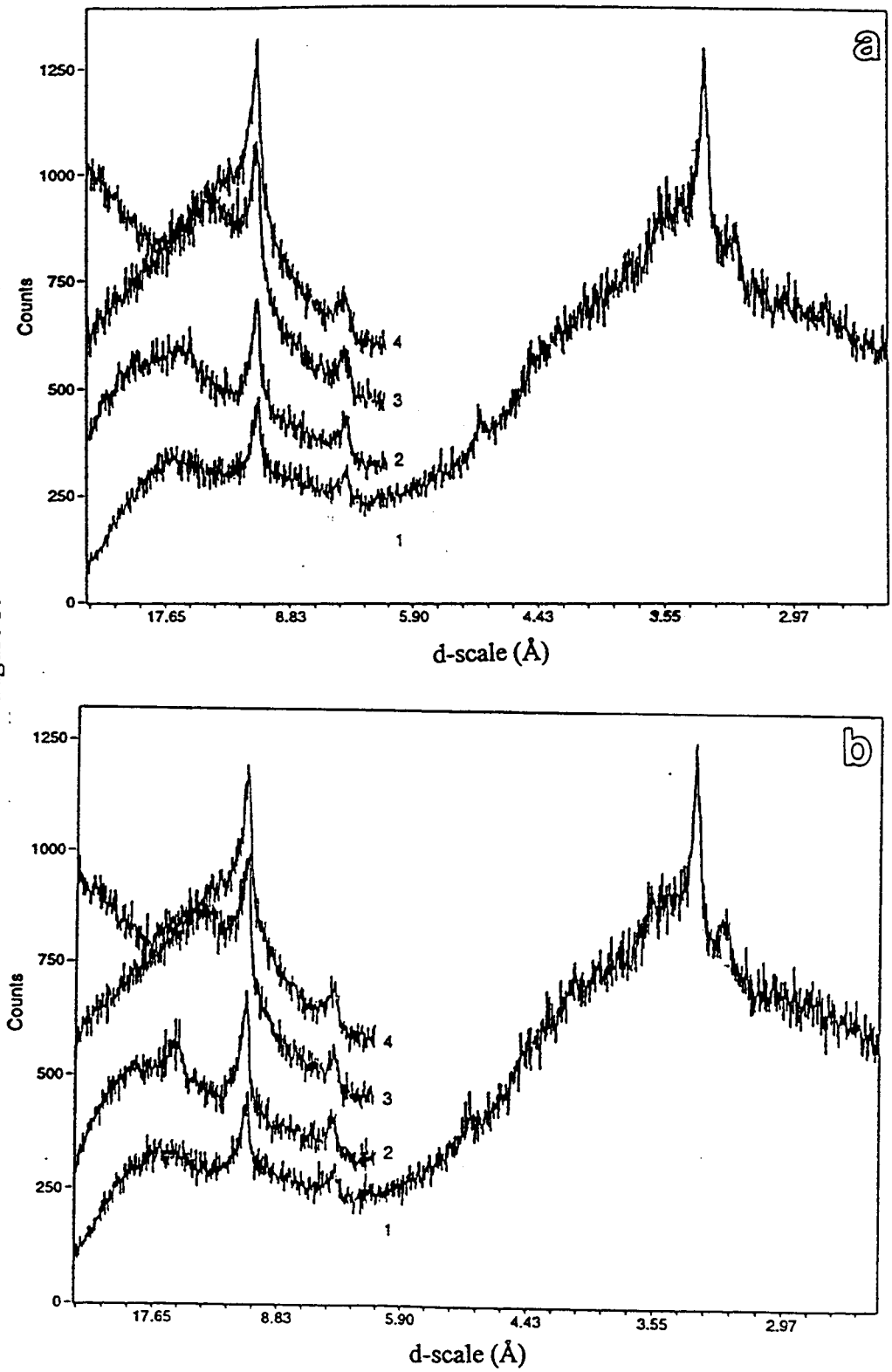
a
b
Counts
d-scale (Å)
17.65
8.83
5.90
4.43
3.55
2.97
1
2
3
4
0
250
500
750
1000
1250

Figure 3.

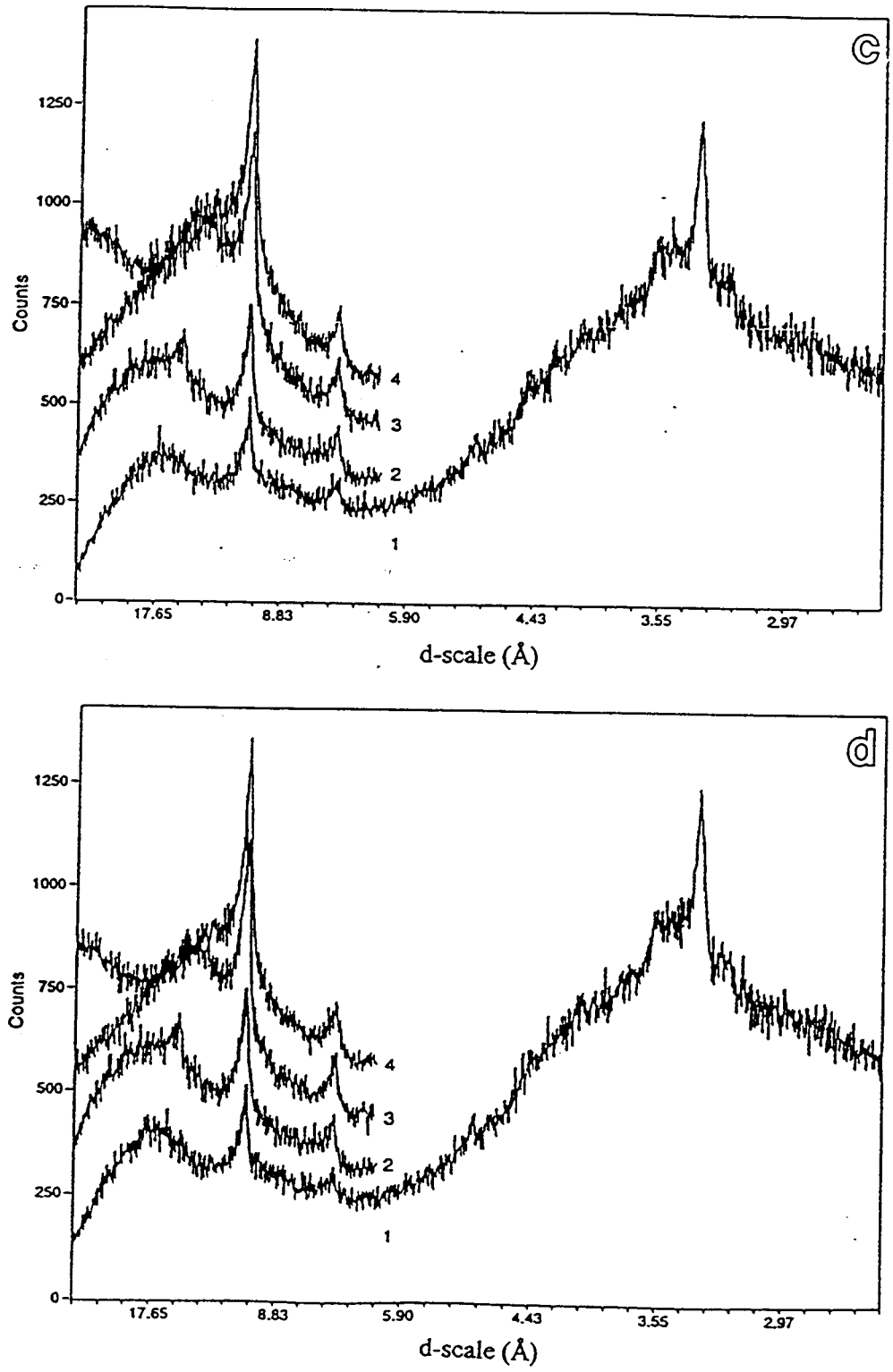

Figure 3. (continued)

Figure 3. (continued)